Evaporative Heat Loss of the Upper Middle Fork of the John Day River, Northeastern Oregon

By

David A. Benner

A Thesis Submitted

to

Oregon State University

In Partial Fulfillment of
The requirements for the
degree of

Master of Science

Presented on December 17, 1999
Commencement June 2000

AN ABSTRACT OF THE THESIS OF

David A. Benner for the degree of Master of Science in Forest Engineering presented on December 17, 1999. Title: Evaporative Heat Loss of the Upper Middle Fork of the John Day River, Northeastern Oregon.

Abstract approved: _____
Robert L. Beschta

Evaporation was studied along the Middle Fork of the John Day River in northeastern Oregon. Evaporation pans and various meteorological sensors recorded data at nine sites during the summer of 1998; measurements were made at each site over a 3-4 day period. A Dalton-type evaporation model was produced using water loss measurements in conjunction with the following meteorological information: pan water temperature, air temperature, relative humidity, and windspeed. This model was highly significant (r^2 = 0.88, $F_{2, 360}$ = 5572, p > F = 0.0001, n = 363). Regression coefficients composing the evaporation relationship were found to vary as a result of unstable atmospheric conditions (overcast periods and/or variable daytime wind direction) and windspeed measurement height.

At each of the nine sites, stream channel characteristics were analyzed to determine potential effects on the streams' capacity to cool by evaporation. The alignment of the stream channel with respect to wind direction, the degree of incision of the stream channel, and the gradient of stream bank side slopes in the direction of wind were found

to potentially affect wind movement at the stream surface, thereby, restricting evaporative cooling.

Water movement was found to increase rates of evaporation relative to non-moving water during periods of low vapor pressure deficit and no air movement. At higher vapor pressure deficits with no wind and during periods of light wind movement with a low vapor pressure deficit, differences in evaporation rates between moving water and non-moving water were less important. Much of the field data used to produce the evaporation relationship presented in this study were recorded during periods of atmospheric conditions similar to those that demonstrated minimal differences in evaporation rates between moving water and non-moving water. Nonetheless, because water loss was measured in stagnant water evaporation pans, it can only be safely assumed that the evaporation relationship presented in this document will tend to underestimate rates of evaporation from streams with moving water.

The evaporation relationship provided in this document is applicable to aridland environments. Application to other climatic regimes is probable but has not yet been validated by additional scientific research.

Master of Science thesis of David A. Benner presented on December, 17, 1999

Approved:

Major Professor, representing Forest Engineering

Head of Department of Forest Engineering

Dean of Graduate School

I understand that my thesis will become part of the permanent collection of Oregon State University Libraries. My signature below authorizes release of my thesis to any reader upon request.

David A. Benner, Author

AKNOWLEDGEMENTS

I would like to thank Oregon State University and the Department of Forest Engineering for providing me the experience of attending graduate school and conducting scientific research. I am particularly grateful to Dr. Bob Beschta who primarily guided me through this academic period. I learned more than just Hydrologic Science from Bob, he is a fine role model and a great man. The following graduate students at Oregon State University deserve thanks for their special knowledge and inspiration: Woodam Chung, Melissa Clark, K.K. McGee, and Matt Rosener.

I also must thank all of the residents of Austin Junction and Prairie City in northeastern Oregon for accepting me with hospitality and helping me to feel welcome in otherwise remote and rugged country. Special thanks to: all the workers at the Austin Junction restaurant, John Forest, and especially the two logging machinery operators who were nice enough to teach me how to negotiate the rough terrain of northeastern Oregon. I had a wonderful time interacting with this group of people, each taught me things that could not be learned in the classroom.

Lastly, I cannot say enough about my family and the support that they have provided. My mother and two brothers are simply the best.

TABLE OF CONTENTS

TABLE OF CONTENTS (continued)

LIST OF FIGURES

LIST OF FIGURES (continued)

LIST OF FIGURES (continued)

Figure Page

LIST OF TABLES

DEDICATION

This thesis is dedicated to the loving memory of my father George Benner

Evaporative Heat Loss of the Upper Middle Fork of the John Day River, Northeastern Oregon

1 - INTRODUCTION

Historical estimations have suggested that the 260,000 square-mile Columbia River basin once supported up to 16 million pacific salmon on a yearly basis. Present estimations suggest that the same area currently supports less than 1 million salmon a year, most of which are hatchery-origin fish (Yuskavitch 1998). Hence, the endangered or threatened species listing of many salmon, steelhead trout, and bull trout populations have attracted considerable attention in the Pacific Northwest. These fishes are also considered to be icons of the Pacific Northwest.

Environmental goals in the Pacific Northwest are clear: to improve the quality of waters to a level that is capable of sustaining historical levels of aquatic life. However, it has been recognized that many habitat components essential to the maintenance of aquatic life have been severely disturbed (Duncan 1998). Much of the aquatic habitat in the Pacific Northwest has been degraded by human practices that include hydroelectric dams, forestry, ranching, farming, hatcheries, and the over harvesting of fish (Duncan 1998). One of the many problems facing aquatic environments in the Pacific Northwest is elevated summertime water temperature.

Parker and Krenkel (1970) noted that any large-scale modification of the thermal regime of a river ecosystem would have drastic effects upon its ecology. Similarly, Smith and Lavis (1975) indicated water temperature is one of the most important of all

water quality criteria. Temperature affects nearly every physical property of concern in water quality management including density, viscosity, vapor pressure, surface tension, gas solubility, and gas diffusion. The solubility of oxygen is perhaps one of the more important of these properties, as reasonable levels of dissolved oxygen are essential to maintain aquatic life. High water temperatures reduce a body of water's capacity to hold oxygen, thereby reducing the oxygen available to aquatic individuals.

The biological effects of elevated water temperatures on stream life have been thoroughly explored by numerous research projects. It has been found that increased temperatures can influence rates of egg development, rearing success, species competition, metabolic rates and the susceptibility of organisms to disease (Kevern 1965, Minshall 1968, Baltz et al. 1982, Heming et al. 1982, Reeves 1985, Beschta et al. 1987, Brown 1989, McGurk 1989).

Because unelevated water temperatures are generally considered essential in the maintenance of diverse and productive aquatic environments for cold water species, it is important to understand the many factors that influence the thermal status of these systems. Essentially, stream temperature is a reflection of energy exchanges between the atmosphere, water surface, terrestrial environment and other interacting water bodies. Of particular importance (relative to this study) is the exchange of energy between the atmosphere and water surface. Figure 1-1 demonstrates the various pathways of energy exchange between a water surface and the atmosphere. This figure also displays the daily magnitude of each pathway that is typical for the middle latitudes of the United States (Parker et al. 1970). The arrows indicate that energy is either entering the system (↓), leaving the system (↑), or both (↓↑).

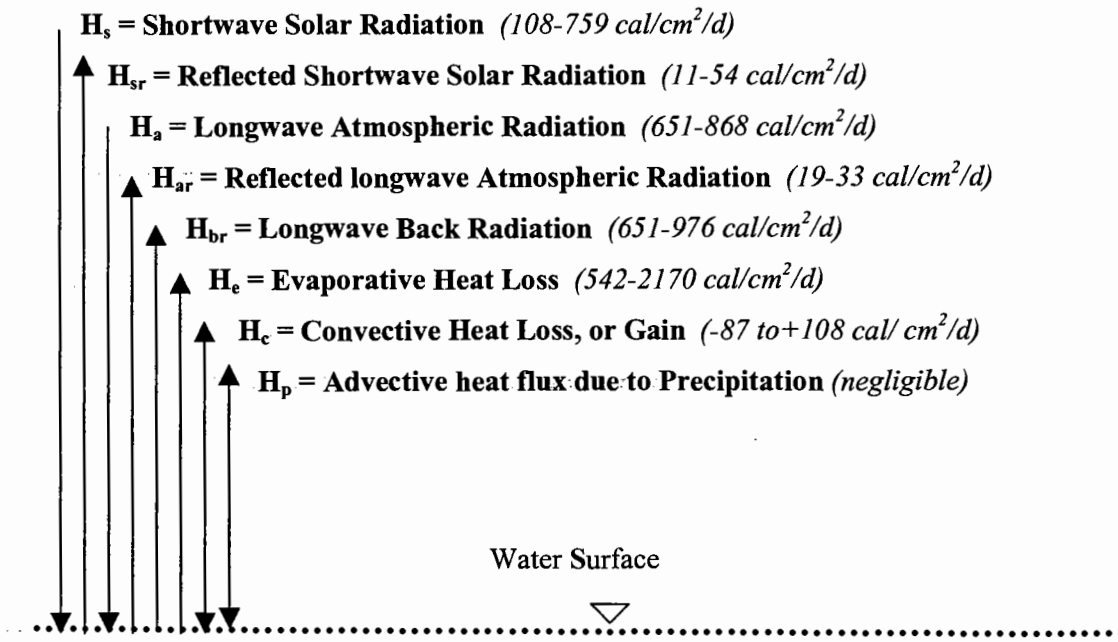

Figure 1-1. Typical mechanisms of heat transfer across a water surface for the middle latitude of the United States (Figure modified from Parker et al. 1970).

To calculate the complete energy budget of a body of water with respect to atmospheric conditions, the heat energy flux S is a simple algebraic sum of all individual energy flux components. Excluding conduction to or from the streambed, hyporeic, exchanges, or groundwater inflows, a typical expression for the total energy flux using the terms in figure 1-1 is as follows:

$$S = H_s - H_{sr} + H_a - H_{ar} - H_{br} - H_e \pm H_c \pm H_p \qquad (1\text{-}1)$$

Estimation of the various energy flux components has been the subject of extensive research projects over the last few decades. A general review of some of the more commonly used equations in water quality models is given in the following sections.

1.1 Net shortwave radiation (H_{sn})

Net shortwave radiation is the difference between the incident and reflected solar radiation ($H_s - H_{sr}$). Incident solar radiation includes both direct and diffuse solar radiation. While direct solar radiation refers to relatively unmodified radiation in the direct beam, diffuse solar radiation includes the reflected and scattered radiation from all parts of the sky (Jones 1992). Accurate estimations of net shortwave radiation require extensive levels of atmospheric information if trying to account for it's reflection, scattering, and absorption as it interacts with gases, water vapor, clouds, etc. when passing through the atmosphere. One of the more common and least data intensive equations for estimating the net shortwave solar radiation available to a water surface is the following (Bowie et al. 1985):

$$H_{sn} = H_s - H_{sr} = 0.94\, H_{sc}\, (1 - 0.65\, C^2) \qquad (1\text{-}2)$$

Where $H_{sn} = H_s - H_{sr}$ = net shortwave radiation, cal/m^2/hr
H_{sc} = clear sky solar radiation, cal/m^2/hr
C = fraction of sky covered by clouds, fraction

Equation (1-2) assumes that the water surface has an average reflectance (albedo) of 0.94. The albedo or reflectance of the stream surface depends largely upon the angle of incoming radiation and the turbidity of the surface water. The albedo of streams typically ranges from 0.06 to 0.12- meaning that 6-12% of the solar radiation incident upon the waters surface will be reflected (Mohseni and Stephan 1999).

Several methods are available for estimating clear sky radiation (H_{sc}) for use in Equation (1-2). The Tennessee Valley Authority (1972) presents a formula for predicting H_{sc} as a function of geographical location, time of year, and hour of the day. It is

important to account for shading by vegetation and/or topography when calculating net shortwave solar radiation. Although equation (1-2) does not directly account for stream shading, it can be easily accomplished by including a multiplier that ranges from 0-1. This multiplier represents an estimation of the ratio of actual solar radiation reaching a surface relative to the unobstructed or "potential" solar radiation reaching the same surface.

1.2 Net atmospheric radiation (H_{an})

Net atmospheric radiation is the difference between longwave atmospheric radiation and the reflected longwave atmospheric radiation ($H_a - H_{ar}$). The atmospheric radiation is composed of much longer wavelengths than solar radiation mostly because the major emitters of this radiation are water vapor, carbon dioxide, and ozone which all have temperatures similar to the earth's approximate temperature. The following formula utilizes an empirical determination of overall atmospheric emissivity and the use of the Stephan-Boltzman law (Bowie et al. 1985). This formula is as follows:

$$H_{an} = H_a - H_{ar} = 0.2712\ [1.16 \times 10^{-13}\ (1 + 0.17C^2)\ (1.8T_a + 492)^6\ ] \qquad (1\text{-}3)$$

Where $H_{an} = H_a - H_{ar}$ = net longwave atmospheric radiation, cal/cm^2/day
C = cloud cover, fraction
T_a = air temperature, °C

1.3 Longwave back radiation (H_{br})

Longwave back radiation is the amount of radiation that is emitted at the surface of a water body. According to the Stephan-Boltzman equation, all matter emits radiation as a

function of its temperature and emissivity (perfect emitter: $\epsilon = 1$) (Satterlund and Adams 1992). Because the emissivity of water is essentially a constant ($\epsilon = 0.97$), the longwave radiation flux from water is mostly a function of its temperature. The basic equation used for determining the longwave back radiation from a water body is as follows:

$$H_{br} = 0.97\sigma T_s^4 \qquad (1\text{-}4)$$

Where H_{br} = longwave back radiation, cal/cm^2/d
T_s = surface water temperature, °K
σ = Stephan-Boltzman constant = 1.19 x 10^{-7}, cal/cm^2/d/°K^4

1.4 Advective heat flux due to precipitation (H_p)

The advected heat flux refers to heat lost or gained by the addition of precipitation. If incoming precipitation is warmer than the temperature of the stream, heat will be gained by the water body, and vice versa. According to Mohseni and Stephan (1999) this heat flux is very small relative to other pathways of heat movement from water bodies and can be ignored when short time scales are used. This term is particularly unimportant during clear-sky conditions in mid-summer.

1.5 Convective heat loss or gain (H_c)

Convective heat is transferred across the air and water interface when the temperatures of the two media are different. The convective rate of heat exchange is proportional to the heat gradient between the two media. Early studies have related this heat flux to the evaporative heat flux by the use of a Bowen ratio (Bowen 1926). A common form of the Bowen ratio is as follows (Parker and Krenkel 1970):

$$R = H_c/H_e = (6.1 \times 10^{-4}) P [(T_s - T_a)/(e_s - e_a)] \quad (1\text{-}5)$$

Where R = Bowen ratio
P = atmospheric pressure, mb
T_a = air temperature, °C
T_s = surface water temperature, °C
e_s = saturation vapor pressure at the surface water temperature, mb
e_a = vapor pressure of the air, mb

If the convective heat flux can be represented as the product of the Bowen ratio and the evaporative heat flux, then reliable estimations of the convective heat flux (via Equation 1-5) are dependent upon accurate estimations of the evaporative heat flux term.

1.6 Evaporative heat loss (H_e)

The heat flux induced by evaporation is a major pathway in which a stream looses heat energy and thus contributes significantly to the cooling of a stream. An equation representing evaporative heat loss is as follows (Boyd 1996):

$$H_e = 8.64 (\rho L_w E) \quad (1\text{-}6)$$

Where ρ = density of water, kg/m^3
L_w = latent heat of vaporization, cal/kg
E = evaporation rate, m/s
H_e = evaporative energy flux, $cal/cm^2/day$

Although the evaporative heat flux is potentially the largest pathway for heat loss from a stream, it is also the pathway that has least been studied.

2 – OBJECTIVES

This study focused on surface water evaporation on the Middle Fork of the John Day (MFJD) River in northeastern Oregon. Along the MFJD River, relatively cool and warm reaches have been documented with FLIR imagery during mid-afternoon conditions in the summer (Torgersen 1997). It was hypothesized that hyporeic flow could explain some of these "thermal patches". However, recent research (Hopson 1997) has indicated that these exchanges were not as common as initially expected and therefore were not a major factor contributing to the occurrence of relatively cool and warm reaches along the MFJD River. Thus, the varying temperature patterns were likely driven by other causes.

Based on preliminary analysis of water temperatures and atmospheric conditions on August 9, 1996, it was concluded that evaporative heat loss may significantly contribute to the energy balance of a streams in the John Day Basin (Appendices A.1 and A.2). Results of this analysis, using the energy balance equations presented in chapter 1, are displayed in Figure 2-1. Based on this analysis, evaporation may have accounted for 37% of the total heat lost from the MFJD River on August 9, 1996.

This study was undertaken to research the role of evaporation in moderating the temperatures of rivers and streams in northeastern Oregon. There is a serious demand for a research project of this nature. Human induced changes of aquatic habitats in the Pacific Northwest and throughout much of the country has increased the awareness of stream temperature problems and the need for additional stream temperature research. It is believed that the study of evaporative cooling is the next logical step in developing a more complete understanding of the factors controlling stream temperatures, particularly

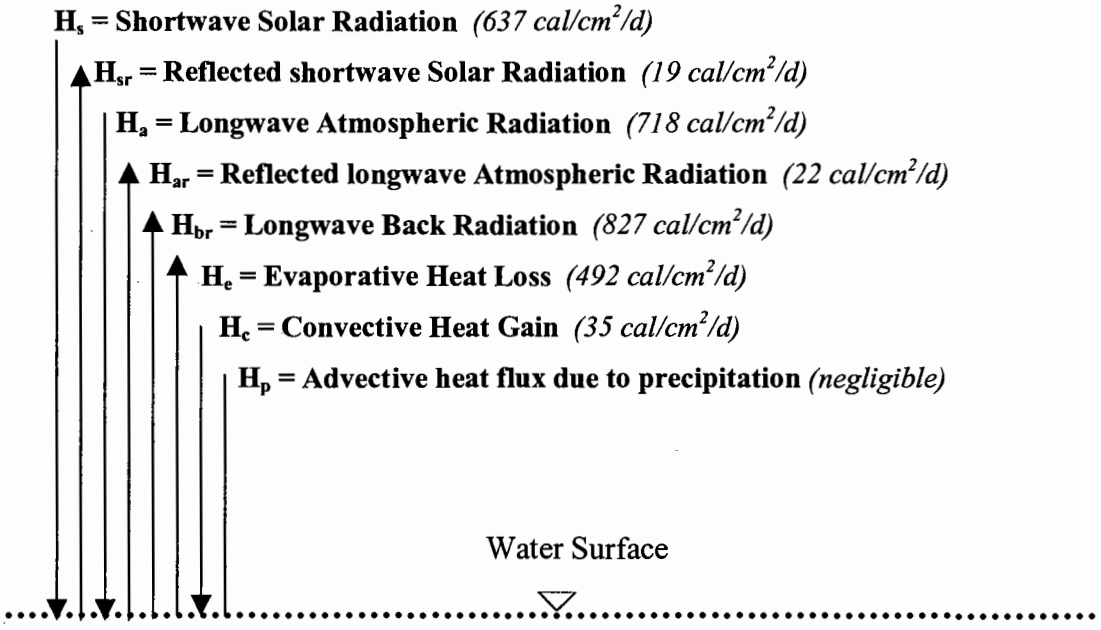

Figure 2-1. Mechanisms of heat transfer at the water surface of the Middle Fork of the John Day River, August 9, 1996. Values in parenthesis estimated from energy balance calculations (Appendices A.1 and A.2).

during clear-sky conditions in mid-summer. Information is generally lacking regarding evaporative heat loss from rivers and streams. Boyd (1996) lists the development and testing of evaporation models for open channels as an area of needed research for an improved understanding of summertime stream temperature dynamics.

The objectives of this study are:

1) To establish an equation relating pan evaporation to several micrometeorological variables including: windspeed, the vapor pressure of the air, and the vapor pressure of the evaporating surface (water). The resulting equation will be used to gauge the effects of stream evaporation upon daily temperature patterns in mid-summer.

2) To evaluate the impact of stream channel characteristics such as the alignment of the stream channel (with respect to average wind direction) and/or channel incision on evaporative potential. Extensive study will be focused in areas of significant channel incision.

3) To attempt to establish a greater understanding of the relationship between water surface turbulence/velocity and resulting evaporation rates. This relationship will be studied with air movement and with no air movement over moving water.

3 - LITERATURE REVIEW

Heat may be transferred away from a body of water at the air-water interface by longwave radiation emission, convection, and evaporation. The relative importance of each of these components depends upon atmospheric conditions and the thermal status of the water. According to Shade and Smith (1968), approximately 50% of the heat imposed on a natural body of water is ultimately lost by evaporation with this influence being most important under summertime conditions. On an average summer day, when stream and air temperatures are often at their highest, evaporation can account for more than two-thirds of the heat transfer away from the water body. During the winter months when air temperatures are low and the sun is in the southern hemisphere (relative to the U.S.), approximately two-thirds of the heat from a body of water maybe lost by means of longwave back radiation and convection and one-third by evaporation (Shade and Smith 1968).

Evaporation is the vaporization of water molecules, i.e., the conversion of liquid water to vapor. This process occurs as a result of molecular motion increasing to a point were the attraction between a single water molecule and adjoining water molecules (hydrogen bonds) is overcome. For water molecules in the liquid state to enter the gaseous state, an amount of energy equal to the latent heat of vaporization must be supplied by the water body. This amount of energy generally varies between 580-585 calories per gram and is a function of the temperature of the evaporating surface. Thus, as evaporation occurs there is a loss of energy away from the water body.

Evaporation from a water surface is directly influenced by the rate in which water vapor is transferred away from the air-water interface (Jackman and Yotsukura 1977). This movement is a function of (1) the vapor pressure deficit between the evaporating surface and the air and (2) the movement of air (wind) over the evaporating surface. When the vapor pressure of the air above a stream is low, the water vapor released from a stream has a lower chance of colliding with other water molecules in the air. In this case, molecules have a greater chance of remaining in the gaseous phase rather than the liquid phase. However, if the vapor pressure of the air is high, the occurrence of molecular collisions is greater and there is an increased tendency for the water vapor to stay in the liquid phase as opposed to entering the gaseous phase (Boyd 1996). In either case, air movement helps to disperse water vapor "ponding" above the evaporating surface. In the absence of air movement, it is possible to form layers of air saturated with water vapor above the water surface, ultimately reducing the vapor pressure deficit and resultant evaporation rates.

The most commonly used evaporation models are mass transfer type models, which are referred to as Dalton-type models (Jobson 1980):

$$E = \psi (e_s - e_a) \tag{3-1}$$

Where E = rate of evaporation in units of length per time
ψ = empirical coefficient or wind function in units of length per time
e_s = saturation vapor pressure of the air evaluated at a temperature equal to that of the water surface in units of pressure
e_a = vapor pressure of the air in units of pressure

According to Jobson (1980), the wind function has the following form:

$$\psi = \alpha + \beta (V) \tag{3-2}$$

Where V = windspeed
α and β = regression constants

Jobson (1980) noted that the evaluation of α and β are difficult for open channel evaporation studies and can change due to varying microclimates.

Jobson (1980) conducted an extensive study of open channel evaporation for the San Diego aqueduct in California. Jobson's study produced one of the few known equations for estimating the wind function and the resulting evaporation from water flowing down an open channel. His equation was developed, calibrated and fit into models used to estimate water temperatures in the San Diego Aqueduct (Jobson 1980). His equation is as follows:

$$E = [3.01 + 1.13(V)](e_s - e_a) \quad (3\text{-}3)$$

Where E = evaporation rate, mm/d
V = windspeed, m/s
e_a = atmospheric vapor pressure, kPa
e_s = vapor pressure of evaporating surface (water), kPa

Jobson's measurement of windspeed and variables associated with atmospheric vapor pressure were recorded at 4 m above the water surface.

Another equation for stream and river evaporation was presented by Krajewski et al. (1982). This equation began as a combination of equations 3-1 and 3-2:

$$E = [\alpha + \beta (V)] \ (e_s - e_a) \quad (3\text{-}4)$$

Krajewski et al. (1982) substituted the following relationships into equation 3-4:

$\alpha = 0$
$\beta = 1.5 \times 10^{-9}$
$e_s = 6.372 \ (1.0646)^{Ts}$
$e_a = [6.372 \ (1.0646)^{Ta}] \ Rh$

The final form of the derived equation is as follows:

$$E = 9.56 \times 10^{-9} \ (V) \ [(1.0646)^{Ts} - (1.0646)^{Ta} \ Rh] \quad (3\text{-}5)$$

Where: E = evaporation rate, m/s
T_s = water temperature, °C
T_a = air temperature, °C
Rh = relative humidity, fraction
V = windspeed, m/s

The regression coefficients that Krajewski et al. (1982) employed in equations 3-4 and 3-5 were taken from Zison et al. (1978). Zison et al. (1978) hypothesized that the values of these coefficients remained relatively constant over a wide range of climatic applications. The measurement height of variables associated with atmospheric vapor pressure was not suggested by Krajewski et al. (1982), however, the wind velocity used in equations 3-4 and 3-5 was that recorded at the stream surface.

Opinions seem to vary regarding potential factors that influence the size of the regression coefficients in the wind function (Equation 3-2). For example, when Jobson used his equation (3-3) in modeling the temperature of the Chattahoochee River in Georgia, the wind function coefficients were reduced by nearly thirty percent (Jobson and Keefer 1979). Jobson believed that this discrepancy was most due to substantially different climatic and exposure regimes between the two areas. While the San Diego Aqueduct was in an arid area that had little shading by vegetation, the Chattahoochee River was located in a humid area that was sheltered by trees and other vegetation. Furthermore, Dingman (1994) indicated that regression coefficients associated with the wind function were dependent largely upon the heights at which the windspeed was measured. He further indicated that they could be affected by atmospheric stability. For example, when the water surface is warmer than the air, vertical convective movements of air could cause water vapor to be transported away from the water body in the absence of any significant horizontal air movement. Although the scientific literature is not

entirely consistent, the coefficients associated with the wind function are likely sensitive to varying climatic regimes.

In the past, most evaporation studies have focused on agricultural or lake (and reservoir) issues. Researchers such as Penman, Ryan and Harleman, Meyer, Harbeck, Turner and Fry have developed some of the more recognized equations dealing with lake and reservoir evaporation (Boyd 1996). Although, numerous studies have been conducted and several equations have been developed to estimate evaporation over lakes and reservoirs, it cannot be safely assumed that the equations derived from these environments can be directly applied to rivers and streams. In spite of the fact that the basic evaporative mechanisms are the same, differences in the two environments have been recognized. The most notable difference is that the regression coefficients α and β (equation 3-2) in lake equations must account for increasing values of e_a as air moves across a lake (increased moisture content as the air traverses the water body). Therefore, the vapor pressure deficit is reduced as air passes over a lake. In fact, some scientists have hypothesized that regression coefficients in these environments are a direct function of the area of the lake (Dingman 1994). This effect is either much smaller or negligible in rivers and streams. If equations with lake-derived regression coefficients were used on streams, actual evaporation rates would likely be underestimated.

In contrast to lake evaporation research, few scientists have chosen to evaluate evaporation from a stream or river type of water body. In fact, early stream temperature research tended to dismiss the role of evaporation as a significant component of a stream systems energy balance (Brown 1969).

4 – STUDY DESIGN AND METHODS

Two separate studies were conducted in an effort to fulfill the objectives of this research plan. The first and most extensive study involved the measurement of evaporation rates and meteorological variables directly from a stream environment (Objectives 1 and 2). The second study involved the measurement of evaporative differences between stagnant and moving water in a controlled laboratory setting (Objective 3).

4.1 Study #1- Site Layout, Selection, Equipment, and Methods

4.1.1 Site Layout

Nine study sites were identified along the upper Middle Fork of the John Day River (MFJD) in arid northeastern Oregon. Figure 4-1 displays the arrangement of the nine study sites relative to one another. Overall, sites were arranged in a longitudinal pattern that proceeded upstream from the fourth order MFJD River to a second order tributary, Squaw Creek. Detailed information is provided for each site in Appendix B.

Each site contained two locations at which water loss (evaporation) and meteorological variables were measured. At each of these locations, two complete experimental setups were employed. Therefore, each site contained two locations and each location contained two evaporation pans (simply called "pans" from here forward), for a total of four pans at each site. At each site, Pans 3 and 4 were placed

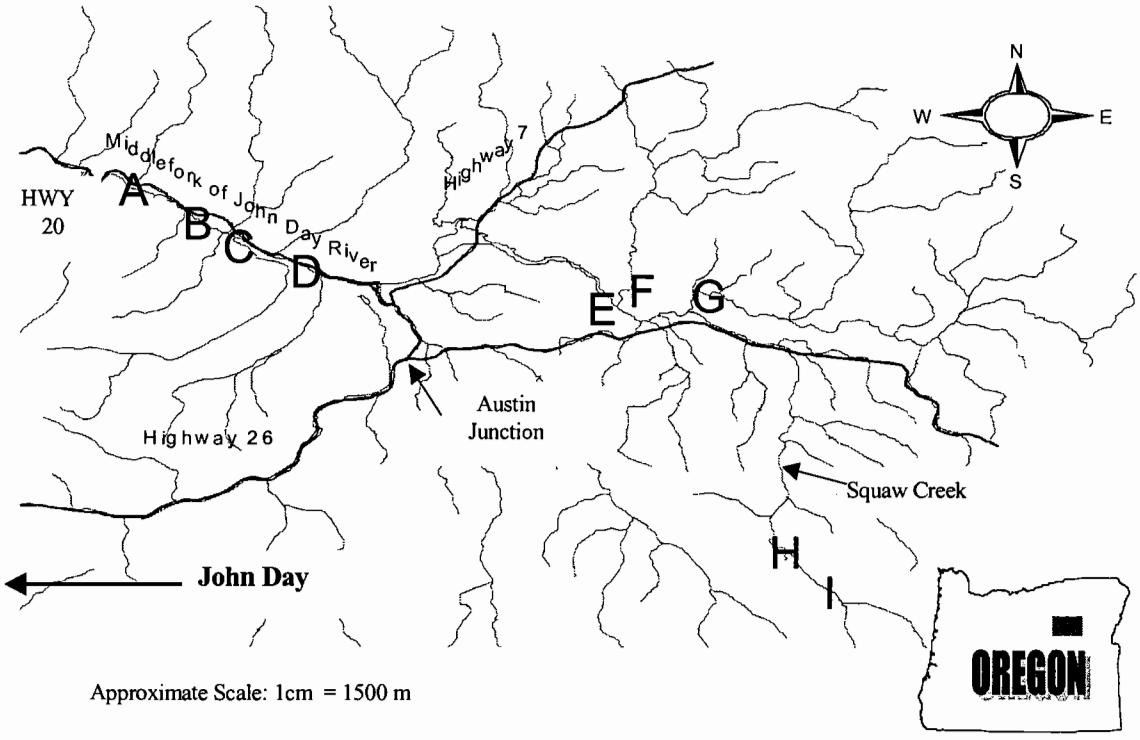

Figure 4.1. Location of the nine study sites along the upper Middle Fork of the John Day River in northeastern Oregon.

downstream relative to Pans 1 and 2. Also, the odd numbered pans (1 and 3) were placed within the stream channel in a region of calm water that was no deeper than a few centimeters less than the height of the evaporation pan. The even numbered pans (2 and 4) were placed on the floodplain surface directly adjacent to their respective in-channel pans.

4.1.2 Site Selection

In general, areas of high potential evaporation (open areas exposed to extensive solar radiation) were chosen as experimental sites. Secondarily, sites were selected based upon degree of channel incision and channel orientation with respect to valley alignment (mean wind direction). For example, a site may have been chosen on the basis that it contained sections of stream that had similar degrees of incision but one was aligned perpendicular to the valley orientation and the other parallel. Most of the sites were located in forested sections of the MFJD River in effort to compare unshaded and unsheltered environments (meadows) to those that were shaded and sheltered by trees (forested). A brief description of each site and the basis for their selection follows:

Site A: Both locations of pans were placed in forested regions of the MFJD (4^{th} order stream) with channels aligned parallel to valley direction This site established the basis for the comparison of evaporative mechanisms associated with forested riparian areas relative to those in open meadow regions with little riparian vegetation.

Site B: Both locations of pans were placed in moderately forested regions of the MFJD (4^{th} order stream) with channels aligned parallel to valley direction. This site established the basis for the comparison of evaporative mechanisms associated with forested riparian areas relative to those in open meadow regions with little riparian vegetation.

Site C: Both locations of pans were placed in open meadow regions of MFJD (4^{th} order stream) with channels aligned at a 45° angle to valley direction. Each location of pans possessed channels with varying degrees of incision. The location of Pans 1 and 2 had a moderately low degree of channel incision, where as, the location of Pans 3 and 4 had a moderately high degree of channel incision. This site was useful in comparing two regions that were identically aligned but had varying magnitudes of channel incision.

Site D: Both locations of pans were placed in open meadow regions of MFJD (4^{th} order stream) with moderately low channel incision. Each location of pans possessed channels that were aligned somewhat differently. The location of Pans 1 and 2 was aligned parallel to the valley direction and the location of Pans 3 and 4 was aligned perpendicular to the valley direction. This site was useful in comparing

regions with moderately low degrees of channel incision but quite different channel alignments relative to valley orientation (mean wind direction).

Site E: Both locations of pans were placed in open meadow regions of the MFJD (4th order stream) with moderately high degrees of channel incision. Each location of pans possessed channels that were aligned somewhat differently. This site was useful in comparing regions with similar degrees of channel incision but quite different channel alignments relative to valley orientation (mean wind direction).

Site F: Both locations of pans were placed in open meadow regions of the MFJD (4th order stream) with moderately high degrees of channel incision. Each location of pans possessed channels that were aligned somewhat differently. This site was useful in comparing regions with similar degrees of channel incision but quite different channel alignments relative to valley orientation (mean wind direction).

Site G: Both locations of pans were placed in open meadow regions of the MFJD (4th order stream) with extremely high degrees of channel incision. Each location of pans possessed channels that were aligned somewhat differently. The location of Pans 1 and 2 was aligned perpendicular to the valley direction and the location of Pans 3 and 4 was aligned parallel to the valley direction. This site was useful in comparing regions with high degrees of channel incision but quite different channel alignments relative to valley orientation (mean wind direction).

Site H: Both locations of pans were placed in an open meadow region of Squaw Creek (a 2nd order tributary to the MFJD) with channels aligned perpendicular to valley direction and moderately incised. Channel topography and alignment made each location of pans susceptible to winds from specific directions.

Site I: Both locations of pans were placed in an open meadow region of Squaw Creek (a 2nd order tributary to the MFJD) with channels aligned parallel to valley direction. Each location of pans had varying degrees of channel incision. The location of Pans 1 and 2 was moderately incised, where as, the location of Pans 3 and 4 was highly incised. This site provided a useful comparison of locations that were aligned identically but had varying degrees of channel incision.

4.1.3 Experimental Equipment

Water loss was measured using evaporation pans constructed from standard 68 liter (18 gallon) galvanized steel tubs made by Northwest Metal Products Corporation in Fife, Washington. Dimensions of the pans were as follows: top diameter = 62-cm, bottom

diameter = 54-cm, and vertical depth = 29-cm. There were several advantages in using these pans for experimental purposes:

1) Weight-- weighed approximately 2.5-kilograms a piece, light weight made for easy transport
2) Tapered shape-- allowed several pans to be stacked for space efficient transport
3) Handles-- pan-side handles made for convenient transport
4) Color-- pans were not colored in a fashion as to be great absorbers of solar radiation, instead galvanized metal reflected most solar radiation

An apparatus similar to a hook and still water measurement device described by the World Meteorological Organization (WMO 1994) was used to measure pan water level. There were essentially two parts to this apparatus: the "still water chamber" and the actual measuring device. The purpose of the still water chamber was to reduce the effects of wind and the resultant rippling of surface water on the measurement of water level inside the evaporation pan. Standard 6.4-cm (2.5-inch) inner diameter white polyvinyl chloride (PVC) piping served as the foundation for this chamber and was supported vertically inside the pan with brackets.

The water level inside the "still water chamber" was measured with a depth-measuring micrometer built by Mitutoyo Corporation (Part # 5C724, Grainger Catalog). The advertised accuracy of this gage was ±0.0254 millimeters (1/1000-th of an inch). Figure 4-2 displays the micrometer as seen in the Grainger catalog. A hook attachment i.e., a 3.8-cm (1.5-inch) fishhook with the barb ground off, was fit to the end of the micrometer rod. Measurements were taken just as the water enveloped the tip of the fishhook when lowering it through the water surface. During preliminary testing, this method proved to give the most reliable and consistent measurements of pan water level.

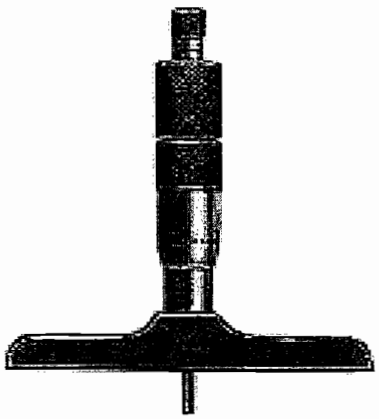

Figure 4.2. Picture of the depth-micrometer used in this study as seen in the Grainger Catalog, micrometer made by Mitutoyo Corporation.

Once fabricated the micrometer and hook attachment would only measure water at levels greater than 3.8-cm (1.5 inches) below the rim of the pan (or the still water chamber). Because it was desired to keep the water level at or near the rim of the pan, an additional modification was needed. A PVC cap was machined so that it could slide onto the 6.4-cm inner diameter PVC piping. When fitted onto the still water chamber setup, the cap protruded approximately 5-cm (2 inches) above the water surface. Two flat grooves were cut into this cap to accommodate the base of the micrometer. During field measurements, the depth micrometer fit onto the cap, which fit onto the 6.4-cm still water chamber housing (Figure 4.3). The addition of the cap was extremely efficient in blocking wind during measurements and could be removed during non-measuring periods as to not alter the movement of air over the water surface of the evaporation pan.

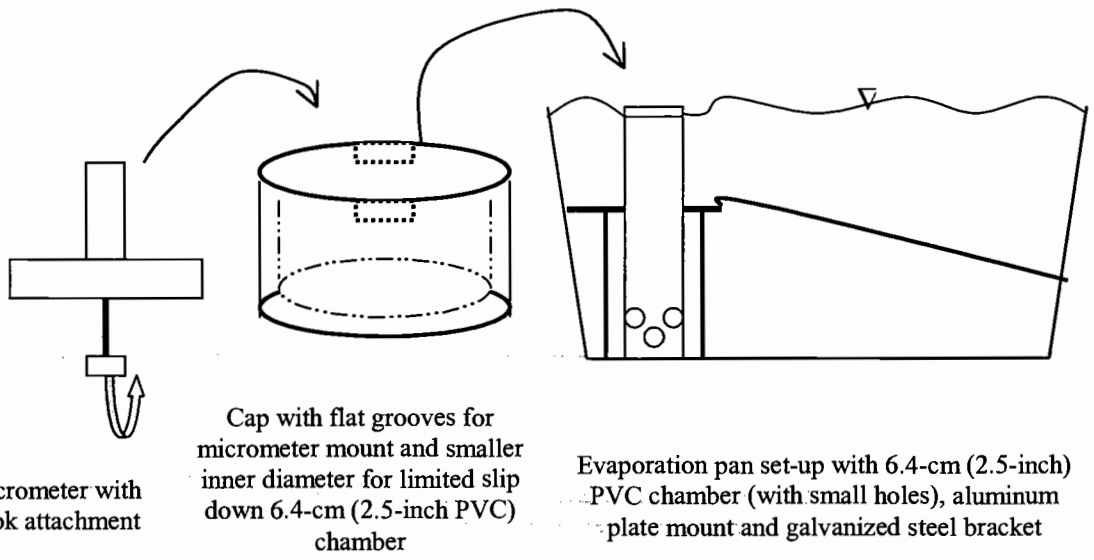

Figure 4.3. Arrangement and operation of constructed water level measuring device.

The constructed water level measuring device proved to be precise. In the field, every measurement was repeated three times and recorded to ensure that measurements were consistent with each other. The average of the three measurements represented the best estimate of the pan water level at a specific time period. Figures 4.4 and 4.5 demonstrate the precision of the described water level measuring device. Figure 4.4 is a plot of the standard deviations of the three measurements taken over the duration of the measurement period at Site A. Site A was a forested site with very little wind movement over the pan. Figure 4.5 is a plot of the standard deviations of the three measurements taken over the duration of the measurement period at Site D. Site D was located in an open, windy meadow and represented the windiest site visited during this study. The average standard deviation of the three measurements under calm conditions (Site A) was 0.051-mm (0.002 inches). The average standard deviation of the three

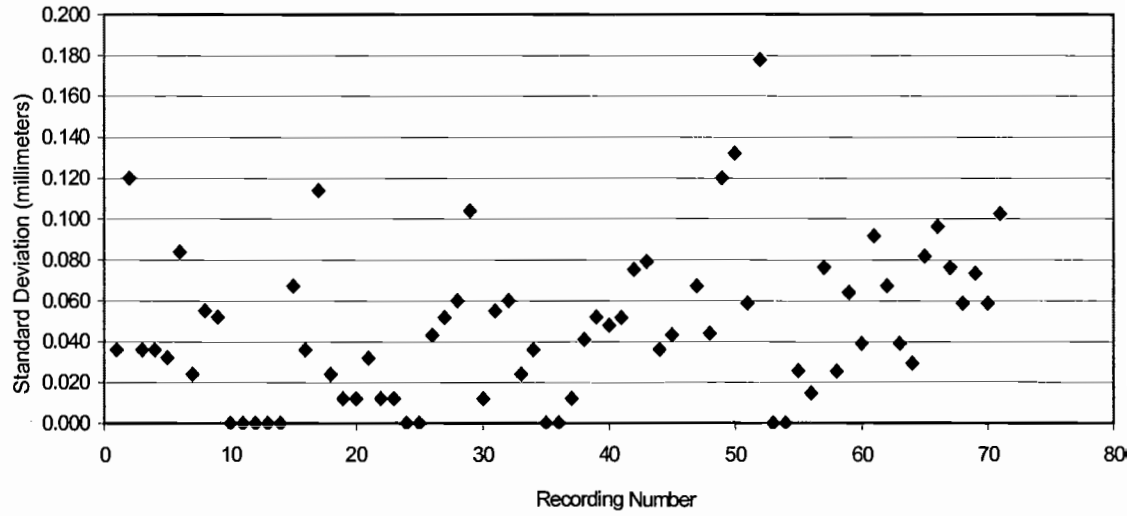

Figure 4.4. Standard deviations of the three water surface measurements taken over the duration of the measurement period at Site A, located in a forested region (average standard deviation = ± 0.051 mm).

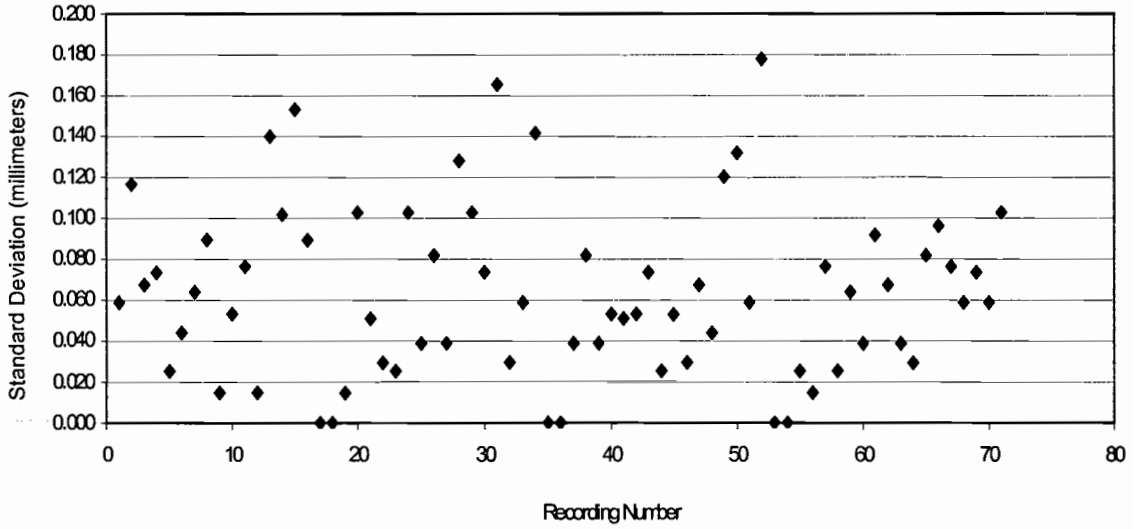

Figure 4.5. Standard deviations of the three water surface measurements taken over the duration of the measurement period at Site D, located in a meadow region (average standard deviation = ± 0.076 mm).

measurements under extreme windy conditions (Site D) was only slightly larger at 0.076-mm (0.003 inches). In either case, deviations between measurements were well within both allowable and expected limits.

Climatic variables were measured by various sensors and recorded by Campbell Scientific CR10 dataloggers. Sensors were used that measured the following atmospheric and water conditions: air temperature, relative humidity, windspeed, wind direction, solar radiation, and water temperature (both inside the pans and stream). These variables were recorded by the dataloggers every five seconds. Every twenty minutes, the proceeding measurements (20 minutes * 12 measurements per minute = 240 measurements) were averaged to produce a single value that was stored by the datalogger to be retrieved at a later time. All of the sensors were connected to the Campbell Scientific CR10 datalogger with the exception of the HOBO® water temperature probe, which had its own internal memory.

The temperature and relative humidity of the air were measured with Campbell Scientific CS500 temperature and humidity probes. This probe measured air temperatures to ± 0.5 °C, where as, relative humidity accuracy ranged from ± 2% at 10% relative humidity to ± 3% at 90% relative humidity. To shield this probe from direct exposure to solar radiation, a Campbell Scientific 41301 radiation shield was used. Figure 4.6 displays the Campbell Scientific CS500 temperature and humidity probe along with the radiation shield. This shield (with probe) was mounted on a tripod approximately 0.5 m above the surface of the evaporation pan water.

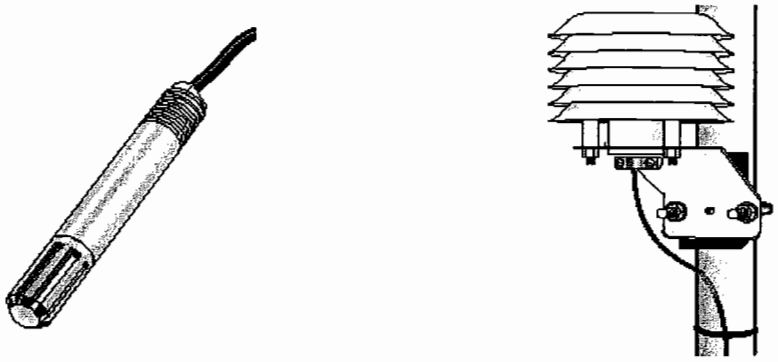

Figure 4.6. Display of the Campbell Scientific CS500 temperature and humidity probe and the probe inserted into the Campbell Scientific 41301-radiation shield as seen in the instruction manual.

Evaporation pan water temperature was measured with a Campbell Scientific 107-temperature probe. This probe was listed as accurate to ±0.2 °C between 0 °C and 70 °C and ±0.3°C at 95 °C. Advertised accuracy was confirmed after extensive laboratory testing by Constantz (1998) who concluded this probe was accurate to ±0.1°C. This probe had a thick waterproof coating made of Santoprene® rubber that surrounded all wiring making it specially adapted to measuring under water and soil temperatures. This probe was placed directly in the evaporation pan; the holes in the bottom of the 6.4-cm (2.5 inch) PVC piping held the probe securely in place and helped limit its exposure to solar radiation.

Windspeed and wind direction were measured with the 03101-5 R.M. Young Wind Sentry Anemometer and the 03301-5 R.M. Young Wind Sentry Vane. Both instruments were obtained through Campbell Scientific. The 03101-5 Anemometer was capable of

accurately measuring windspeeds of up to 50 m/s. A wind velocity in excess of 0.2 m/s was needed to initiate the movement of the cup wheel assembly. If wind movement was at or below this critical threshold, the instrument recorded a constant value of 0.2 m/s. Therefore, all data that contained windspeed values that were recorded as 0.2 m/s were discarded from analysis. If the instrument recorded a value of 0.2 m/s, it could have represented any level of windspeed between 0 and 0.2 m/s. The 03301-5 R.M. Young wind vane measured wind direction on a degree scale with 0° representing due north and 180° representing due south. The advertised accuracy of this instrument was ± 5°. The wind vane was mounted on a cross arm opposite the anemometer as shown in Figure 4.7. Both instruments were located approximately 0.5-m above the water level in the evaporation pans.

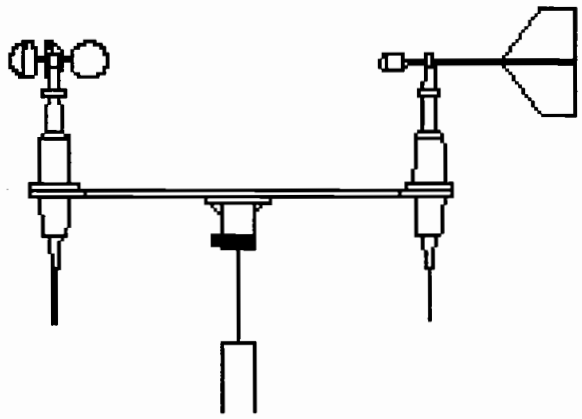

Figure 4.7. The 03101-5 R.M. Young Wind Sentry Anemometer and 03301-5 R.M. Young Wind Sentry Vane mounted side by side on cross arm as seen in the instruction manual provided by Campbell Scientific.

Solar radiation was measured using a sensor made by LI-COR ®. The sensor used was a Quantum Sensor (LI-190SA) purchased from Campbell Scientific. This sensor measured the photosynthetically active radiation (PAR) in the 400 to 700 nanometer waveband passing through a horizontal plane of known area (units = μmol s^{-1} m^{-2}). The U.S. National Institute of Standards and Technology (NIST) calibrated the LI-190SA to a standard lamp. The LI-190SA gave measurements that were within ± 5% of the values recorded by the NIST lamp. This sensor was also placed approximately 0.5-m above the water level in the evaporation pans.

HOBO® temperature sensors recorded the temperature of the actual stream water. This sensor was used to monitor the agreement between stream temperatures and the recorded water temperatures of the in-stream evaporation pan. Figure 4.8 displays the agreement between the temperatures recorded by a HOBO® sensor in the actual stream channel and the temperature sensor residing within the in-channel pan located at Site I.

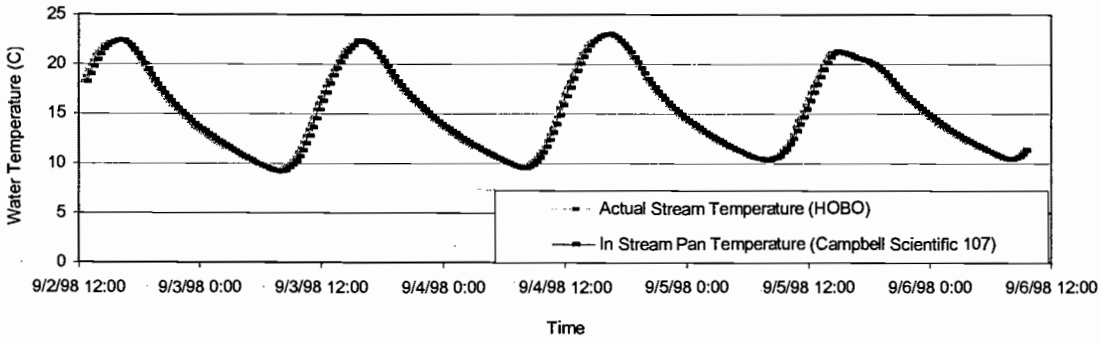

Figure 4.8. Comparison of stream temperatures and the water temperatures of the in-stream evaporation pan at Site I from 9-2-98 to 9-6-98.

Inspection of Figure 4.8 indicates that the two bodies of water are thermally identical for the period between 9-2-98 and 9-6-98. It was expected that the pans placed outside the stream on the floodplain would tend to heat at a greater rate throughout the duration of the day than the pans in the stream as a result of not being bathed by stream water. The purpose of these additional pans was to increase the number of recordings of evaporation and associated meteorological variables. In short, these pans were not intended to represent actual stream conditions; it was expected that these pans would experience more evaporation than those located inside the stream. Nonetheless, they did provide useful data for derivation of evaporation relationships.

All meteorological instruments (except water temperature probes) were located on a horizontal 1-m-long bar that was attached to a tripod. The wind vane and anemometer assemblies were attached to one end of this bar (perpendicular to the bar) and the air temperature and relative humidity sensor with the radiation shield was attached to the opposite end. The Quantum sensor was located at approximately the middle point of the bar, directly over the center portion of the tripod. With this tripod device, all sensors could be adjusted to the desired height (0.5-m) above the evaporation pan water.

Dataloggers recording information from the sensors on the tripods were located in a shaded region near the tripod and/or also covered with grass to protect their black exteriors from heating by solar radiation. At each location of pans, both the in-stream and out-of-stream tripod setups were orientated identically.

Measurements using the described equipment were recorded between July 21, 1998 and September 8, 1998. Between these dates, 31 days of complete data were recorded. Complete data consisted of pan water level measurements approximately every two to

three hours during the sunlight period with accompanying meteorologic measurements. Over a two to three hour period, water losses were typically much greater than 1mm (0.039 in). In general, as overall water losses increased, the error in measurement decreased, as water losses were much larger than measurement errors (0.051-0.076 mm). Data from the meteorological sensors were stored in the dataloggers and "dumped" on a daily basis to storage modules, where the data could be imported to a laptop computer.

4.2 Study #2- Design, Layout, Methods, and Equipment

The second part of this research plan compared evaporation rates from stagnant and moving water. This study was undertaken to compliment Study #1. All field measurements of evaporation recorded in Study #1 occurred in stagnant water (pans), however, the stream water surrounding each pan was in motion. To help better understand evaporation from streams, additional exploration of the effects of water velocity/turbulence was needed. Early on, it was hypothesized that a moving body of water would tend to evaporate more water than a stagnant body of water that was subject to the exact same set of atmospheric conditions. Furthermore, it was thought that this difference would increase as the velocity of the water increased. As part of field measurements (Study #1, Appendix B), the surface velocity of the water was measured at the location of each in-stream evaporation pan. It was anticipated that a correction coefficient could be developed to adjust evaporation rates to account for the velocity of the stream water.

Three separate experimental tests were associated with Study #2. The first test involved comparing pan evaporation rates from stagnant water (E_s) to that of a pan with moving water (E_m). This test was executed under laboratory conditions with a relatively constant vapor pressure deficit and with no air movement. The second test involved a similar experimental design with a larger vapor pressure deficit than the first experiment, but again no air movement across the pan water surface. The third experimental test had a vapor pressure deficit similar to that of the first experiment, but introduced air movement across the surfaces of both pans.

4.2.1 Test #1

This experimental test consisted of comparing the water loss from two separate pans. The pans used for this test were the same as those used for field measurement (i.e., Study #1). Although both pans were subject to exactly the same atmospheric vapor pressures, one experimental pan had a device installed that moved pan water at a constant rate. Water movement was provided with a power drill (i.e., 13-mm (0.5-inch) 4.0 Amp Skil® Drill; part # 6355) suspended approximately 40-cm above the rim of the evaporation pan. A "mixing wheel" was attached to an extension rod that fit into the chuck of the drill. The mixing wheel was positioned approximately 10-cm above the bottom of the pan. This drill came equipped with a trigger that could be used to adjust the number of revolutions per minute (RPM) until the desired movement of water was observed in the pan. Because this drill cooled its inner components by an internal fan with external air vents, high RPM increased air movement around the drill. To ensure that this air

movement did not influence evaporation at the water surface, a 0.5 x 0.5-m shield was installed between the drill and water surface. Because it was also important that the breeze did not reach the neighboring evaporation pan, a 1.5 x 1.5-m barrier was placed in between the two pan setups (Figure 4.9). For this test of Study #2, three different rates of water movement were simulated: 0.03-0.06 m/s (0.1-0.2 ft/s), 0.09-0.12 m/s (0.3-0.4 ft/s), and 0.24-0.30 m/s (0.8-1.0 ft/s); three sets of measurements were taken at each water movement setting. Because of the somewhat low vapor pressure deficit (1 kPa) between the air and water, a measurement period often consisted of 24 hours or more. This amount of time was needed to record a water loss of around 2.5-mm (0.1 inch) in the pan

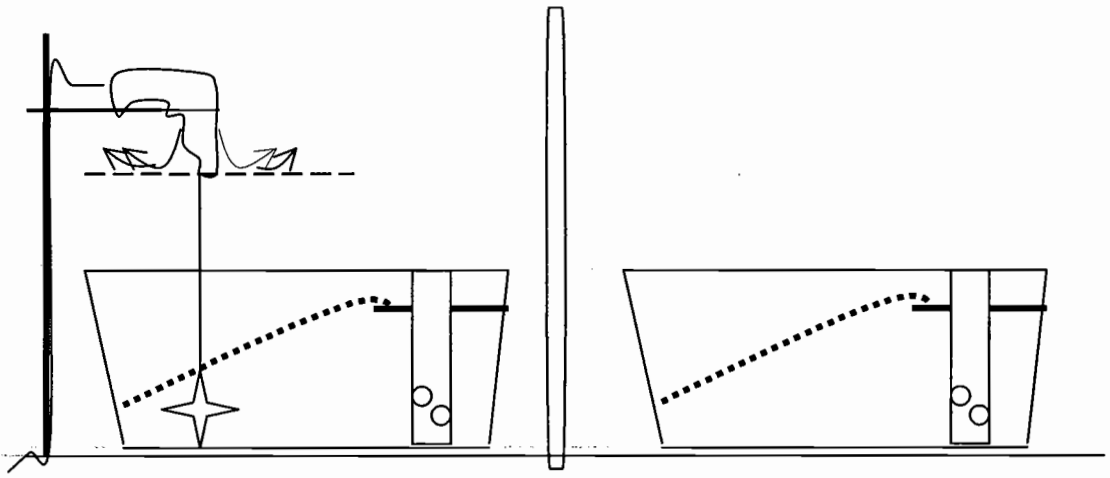

Figure 4.9. Arrangement of evaporation pans and water mixing device for Test #1, Study #2.

with stagnant water. As indicated previously, the error in measurement of water surface elevation is approximately ±0.051-mm (0.002 inches) under calm conditions. Therefore, as total evaporative losses over a measurement period increase, this error becomes less significant. As with Study #1, three recordings of pan water level were averaged in effort to produce a reliable estimate of pan water level at a specific time.

The temperature of the water inside each of the pans was recorded with each measurement of water level. In all instances, water temperatures within the two pans remained identical. Appendix D displays all data recorded during this part of Test #1, Study #2.

Water velocities inside the evaporation pans were difficult to determine. Several methods of water velocity measurement were used in effort to discover the most reliable technique of estimating water movement. Very little success was had using several different current meters to measure water movement. This situation may have occurred because of secondary currents within the pan in conjunction with a relatively high degree of random water movement (created by the stilling well). It was finally decided that an "eye ball" method would be used to estimate water velocity. Using this method, the "average" velocity was estimated, by eye, based upon the average distance traveled by particulate material (i.e., small pine needles obtained during field duties) over a specific period. Although the absolute accuracy of this approach is not known, it was a consistent methodology for estimating velocities.

4.2.2 Test #2

After completing Test #1, it was hypothesized that the relationship between the ratio of $[(E_m)/(E_s)]$ would vary as a function of vapor pressure deficit. To test this hypothesis, an experiment similar to Test #1 was employed, but with an increased vapor pressure deficit. A hot-dry controlled condition room in Richardson Hall at Oregon State University provided an environment that maintained a large vapor pressure deficit. The experimental setup (exactly identical to that described in Test #1) was transferred to this room, which provided a vapor pressure deficit of approximately 2 kPa. This experimental test was performed at a water velocity of 0.12-0.18 m/s (0.4-0.6 ft/s).

The purpose of this test was not to establish a complete relationship between $[(E_m)/(E_s)]$ and water velocity as was the intent of Test #1. Instead, it was desired to check if the relationship obtained in Test #1 was valid for larger vapor pressure deficits. For this reason, measurements were only recorded at one water velocity and compared with those predicted by the relationship derived in Test #1 for the same velocity but at a lower vapor pressure. The water temperature of the evaporation pan water was recorded and remained consistent throughout this experimental test (Appendix D).

4.2.3 Test #3

Test #3 was performed under the same conditions as Test #1 (vapor pressure deficit approximately 1 kPa) with the addition of a slight wind blowing over the surfaces of both evaporation pans. In this part of Study #2, all equipment was set-up in the same exact location and arrangement as in Test #1. However, a large household fan was installed

that delivered a slight wind (approximately 0.3 m/s) evenly to the water surfaces of the two evaporation pans. This experimental test was performed at a water velocity of 0.12-0.18 m/s (0.4-0.6 ft/s). The temperature of the water inside each evaporation pan was again monitored and remained consistent between pans throughout the duration of this study (Appendix D).

5 – DATA ANALYSIS

Data analysis was separated into two sections in accordance with the separate studies and objectives of this research plan. Data analysis associated with Study #1 aimed at fulfilling objectives 1 and 2. Analysis connected with Study #2 focused on meeting the requirements of objective 3.

5.1 Study #1

Analysis of this study was divided into two parts, corresponding to objectives 1 and 2. Analysis of each objective was evaluated separately and collectively. Often, analysis of one objective included using information that was learned in the evaluation of another objective.

5.1.1 Objective 1

This objective called for the derivation of a single mathematical equation that related pan evaporation to meteorological variables measured approximately 0.5-m above the pan water surface. To begin, it was important to certify that all meteorological sensors of the same type recorded consistent information throughout the entire period of data collection. This verification was established by the analysis of meteorological data recorded before and after field study. All sensors and data loggers were set up for several days in a small courtyard at Oregon State University. This environment contained spatially uniform air temperature and relative humidity that varied naturally with time of

day. In contrast, windspeed and wind direction varied throughout this area depending on location and time of day (the courtyard contained some degree of turbulent air movement) causing difficulty in the calibration of wind sensors. Figure 5.1 demonstrates the relationship between air temperature and time recorded by the four data loggers before the start of field observation. It is clear that all four sensors recorded air temperature information that was very consistent with one another for the calibration period on 7-14-98. Plots of this nature were also plotted for relative humidity and all sensors yielded results within 2% of one another.

Upon completion of field analysis, sensors were again calibrated and checked for consistency. Figure 5.2 demonstrates the relationship between air temperature and time recorded by the four data loggers after the completion field observation.

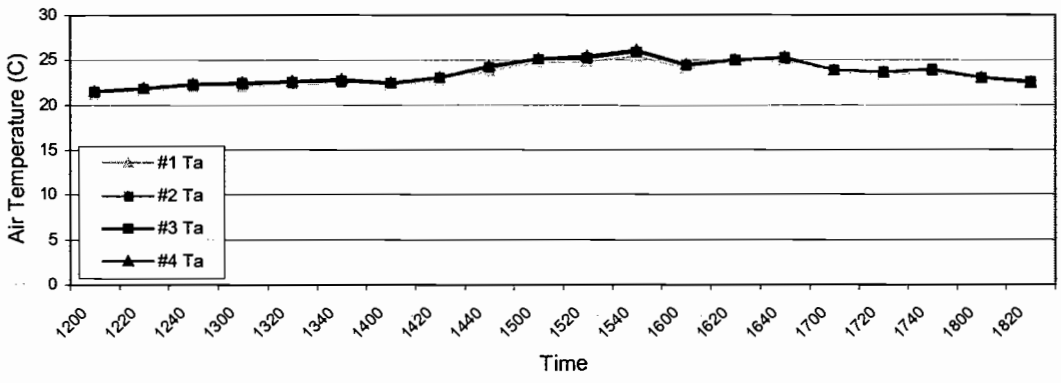

Figure 5.1. Air temperature data recorded on 7-14-98, before the start of field analysis; used to verify that all four air temperature sensors recorded consistent results.

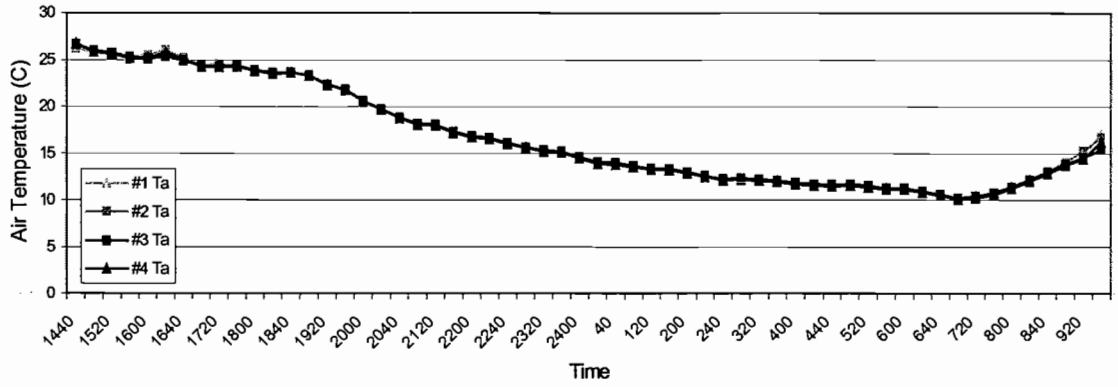

Figure 5.2. Calibration of air temperature data recorded on 9-12-98, after the completion of field analysis; used to verify that all four sensors recorded consistent results after extensive field use.

Again, it is clear that sensors provided consistent results after use in the field. In addition to the above calibration relationships, all sensor data from each site (four like sensors per site) was plotted against comparable sensors to ensure they were operating correctly and recording similar data. The fact that many measurements were taken in open meadows under clear-sky conditions made analysis simple, as these conditions favored a uniformly changing environment and many of the sensors theoretically should have been recording similar information. For example, during a clear day all air temperature sensors should have recorded similar field data; any large differences between one sensor and the rest would indicate a malfunctioning sensor. In a few instances where problems were discovered concerning the sensors, these data were eliminated from use in subsequent analysis. Overall, excellent confidence was had in the information recorded by the meteorological sensors.

The first step in the analysis of field data was to average and weight all 20-minute meteorological variables with respect to periods in which water loss was measured. For example, if pan water loss was measured from 12:13 pm to 14:14 pm, a weighted average of meteorological variables had to be calculated for this same time period. In this weighting procedure, variables measured between 12:00 pm and 12:20 pm (recorded by datalogger as 12:20 pm) were given a weight of 7/20 because only 7 minutes of its measurement interval fell within the time period of water loss measurement. Data recorded from 12:20 pm to 12:40 pm (recorded by datalogger as 12:40 pm) would receive a full weight of 20/20 because all of its minutes of measurement were included in the water loss period. Each weight was then multiplied by its respective meteorological measurements. Next, individual weighted variables were totaled and divided by the summation of the weights. Table 5.1 demonstrates this procedure for the weighting and averaging of variables.

Because the weighting procedure had to be repeated upwards of fifty times per site with a total of nine sites, there was concern with regard to potential errors. For this reason, a program was written using EXCEL© software that performed the previously described calculations. This program enabled all initial calculations to be checked a second time and any existing errors worked through. Therefore, the weighting and averaging of all meteorological variables was calculated by two procedures, resulting in a high degree of confidence in this portion of the data set.

Table 5.1. Example calculation demonstrating the weighting and averaging of meteorological variables for a hypothetical period of water loss measurement (12:13 pm to 14:14 pm).

Time	Weight	Windspeed (m/s)	Weight * Windspeed (m/s)
12:20	7/20 = 0.35	1.20	0.4
12:40	20/20 = 1.00	1.00	1.0
13:00	20/20 = 1.00	0.80	0.8
13:20	20/20 = 1.00	0.50	0.5
13:40	20/20 = 1.00	1.60	1.6
14:00	20/20 = 1.00	1.70	1.7
14:20	14/20 = 0.70	1.20	0.8
SUM	6.05		6.9
Weighted Average of Windspeed Over Period = of Evaporation Measurement			6.9/6.05 = 1.1m/s

Before relationships could be established, the vapor pressures of the air and evaporating surface had to be calculated for the period of water loss measurement. The equation used to calculate the vapor pressure of the air from the weighted and averaged air temperature and relative humidity is as follows:

$$e_a = 0.1\ [R_h\{6.11\ \exp((17.3T_a)/(T_a + 237.3))\}] \quad (5\text{-}1)$$

Where: e_a = vapor pressure of the air, kPa
R_h = relative humidity expressed as a fraction
T_a = temperature of the air, °C

Similarly, the equation used to calculate the vapor pressure of the evaporating surface from the weighted and averaged pan water temperature is as follows:

$$e_s = 0.1\ [6.11\ \exp((17.3T_s)/(T_s + 237.3))] \qquad (5\text{-}2)$$

Where: e_s = saturation vapor pressure of the air evaluated at a temperature equal to that of the water surface, kPa
T_s = temperature of the water surface, °C

The weighted averages of all meteorological variables (except wind direction) along with measurements of water loss (evaporation) and vapor pressure calculations for all periods of field research are provided in Appendix C-1.

As stated in the methods section, data that included windspeeds of 0.20 m/s were not included in subsequent analysis. Explanation of the problem associated with windspeeds of this magnitude can be found in the experimental equipment section of the study design and methods chapter under the explanation of the anemometer. All weighted and averaged data points that had significant periods of windspeed at this velocity were eliminated. This included every nighttime period, much of the data from the forested sections (particularly Site A), and some data from calmer and overcast days. Although the majority of data points were eliminated based on the wind criteria, others were discarded due to the following problems: malfunctioning sensors, animal interference, and rain. Nearly all clear-sky daytime data was preserved and fit into the regression relationships. These periods were the most important to this study simply because the largest percentage of evaporation occurred during daytime periods. Overall, fewer than 20% of the data points were eliminated leaving 363 points available for analysis.

SAS© statistical software was used to determine the most suitable form of a model relating evaporation rate to meteorological variables. Initially, all useable data (363 points) were used to fit a rich multiple regression model that included many possible

combinations of the explanatory variables (e_s-e_a, V) known to influence rates of evaporation. The following multiple regression model was tested:

Rich Model

Response variable:
Evaporation rate (E), mm/hr

Explanatory variables:
Vapor pressure deficit (e_s-e_a), kPa
Windspeed (V), m/s
Square of vapor pressure deficit [$(e_s-e_a)^2$], $(kPa)^2$
Square of windspeed (V^2), $(m/s)^2$
Vapor pressure deficit multiplied by windspeed, [$(e_s-e_a)V$], [kPa (m/s)]
Square of vapor pressure deficit multiplied by windspeed [$(e_s-e_a)^2$ V], [$(kPa)^2$ (m/s)]
Vapor pressure deficit multiplied by square of windspeed, [(e_s-e_a) V^2], [kPa $(m/s)^2$]
Square of vapor pressure deficit multiplied by square of windspeed [$(e_s-e_a)^2$ V^2], [$(kPa)^2$ $(m/s)^2$]

SAS© calculated the probability that the regression coefficient for each explanatory variable in the rich model was zero. All explanatory variables that had regression coefficients with a probability greater than 5% ($p > 0.05$) of being zero were eliminated from the model. After each variable that was not significant was eliminated, the following reduced multiple regression model was tested:

Reduced Model

Response variable:
Evaporation rate (E), mm/hr

Explanatory variables:
Vapor pressure deficit (e_s-e_a), kPa
Vapor pressure deficit multiplied by windspeed, [(e_s-e_a) V], [kPa (m/s)]

Again, SAS© calculated the probability that the regression coefficient for each variable was equal to zero. The square of the correlation coefficient and the analysis of variance F-statistic were calculated for both the full and reduced regression models. The F-statistic tests the hypothesis that all regression coefficients in the model are equal to zero. Appendix C-2 displays the stepwise determination of the evaporation model.

After determining an accurate evaporation model that suitably represented all recorded data, several graphs were produced using EXCEL© spreadsheet software. Plots demonstrating the following relationships were constructed:

1) Evaporation rate regressed individually against vapor pressure deficit, $(e_s - e_a)$
2) Evaporation rate regressed individually against vapor pressure deficit multiplied by windspeed, $[(e_s - e_a)\ V]$
3) Evaporation rate predicted by the reduced form of the evaporation model versus the actual rate of recorded evaporation
4) Residuals of the predicted versus actual evaporation rate relationship
5) Plots showing evaporation rates predicted by Equation 6-2 versus actual evaporation using data from individual sites, along with the regression line produced using the entire data set.

Next, analysis focused on between-site variation of the regression coefficients that composed the evaporation model. To begin this analysis, all 363 useable data points were divided into 18 sub-sites representing the in-stream and out-of-stream pans at each site. For each sub-site, regression coefficients were calculated (only using data collected at the sub-site) using the same form as the reduced evaporation model as determined in previous analysis (explanatory variables = $(e_s - e_a)$ and $[(e_s - e_a)\ V]$). Confidence intervals (95%) were calculated for each regression coefficient at each sub-site. Plots were developed and used to demonstrate the variability in confidence intervals for each regression coefficient between all 18 sub-sites. Also, a simple statistical test was used to

assess whether regression coefficients calculated at individual sub-sites were significantly different from those calculated using the entire data set (excluding the data linked to a sub-site of comparison). In this test, if the mean of the regression coefficient for the entire data set (excluding data from the sub-site of comparison) fell with the 95% confidence interval of the regression coefficient for the sub-site, then the means of the regression coefficients were declared equal at a 5% level of significance. If the mean regression coefficient of the larger data set fell outside the 95% confidence interval for the sub-site regression coefficient, then the means were considered unequal. Appendix C-3 displays the regression coefficients for each sub-site and provides additional information regarding the results of statistical tests.

The last analytical component concerning this objective dealt with comparing daily amounts of energy gained by solar radiation and lost by evaporation for streams along the MFJD River. For this comparison, complete days of 20-minute continuous data (i.e., midnight to midnight) were obtained from data recorded at each site. During these periods, estimations of 20-minute solar energy inputs and evaporation energy outputs were made for each pan set-up (1, 2, 3, 4) within each site.

Evaporation rates were calculated for all 20-minute periods at each location using the reduced form of the evaporation model. The following information was utilized at each pan location: air temperature, relative humidity, windspeed, and actual stream temperature (represented well by the water temperatures in Pans 1 and 3). Vapor pressures were calculated using equations 5.1 and 5.2 before actual input into the reduced form of the evaporation model. Because the model estimates evaporation rate in units of millimeters per hour of evaporation, each estimate was divided by three to provide units

of millimeters of evaporation per 20-minute period. For this amount of evaporation to be converted to units of energy, the latent heat of vaporization (LHV) had to be calculated. This term was found using the following equation:

$$LHV = 597.3 - 0.564\ (T_s) \tag{5-3}$$

Where: LHV = latent heat of vaporization, cal/g
T_s = temperature of the pan water, °C

The amount of evaporation occurring over each 20-minute interval was then converted to units of energy/area/time via the following equation:

$$H_e = 0.10\ [(LHV)\ E\ \rho] \tag{5-4}$$

Where: H_e = evaporative heat energy, cal/cm^2/time
LHV = latent heat of vaporization, cal/g
E = evaporation, mm/time
ρ = density of water, g/cm^3 (assumed to be 1)

Solar radiation (direct and diffuse beam) was estimated using the photosynthetically active radiation (PAR) measured in the field. To begin this estimation, PAR measurements were converted to units of cal/cm^2/20-minute period (from units of μmol/s/m). Next, a correction ratio, relating PAR to total solar radiation, was computed. For the purposes of this correction, incoming solar radiation was estimated every 20-minutes for a clear-sky day (7-22-98) using TEMP86, a stream temperature prediction model. Because PAR was also measured on this day in the field, a simple correction could be made that related 20-minute values of PAR and solar radiation. PAR was found to be 36% of total solar radiation (standard deviation = ± 0.4 %). With the above correction, each 20-minute value of PAR (at each pan within each site) was corrected to represent estimates of solar radiation. Resulting plots demonstrated a combination of:

continuous stream energy gains by solar radiation, losses by evaporation, and recorded stream temperatures. All plots and calculations were made using EXCEL© spreadsheet software.

5.1.2 Objective 2

Objective 2 aimed at studying the influence of channel alignment and wind direction on the amount of wind exposed to a stream water surface. Studies were especially focused on how channel incision may compound or retard the above influence. For example, it was hypothesized that streams with channels aligned perpendicular to wind direction would tend to have less wind exposed to their water surface than would channels aligned parallel to wind direction. In this case, the incision of stream channels would compound the loss of wind at the stream surface. On the other hand, if deeply incised channels were aligned parallel to wind direction, the incised reach may have a "funneling" effect and accelerate the movement of wind over the water surface.

The first step in the analysis of this objective was to compile all recorded wind direction information. Wind direction was recorded continuously throughout the duration of the day at both of the evaporation pan set-ups located outside of the stream channel, i.e., Pans 2 and 4. Analysis of wind direction data was especially critical during daytime periods when air movement was significant. Wind movement was, for the most part, non-existent during the overnight periods from 9:00 PM to 8:00 AM. For each day, wind directions were divided into blocks of similar direction and average wind directions were calculated for each block. For the value of easy comparison, averaged wind directions

were placed in general categories. The eight categories included winds out of the N, NW, W, SW, S, SE, E, and NE. Many days contained winds that occurred predominantly in one direction, so all recorded wind directions were simply averaged and an approximate wind direction was obtained. In some cases, two periods of wind movement were noticed throughout the duration of the day. These periods were separated and approximate wind directions for each period were determined.

Using the wind direction and windspeed information, individual sites were subjected to "wind analysis". This analysis included comparing and contrasting channel alignment and blocks of daily wind direction with the relative velocity of wind within and outside of the channel. For each blocked period of wind direction, average windspeed was determined for each of the pans. Over this period of time, the ratio of in-stream pan to out-of-stream pan windspeed was calculated. The average windspeed of Pan 1 was compared to Pan 2; Pan 3 was compared to Pan 4. This compilation of data allowed for site-by-site analysis of how the alignment and incision of the channel affected the wind reaching the stream surface for varying wind directions.

For analytical purposes, it was necessary to derive an estimation of the extent to which a stream water surface was exposed to wind relative to that of the adjacent floodplain surface. This estimation was based upon an equation presented by Yoshino (1975) used to predict ventilation in valleys. Although it was recognized that this equation was intended for use on larger topographic scales than incised stream channels, the elementary principles involved in an equation of this nature may be applicable at both scales. The equation presented by Yoshino (1975) did not differentiate between V-

shaped mountain valleys and those associated with erosional down-cutting on otherwise flat terrain (e.g., the Grand Canyon). Incised stream channels may represent miniature valleys of the later kind. Thus, Yoshino's formula was employed and evaluated to see if results seemed reasonable. The evaluation of Yoshino's equation is provided in Appendix E along with the definition of necessary variables. Information provided in this appendix indicates that this equation provides a reasonable representation of channel incision for a range of hypothetical stream cross-sections. Thus, Yoshino's formula was used to calculate a "Wind Exposure Index" for each location where data was collected for Study #1.

Yoshino's equation required the knowledge of several channel characteristics. As part of data collection at each site, channel cross-sections at each location were measured along with the wetted channel dimensions. From this information, the calculation of numerous channel characteristics was made through the use of FLOWMASTER© software. Channel cross-sections and various channel characteristics are provided along with the wind analysis and wind exposure indices for each location in Appendix B.

5.2 Study #2

Analysis of Study #2 corresponded to the goals of Objective 3. For each test within each experiment, water loss in the treatment pan (moving water) was expressed as a ratio of water loss in the control pan (stagnant water). Calculations were made using EXCEL© software. Results of tests and calculations are presented in appendix D.

6 – RESULTS AND DISCUSSION

The results and discussion of data analyses was divided into major categories that focused on the objectives of this study.

6.1 Study #1

6.1.1 Objective 1

A single mathematical expression that related pan evaporation to meteorological variables, measured approximately 0.5-m above the pan water surface, was successfully produced. This equation included data taken from all nine experimental sites (363 data points) and was created using stepwise regression with SAS© statistical software (Appendix C-2). This relationship is as follows:

$$E = 0.144(e_s-e_a) + 0.085[V\ (e_s-e_a)] \qquad (6\text{-}1)$$

This form of the evaporation equation was referred to as the reduced evaporation model in the data analysis section and was highly significant ($r^2 = 0.88$, $F_{2, 360} = 5572$, $p > F < 0.01$). In addition, the regression coefficients for the variables in this relationship had a very low probability ($p < 0.01$) of being zero (Appendix C-2). Figure 6.1 demonstrates the predictive power of Equation 6-1; differences between measured pan evaporation rates and those predicted by Equation 6-1 are illustrated in Figure 6.2.

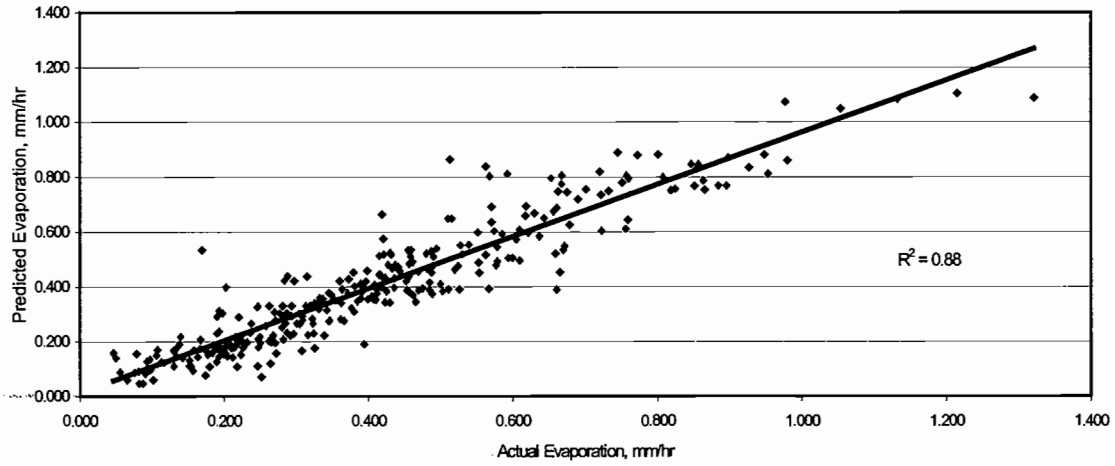

Figure 6.1. Actual measured pan evaporation rates versus those predicted by Equation 6-1 (n = 363).

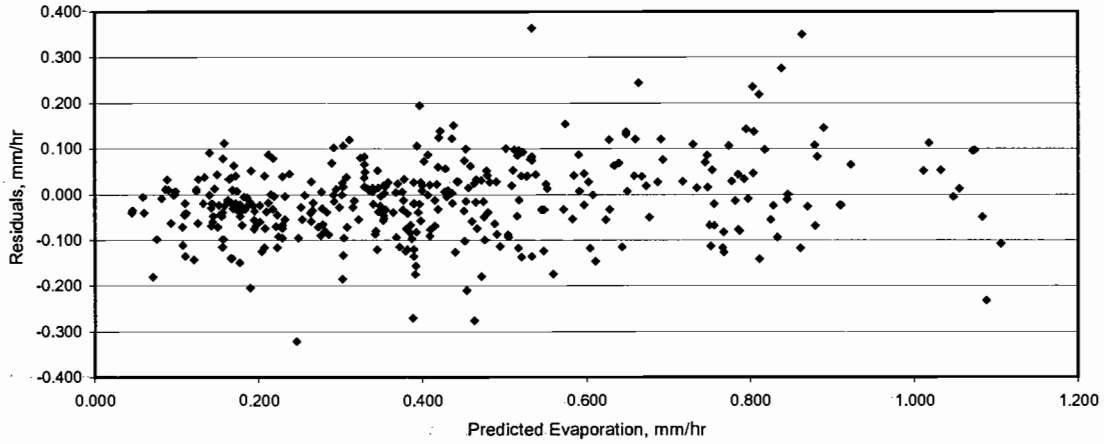

Figure 6.2. A plot of the residuals versus predicted evaporation rates using the data in Figure 6-1.

It is clear that Equation 6-1 provides an excellent representation of rates of pan evaporation from the upper Middle Fork of the John Day River. In addition, the residual

plot (Figure 6.2) tends to confirm that this multiple regression model is appropriate for the data. Plots of recorded evaporation rates versus each individual variable of Equation 6-1 (e_s-e_a, V (e_s-e_a)) can be found in Appendix C-4.

Equation 6-1 was rearranged slightly to match the form of the theoretical equations presented in the literature review. In rearranging Equation 6-1, the vapor pressure deficit (e_s-e_a) was factored out of the form yielded by the statistical software. Factoring resulted in the exact form of evaporation equation as theory had indicated, a wind function (with regression coefficients α and β) multiplied by a vapor pressure deficit (e_s-e_a). The rearranged equation for predicting evaporation with definition of terms is as follows:

$$E = [0.144 + 0.085(V)](e_s - e_a) \qquad (6\text{-}2)$$

Where E = evaporation rate of pan water, mm/hr
V = windspeed measured at 0.5-m above the pan water surface, m/s
e_a = vapor pressure of the air above the pan, calculated using the air temperature and relative humidity measured at 0.5-m above pan water surface (Equation 5-1), kPa
e_s = vapor pressure of air immediately above pan water surface, calculated using the temperature of the pan water (Equation 5-2), kPa
0.144 = α = alpha wind function regression coefficient
0.085 = β = beta wind function regression coefficient

Additional analysis shows there are minor sub-site differences in the regression coefficients α and β. As stated in the analysis section, the coefficients α and β were calculated for each of the sub-sites (in-stream and out-of-stream sub-sites within each site). The separate evaporation equations for each sub-site along with the standard errors of each regression coefficient can be found in Appendix C-3. The following figures demonstrate the variability of these coefficients between sub-sites.

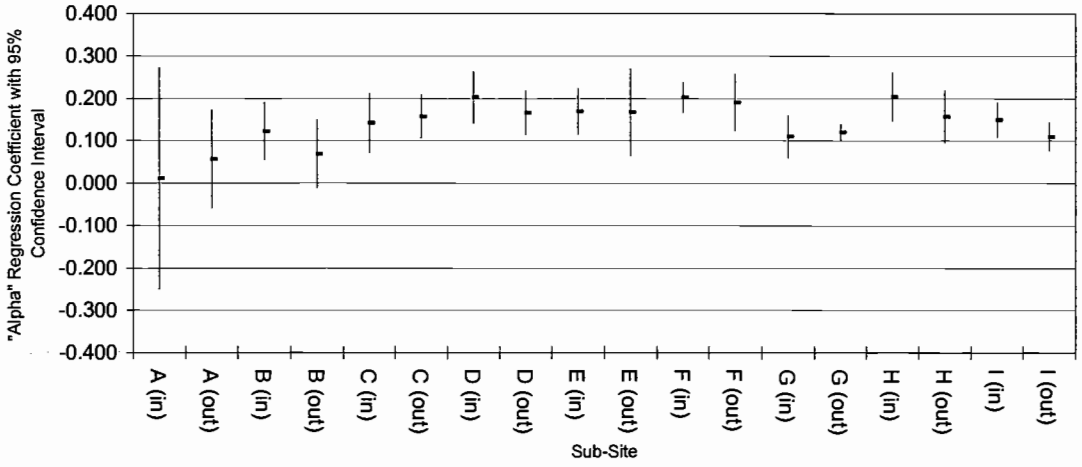

Figure 6.3. Mean estimates of the alpha (α) regression coefficients with 95% confidence intervals for each of the 18 sub-sites.

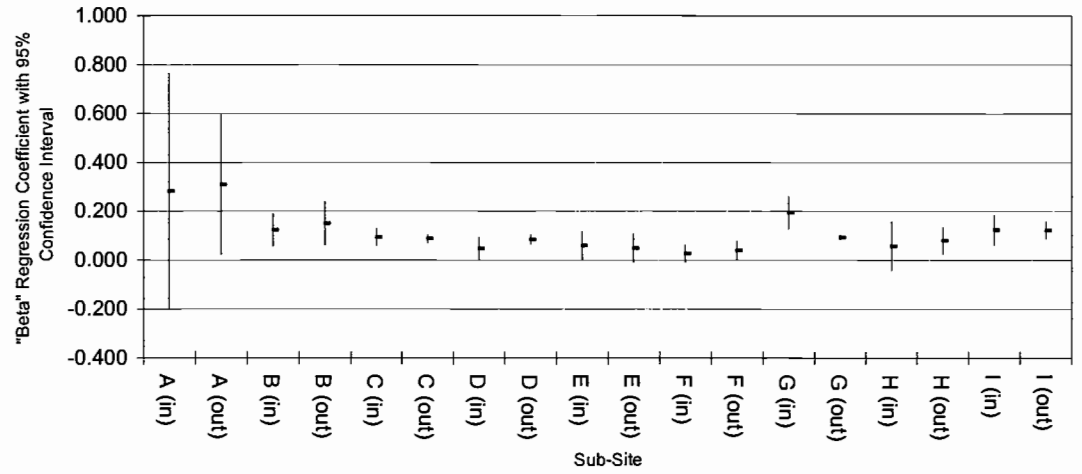

Figure 6.4. Mean estimates of the beta (β) regression coefficients with 95% confidence intervals for each of the 18 sub-sites.

A moderate degree of variation exists between sub-sites for both the regression constants α and β. Figure 6.3 and Appendix C-3 indicate that the mean estimates of the

alpha (α) regression coefficient range from 0.011 to 0.204 between sub-sites. In addition, figure 6.4 and Appendix C-3 demonstrate that mean estimates of the beta (β) regression coefficient range from 0.026 to 0.309 between sub-sites. Other researchers have also noted variation in the coefficients that compose the wind function. For example, wind function coefficients in Jobson's (1980) study varied from day to day as a suggested result of varying wind direction and meteorological conditions. Jobson's conclusions are consistent with regression coefficient variability recorded in this study.

Figures 6.3 and 6.4 are useful in the exploration of factors affecting variability in the regression coefficients. Sites A and B were located not more than 1000 meters from one another in forested sections of the MFJD River. Assuming roughly consistent meteorological regimes, both sites would be expected produce similar wind function regression constants. However, Site A yielded not only lower mean alpha (α) regression constants, but also higher mean beta (β) regression constants than observed for Site B. Information in Appendix C-1 indicates that the meteorological conditions between these sites were variable. Measurements were recorded at Site A during a predominantly overcast period, whereas those recorded at Site B involved clear-sky atmospheric conditions. During the overcast measurement period at Site A, air temperatures were moderate, relative humidity was high, and limited solar radiation prohibited the ordinary daytime warming of the land surface, which typically governed afternoon air movement (convectively driven air movement). All of these factors led to lower vapor pressure deficits and lower windspeed at Site A compared to Site B. This example indicates that the regression constants involved in evaporation relationships in forested regions may be sensitive to local atmospheric conditions.

Figures 6.3 and 6.4 are also useful in comparing the wind function regression coefficients produced in forested and meadow environments under the influence of similar atmospheric conditions. For example, Sites B, C, and D were all located within the same valley with approximately consistent meteorological conditions. However, Site B was located in a forested section of the valley in contrast to Sites C and D, which presided in open meadow regions. From figure 6.3 and 6.4, it can be seen that the mean regression coefficients between these sites varied only slightly. Data from the Site B floodplain location appear to yield slightly lower mean estimates of the alpha (α) regression coefficient than does data from the other 5 sub-sites of comparison (B_{in}, C_{in}, C_{out}, D_{in}, D_{out}). This small difference may have been a result of streamside vegetation (tall grasses, shrubs, etc.) causing the micrometeorological environment at the pans on the floodplain to vary more than those located in the stream (at Site B) or in predominantly unvegetated environments (Sites C and D). Records show that winds on the floodplain at Site B were prone to random periodic direction changes. Never the less, Figures 6.3 and 6.4 suggest that the evaporative relationships in a forested environment (at least in the stream channel) do not differ greatly from those in open meadow environments under similar atmospheric regimes.

Further inspection of Figures 6.3 and 6.4 indicates that under consistent meteorological conditions, the mean regression coefficients found in open meadow environments are generally similar. Meteorological conditions at Sites C, D, and E were quite similar: clear-sky days with gradually increasing air temperature and solar radiation, gradually decreasing relative humidity, and uniform wind direction. However, meteorological variation was recorded in each of the other four sites located in open

meadow environments (Sites F, G, H, and I) and these four sites appear to produce more variable regression coefficients than does the sites located in open meadows with non-changing meteorological conditions (Sites C, D, and E). For example, both sub-sites within Site F appear to yield slightly higher mean alpha (α) and lower mean beta (β) regression coefficients than the sub-sites within Sites C, D, and E. At Site F, extensive fluctuations in air temperature, relative humidity, solar radiation, and wind direction were noticed throughout daytime periods. It is hypothesized that the somewhat more variable meteorolgic regime witnessed at Site F resulted in regression coefficients that were somewhat different than were obtained at Sites C, D, and E. Atmospheric variability over the data measurement periods at Sites G, H, and I, much like Site F, likely contributed to regression coefficient differences between these sites and those in open meadow environments with more uniform atmospheric conditions.

Regression coefficients produced at Site E and G provide a useful comparison of sites where atmospheric conditions are similar, with the exception of daily wind direction. Both Sites E and G were located in the same valley, had similar degrees of channel incision, and experienced roughly similar daytime air temperature, relative humidity, and solar radiation regimes over their respective study periods. However, differences in wind direction were recorded between the two sites. Site E experienced relatively uniform wind direction (predominantly out of the NW) over the period of observation, where as; Site G experienced winds that varied in direction from day to day (Appendix B). From Figure 6.3, the mean alpha (α) regression coefficients calculated at Site G appear to be consistently smaller than those calculated at Site E. In addition, the mean estimate of the

beta (β) coefficient produced using the data collected from inside the stream channel at Site G appears to be somewhat larger than those calculated from the data recorded from the floodplain at Site G and both sub-sites within Site E. This would seemingly imply that the "wind term" in evaporation relationships [V (e_s-e_a)] is especially sensitive to variable wind directions in channels that are heavily incised (Site G contained some of the more incised channels in this study).

The above examples suggest that the regression coefficients α and β that comprise the evaporation relationship established in this study may be sensitive to varying climatic conditions. In particular they seem sensitive to unstable atmospheric conditions (cloudy days, etc.), especially periods with changing wind direction. It is also suggested that channel incision may compound the above influence.

Despite the fact that a moderate degree of variation exists in regression coefficients between sites, the evaporation relationship (Equations 6-1 and 6-2) established in this study generally defines the entire data set. Few regression coefficients calculated from individual sub-site data were significantly different from those coefficients calculated using all other data other than that from the sub-site of comparison (Appendix C-3). All of the sub-sites with statistically different coefficients were associated with sites containing considerable meteorologic variation (Sites F, G, H, I). Figure 6.5 displays plots of the evaporation predicted by Equation 6-2 versus the actual measured evaporation using individual data sets from each of the nine experimental sites that composed this study. Also included within each plot is the regression line relating predicted to actual evaporation calculated using the entire dataset.

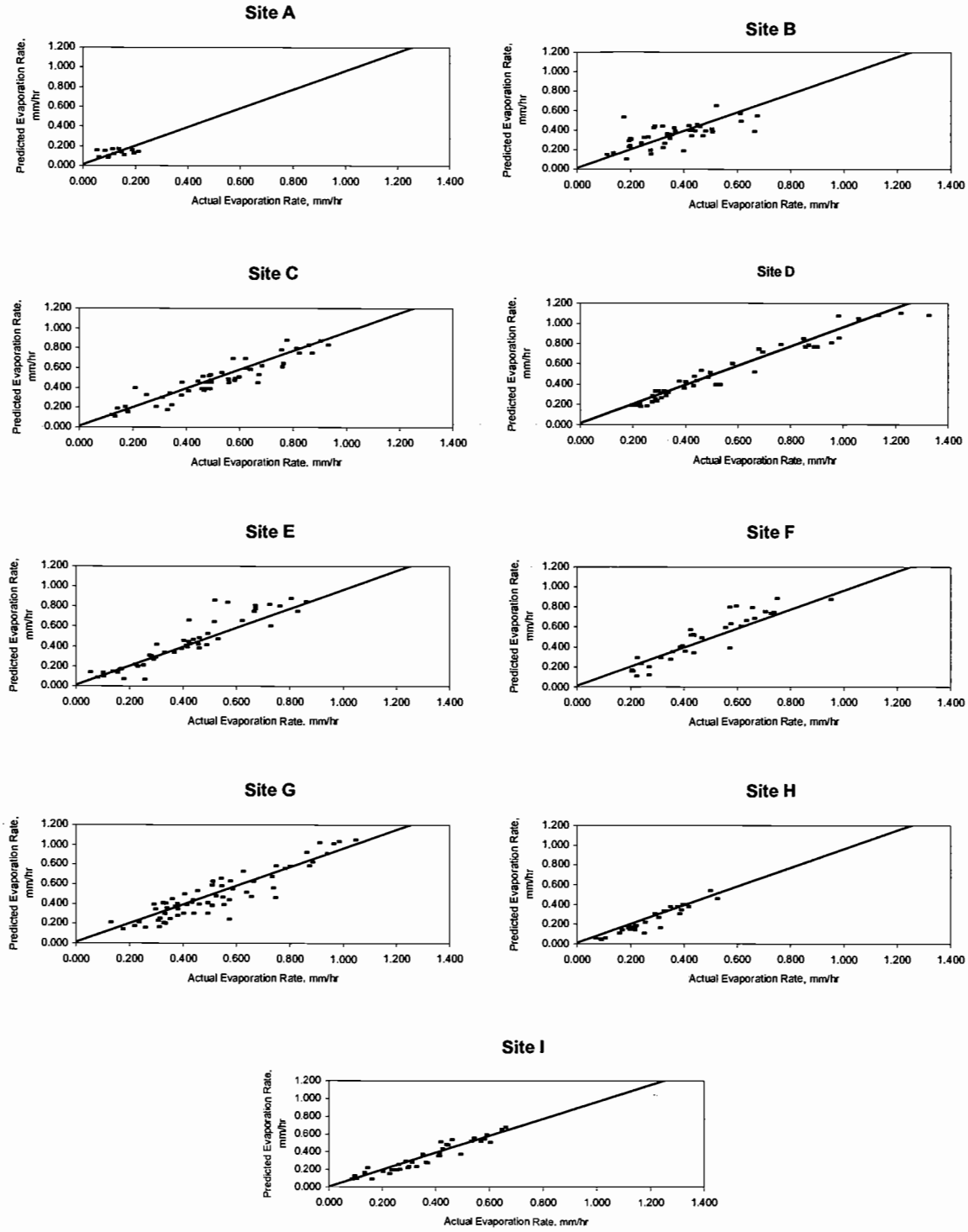

Figure 6.5. Plots of the evaporation rates predicted by Equation 6-2 versus actual recorded evaporation rates for each site along with the regression line produced using the entire data set (all nine sites, 363 points).

Equation 6-2 was used to construct comparisons of incident solar (including both direct and diffuse beam) and evaporative energy transfers over complete days at each site. Methods used for calculating the energies in this comparison are outlined in the data analysis section. Graphical representations of this analysis are demonstrated in Figures 6.6 and 6.7. These figures show three curves: the solar energy gained by the stream every 20-minutes, the energy lost from the stream by evaporation every 20-minutes, and measured stream temperature.

According to Figures 6.6 and 6.7, a common trend persists over each daytime period at Pans 1 and 2 at Site D. Specifically, it appears that stream temperatures respond rapidly to solar energy inputs, however, as the ratio of stream energy lost by evaporation to that gained by solar radiation (H_e/H_a) increases, the rate of stream temperature increase begins to slow. Stream temperatures appear to peak in mid-afternoon at approximately the point when solar radiation inputs are equalized by evaporative energy losses ($H_e/H_a = 1$), this being the point of intersection between the two curves. Finally, as the ratio of H_e/H_a increases beyond the intersection of the two curves, stream temperatures experience a general decrease. Although it is important to note that other mechanisms of heating and cooling also contribute to the temperature trends seen in Figures 6.6 and 6.7, both figures indicate that evaporation can be an important mechanism in the cooling of a stream.

Table 6.1 displays total daily wind run, evaporative energy losses, available solar radiation, time of maximum stream temperature, and the time when evaporative energy loss offsets available solar energy ($H_e/H_a = 1$) for streams at the location of each pan.

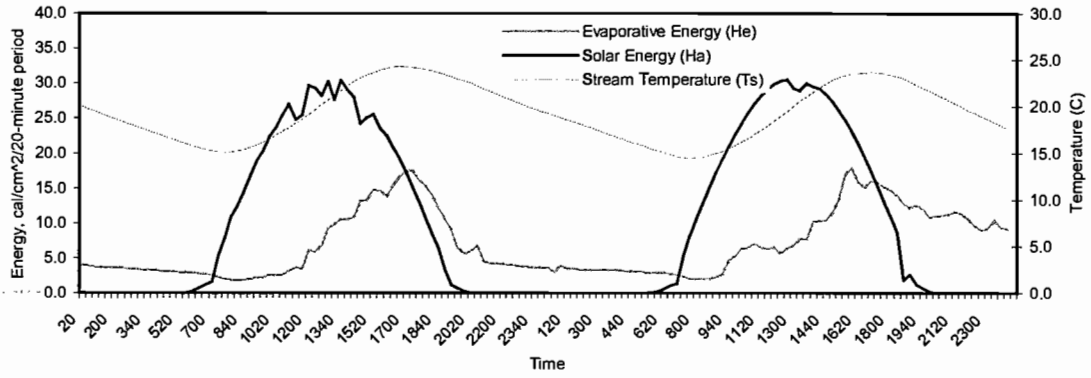

Figure 6.6. Plot of available solar energy (H_a) and evaporative energy (H_e) lost from the stream every 20-minutes, in addition to stream temperature, at Pan 1 (Site D) from August 14, 1998 to August 15, 1998.

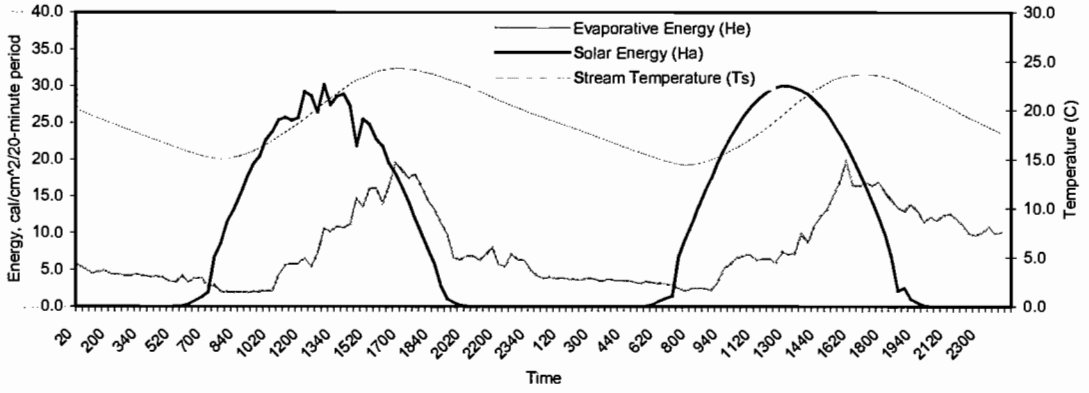

Figure 6.7. Plot of available solar energy (H_a) and evaporative energy (H_e) lost from the stream every 20-minutes, in addition to stream temperature, at Pan 2 (Site D) from August 14, 1998 to August 15, 1998.

Table 6.1. Total daily (midnight to midnight) wind run, evaporative energy (H_e) losses, available solar energy (H_a), time of daily maximum stream temperature, and time when evaporative energy loss offsets available solar energy ($H_e/H_a = 1$) for stream sections along the MFJD River.

Site	Pan	Date	Wind Run (Km)	Daily Evaporation Energy (He) (cal/cm^2/d)	Daily Solar Energy (Ha) (cal/cm^2/d)	He/Ha	Time of Max. Stream Temp.	Time When He/Ha = 1
A	1	20-Aug	19	189	263	0.72	1340	1320
	2	20-Aug	7	180	170	1.05	1400	1500
	3	20-Aug	14	190	230	0.83	1300	1300
	4	20-Aug	12	190	66	2.88	1300	1240
B	1	12-Aug	23	307	498	0.62	1700	1520
	2	12-Aug	27	306	443	0.69	1700	1500
	3	12-Aug	19	309	375	0.83	1720	1420
	4	12-Aug	27	335	453	0.74	1700	1500
C	1	17-Aug	130	433	749	0.58	1700	1740
	2	17-Aug	189	530	742	0.71	1640	1700
	3	17-Aug	97	395	658	0.60	1640	1720
	4	17-Aug	183	536	770	0.70	1640	1640
D	1	14-Aug	80	450	728	0.62	1640	1700
	2	14-Aug	124	518	715	0.72	1640	1640
	3	14-Aug	41	365	630	0.58	1620	1700
	4	14-Aug	124	536	738	0.73	1620	1600
	1	15-Aug	154	546	748	0.73	1700	1720
	2	15-Aug	176	585	737	0.79	1700	1700
	3	15-Aug	65	387	644	0.60	1640	1720
	4	15-Aug	172	597	760	0.78	1640	1620
E	1	22-Jul	26	339	809	0.42	1720	1900
	2	22-Jul	56	420	839	0.50	1720	1820
	3	22-Jul	30	362	755	0.48	1620	1820
	4	22-Jul	54	429	877	0.49	1620	1800
	1	23-Jul	11	157	228	0.69	1840	1920
	2	23-Jul	22	170	252	0.67	1840	2000
	3	23-Jul	9	162	215	0.76	1800	1900
	4	23-Jul	20	177	263	0.67	1800	1900
F	1	26-Jul	28	211	487	0.43	1840	1920
	2	26-Jul	38	216	479	0.45	1840	1900
	3	26-Jul	10	199	437	0.45	1800	1820
	4	26-Jul	32	221	494	0.45	1800	1820
	1	27-Jul	34	282	633	0.45	1840	1900
	2	27-Jul	52	315	622	0.51	1840	1840
	3	27-Jul	16	255	571	0.45	1800	1800
	4	27-Jul	44	314	649	0.48	1800	1800
G	1	3-Aug	18	296	776	0.38	1720	1820
	2	3-Aug	37	345	802	0.43	1720	1840
	3	3-Aug	13	300	724	0.41	1700	1800
	4	3-Aug	29	340	829	0.41	1700	1800
	1	4-Aug	31	340	771	0.44	1700	1820
	2	4-Aug	91	480	798	0.60	1700	1720
	3	4-Aug	36	369	723	0.51	1640	1720
	4	4-Aug	83	480	826	0.58	1640	1700
H	1	7-Sep	20	103	373	0.27	1540	1740
	2	7-Sep	41	128	370	0.35	1540	1740
	3	7-Sep	15	115	337	0.34	1500	1700
	4	7-Sep	40	139	384	0.36	1500	1700
I	1	4-Sep	32	248	607	0.41	1600	1800
	2	4-Sep	38	273	604	0.45	1600	1740
	3	4-Sep	9	206	517	0.40	1520	1640
	4	4-Sep	39	287	624	0.46	1520	1640
	1	5-Sep	20	224	626	0.36	1620	1800
	2	5-Sep	33	264	623	0.42	1620	1800
	3	5-Sep	7	199	533	0.37	1540	1640
	4	5-Sep	24	257	642	0.40	1540	1700

From Table 6.1 it can be seen that the daily wind run on August 15, 1998 for Pans 1 and 2 (Site D) was somewhat larger than that seen on August 14, 1998. The larger wind run resulted in larger daily amounts of evaporation on August 15, 1998. Because solar radiation was approximately consistent between these dates, increased evaporative energy losses resulted in larger ratios of H_e/H_a on August 15, 1998 as compared to August 14, 1998. In general, on days of clear-sky atmospheric conditions, regions that experience the most wind (larger wind run) have the highest ratio of H_e/H_a.

Total daily amounts of solar and evaporative energy were determined for each pan (e.g., the area under the curves in Figures 6.6 and 6.7). Using the pans and sites represented in Figures 6.6 and 6.7 as an example, total evaporative losses on August 14, 1998 were 62% (H_e/H_a * 100%) of the solar energy available to the stream at Pan 1 (Site D) and 72% at Pan 2 (Site D). Similarly, total evaporative losses on August 15, 1998 were 73% of the solar energy available to the stream at Pan 1 (Site D) and 79% at Pan 2 (Site D).

In addition, according to Table 6.1, over 64% of stream temperatures were at their maximum within 1 hour of the time when evaporative energy losses offset available solar energy ($H_e/H_a = 1$).

The last result associated with this objective dealt with comparing the equation presented in this study with other equations used to predict evaporation rates from open channels. Several days of meteorological data recorded at Site D were used as input to the following evaporation relationships:

1) Equation 6-2 presented in this study
2) Equation 3-3 presented in Jobson (1980)
3) Equation 3-5 presented in Krajewski et al. (1982)

Windspeeds recorded at Site D were adjusted to accommodate the suggested measurement heights of wind velocities for use in Equations 3-3 and 3-5. Krajewski et al. (1982) suggested that wind velocity be measured directly above the water surface for use in Equation 3-5. A height of 0.05-m (5-cm) was chosen as suitable to represent 'directly over the water surface.' Jobson's equation (3-3) was derived using wind velocities recorded at 4.0-m above the water surface. Therefore, wind velocities recorded at Site D were adjusted from an initial measurement height of 0.5-m to 0.05-m and 4.0-m for windspeed input into Equations 3-5 and 3-3, respectively. Windspeed adjustments assumed that 0.15-m grass was the predominant surface that wind was moving over within the valley at Site D. Adjustments were made using Equations 3.36, 3.37, and 3.38 presented in Jones (1992). Air temperature and relative humidity measurements recorded at Site D were not corrected for the measurement heights suggested for use in Equations 3-3 and 3-5. Jobson (1980) indicated that corrections were not needed for the heights of measurement of variables relating to vapor pressures when using time periods of one day or less. Therefore, it was assumed that the measurement height of air temperature and relative humidity had little effect upon the coefficients in the wind function. Figure 6.8 demonstrates how each of the above equations (adjusted for windspeed measurement heights) predicts evaporation rates on a stream using recorded meteorological information from this study.

Figure 6.8 indicates that the predictive methods provided in this study and by Jobson (1980) estimate very similar rates of evaporation at Site D. However, the equation

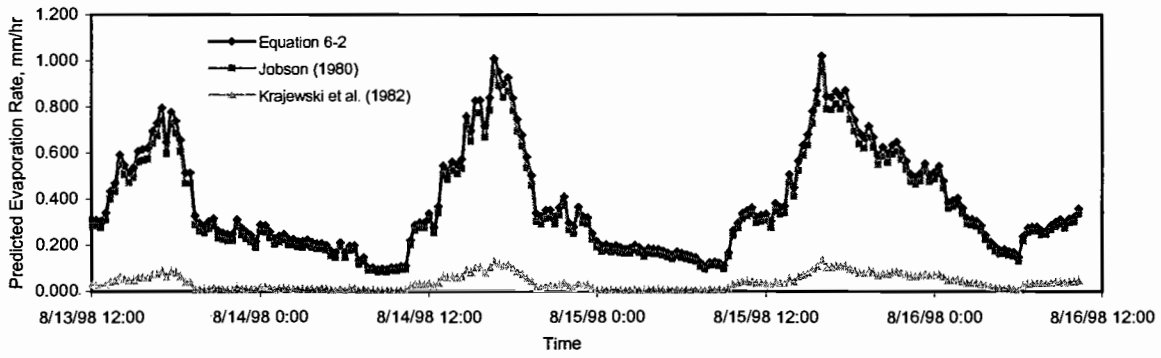

Figure 6.8. Comparison of the evaporation rates predicted by several recognized equations using meteorological information recorded at Site D from 8-13-98 to 8-16-98.

presented by Krajewski et al. (1982), which assumed the alpha (α) regression coefficient to be zero, provides much lower estimates of evaporation rates relative to the other two methods. This equation essentially implies that if wind movement is nonexistent then rates of evaporation are also nonexistent regardless of any existing vapor pressure deficit (see page 14). Therefore, this estimator only responds during periods of air movement. Even then, it appears to seriously underestimate evaporation rates.

Evaporation rates predicted by the equation presented in this study and that obtained from Jobson (1980) are very similar. The equations for these methods of evaporation rate prediction, in exactly the same form with uniform units, are as follows:

Jobson's Equation: $E = (0.125 + 0.047V)(e_s - e_a)$
Equation 6-2: $E = (0.144 + 0.085V)(e_s - e_a)$

Where E = evaporation rate, mm/hr
V = windspeed, m/s
e_a = atmospheric vapor pressure, kPa
e_s = vapor pressure of evaporating surface (water), kPa

Comparison of the above equations validates the hypothesis proposed by Dingman (1994) that the regression coefficients (α and β) vary in accordance with the measurement height of windspeed. Atmospheric conditions in this study were measured at 0.5-m, where as, Jobson (1980) recorded conditions at 4.0-m above the water surface. Once windspeed values recorded at 0.5-m are adjusted for the measurement height used in Jobson's study (4.0-m), both equations produce very similar estimates of evaporation rates throughout the period of measurement at Site D.

Similarity between Equations 6-2 and Jobson's (3-3) indicate that evaporative mechanisms are consistent for aridland environments. Jobson's evaporation model was produced from data collected along the San Diego Aqueduct in aridland California. Likewise, data used in the production of Equation 6-2 was recorded in arid northeastern Oregon. Both equations were produced from different locations of the U.S. (with similar climatic regimes), but yielded similar estimates of evaporation rates. The application of Equation 6-2 and/or Jobson's Equation to less extreme environments is uncertain. However, comparison of regression coefficients derived at sites in this study that experienced relatively humid conditions indicate a potential for application to environments other than aridlands.

The comparison of wind function regression coefficients at Sites C and D suggest that evaporation relationships may not differ largely between arid and more moderate climatic regions during periods of clear-sky atmospheric conditions. Throughout the study period at Site C, both daily maximum air temperature and minimum relative humidity were moderate ($T_{a(max)}$ = 22-24°C, $R_{h(min)}$ = 30-40%). It is assumed that the meteorological conditions experienced at this site are representative of clear-sky summertime

atmospheric conditions in moderate environments (i.e., western Oregon). Throughout the study period at Site D, maximum air temperature and minimum relative humidity were more extreme ($T_{a(max)}$ = 32-35°C, $R_{h(min)}$ = 18-21%). The meteorological conditions at Site D are characteristic of clear-sky summertime atmospheric conditions in aridland environments. From Figures 6.3 and 6.4, the wind function coefficients produced at Sites C and D are very similar. Although this example suggests that Equation 6-2 may be applicable to environments other than only aridlands during summertime conditions, caution must be taken until validated by additional research.

6.1.2 Objective 2

This objective studied the influence of channel alignment, channel incision, channel topography, and wind direction on the availability of wind at a stream water surface in an open meadow with little streamside vegetation. The results associated with the analysis of this objective are presented on a site-by-site basis. Sites C, D, E, F, G, and I represent the study group for this analysis. Forested Sites A and B were excluded from this analysis primarily because of the potential sheltering effects of the vegetation. Site H was not included in this analysis due to the presence of high levels of sagebrush, which generally had a large influence on the movement of air near a stream. Overall, vegetation at Sites A, B, and H influenced air movement near the stream more so than did channel alignment, incision, and topography.

6.1.2.1 SITE C, CASE STUDY

Stream channels for locations at Site C were aligned identically to wind direction, but each contained varying magnitudes of channel incision. Data was recorded at Site C during a period of intense daytime winds moving in a uniform direction (see Appendix B). Channels at both locations were aligned in an N←S direction (arrow indicates direction of flow) with daytime winds that originated from the NW. The channel cross-section at the location of Pans 1 and 2 had a high Wind Exposure Index (low degree of channel incision, Appendix E). The channel cross-section at the location of Pans 3 and 4 had a lower Wind Exposure Index (higher degree of channel incision, Appendix E). From Appendix B, the ratio of wind reaching the stream to that reaching the floodplain surface ($V_{in\text{-}stream}/V_{out\text{-}of\text{-}stream}$) was lower at the location of Pans 3 and 4 relative to that calculated for the location of Pans 1 and 2. In-stream Pan 1 experienced an average of 74% [($V_{in\text{-}stream}/V_{out\text{-}of\text{-}stream}$) * 100%] of the windspeed that was recorded on the floodplain surface. In contrast, in-stream Pan 3 experienced an average of 57 % of the windspeed that was recorded on the floodplain surface.

These results indicate a limited ability of wind to penetrate into incised stream channels to the stream water surface. Because the movement of wind plays a dominant role in the process of evaporation (Equation 6-1, 6-2), the result of limited wind movement at the stream surface is a reduction of cooling potential.

6.1.2.2 SITE D, CASE STUDY

Channels within locations at Site D had similar low levels of channel incision (high WEI), but were aligned much differently with respect to wind direction. Data was recorded at Site D during a period of medium wind moving in a uniform NW direction (Appendix B). The channel at the location of Pans 1 and 2 was aligned parallel to wind direction (NW←SE). The channel at the location of Pans 3 and 4 was aligned perpendicular to mean wind direction (NE←SW). From appendix B, it can be seen that the ratio of wind movement ($V_{in\text{-}stream}/V_{out\text{-}of\text{-}stream}$) is much lower at the location of Pans 3 and 4 relative to that at Pans 1 and 2. An average of 90% of the wind velocity experienced at the floodplain surface was recorded at in-stream Pan 1. In contrast, an average of less than 42% of the wind velocity experienced on the floodplain reached in-stream Pan 3.

This example indicates that the alignment of a stream channel with respect to wind direction is a very relevant factor in determining the amount of wind reaching a stream at even low levels of channel incision (high WEI). It is hypothesized that the effect seen in the above example would be magnified at larger levels of channel incision (lower WEI). This example implies that channel incision may have a greater influence on the cooling of streams at locations that are highly sinuous as compared to locations where streamflow is predominantly in the direction of valley orientation (wind direction).

6.1.2.3 SITE E, CASE STUDY

At Site E, stream channels at both locations of pans had similar high levels of incision (low WEI), but were aligned somewhat differently. The channel at the location of Pans 1 and 2 was aligned in a NE←SW direction; where as, the channel at the location of Pans 3 and 4 was aligned in a NW←SE direction. Daytime wind direction at this site was predominantly out of the NW, however, one period of data contained winds originating from the NE. When winds were out of the NW (4 periods), an average of 49% [($V_{in\text{-}stream}/V_{out\text{-}of\text{-}stream}$) * 100%] of the wind movement recorded on the floodplain was measured at in-stream Pan 1. However, during the period of NE winds, an average of 82% of the wind recorded at the floodplain was recorded at in-stream Pan 1. The location of Pans 3 and 4 was bordered on one side by a channel aligned in a NW←SE direction and on the other side by a channel aligned in a NE←SW direction. At this location, a difference in wind direction from NE to NW made little difference (56% to 60% reaching Pan 1 relative to the floodplain) in the amount of wind reaching the stream.

The results from this site again indicate that the alignment of a stream channel with respect to wind direction can be an important variable when attempting to determine the effects of wind upon evaporative heat loss from streams.

6.1.2.4 SITE F, CASE STUDY

At Site F, stream channels associated with pan locations had similar high levels of channel incision (low WEI), but were aligned somewhat differently. The channel at the location of Pans 1 and 2 was aligned in an NW←SE direction; whereas the channel at the

location of Pans 3 and 4 was aligned in an N←S direction. Winds at this location were consistently out of the west. At this site, variations in channel topography created a notable difference in the ratio of wind movement ($V_{in\text{-}stream}/V_{out\text{-}of\text{-}stream}$) between the locations of both sets of pans. Channel cross-sections plotted for each location (Appendix B) show that the slopes of the west stream banks differ between locations. At the location of Pans 1 and 2, the west bank gradually slopes downward from the floodplain to the stream water surface. In contrast, the west stream bank at the location of Pans 3 and 4 contained a very steep sidewall. In the previous case, wind had a greater opportunity to follow the stream bank to the stream water surface. In the later case, the steep sidewall promoted the movement of wind over the incised channel to the opposite floodplain surface, instead of toward the stream. From Appendix B, the ratio of wind movement ($V_{in\text{-}stream}/V_{out\text{-}of\text{-}stream}$) was much higher at the location of Pans 1 and 2 relative to Pans 3 and 4. Wind velocities at in-stream Pan 1 averaged 76% of that measured on the adjacent floodplain. In contrast, an average of less than 30% of the wind velocity experienced at the floodplain reached in-stream Pans 3.

This example indicates that (in addition to channel incision) the local topography of the channel bank in the direction of wind movement can influence the availability of wind to a stream. In general, gently sloping stream banks allow greater wind movement at the stream, where as steep stream banks tend to retard wind movement within the channel.

6.1.2.5 Site G, Case Study

Stream channels at both locations of pans at Site G had very high levels of channel incision (low WEI), but were aligned much differently. The channel at the location of Pans 1 and 2 was aligned in a NW←SE direction, where as, the channel at Pans 3 and 4 was aligned in a NE←SW direction. Data was recorded at Site G during a period of moderately intense wind that varied in direction from day to day. Wind data at this site was quite erratic which prohibited detailed comparisons between locations. However, this site did provide useful information that reinforced the results discovered at Site D.

One period of winds that originated from the NW enabled the between location comparison of channels aligned parallel and perpendicular to wind direction with relatively high levels of incision (low WEI). Wind out of the NW moved approximately parallel to the channel at the location of Pans 1 and 2 and perpendicular to that of Pans 3 and 4. During this block of wind direction, 52% of the wind movement experienced at the floodplain was recorded near the stream at Pan 1 (parallel). In contrast, only 36% of the wind experienced at the floodplain was recorded near the stream surface at the location of Pan 3 (perpendicular). These results support a hypothesis proposed for Site D, that increasing levels of incision (concerning stream channels aligned perpendicular to wind direction) may increasingly reduce wind movement in the channel.

6.1.2.6 SITE I, CASE STUDY

Site I was located within a second order tributary to the MFJD River. At this site, stream channels at both locations of pans were aligned identically, but had different levels of incision (WEI). Both stream channels were aligned in a NW←SE direction. The channel at the location of Pans 1 and 2 was moderately incised; where as, the channel at the location of Pans 3 and 4 was extremely incised. Winds at Site I originated from the NW for three full days of study and from the SE for one day of study. When winds were out of the NW, an average of more than 72% of the wind velocity recorded at the floodplain reached in-stream Pan 1. In contrast, an average of less than 35% of the wind velocity experienced at the floodplain was recorded for in-stream Pan 3. When winds originated from the SE, 91% of the wind experienced at the floodplain reached the stream at the location of Pan 1. However, at Pan 3, only 25% of the wind recorded on the floodplain was experienced near the stream. These results indicate that channel incision (at least on smaller streams) can effectively regulate the amount of wind reaching the stream even at locations where the wind direction and stream channel are aligned.

The last component of this objective dealt with creating a visual representation of the impact of channel incision on evaporative potential. For this representation, graphs identical to Figures 6.6 and 6.7 were created for Pans 3 and 4 at Site D. Pan 3 (at Site D) was located in a moderately incised stream channel that was aligned perpendicular to wind direction. Pan 4 (at Site D) presided on the floodplain directly adjacent to Pan 3. Figures 6.9 and 6.10 display the profiles of solar and evaporative energy for Pans 3 and 4 from August 14, 1998 to August 15, 1998.

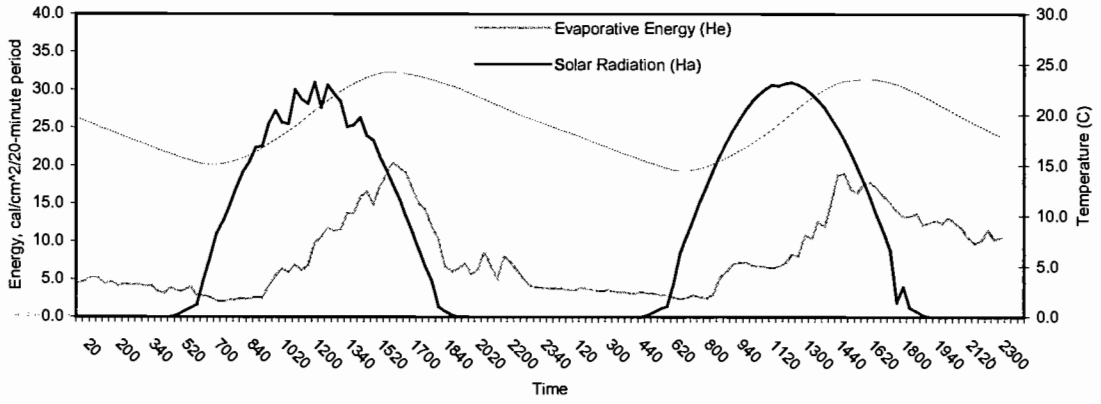

Figure 6.9. Plot of available solar energy (H_a) and evaporative energy (H_e) lost from the stream every 20-minutes, in addition to stream temperature, at Pan 4 (Site D) from August 14, 1998 to August 15, 1998.

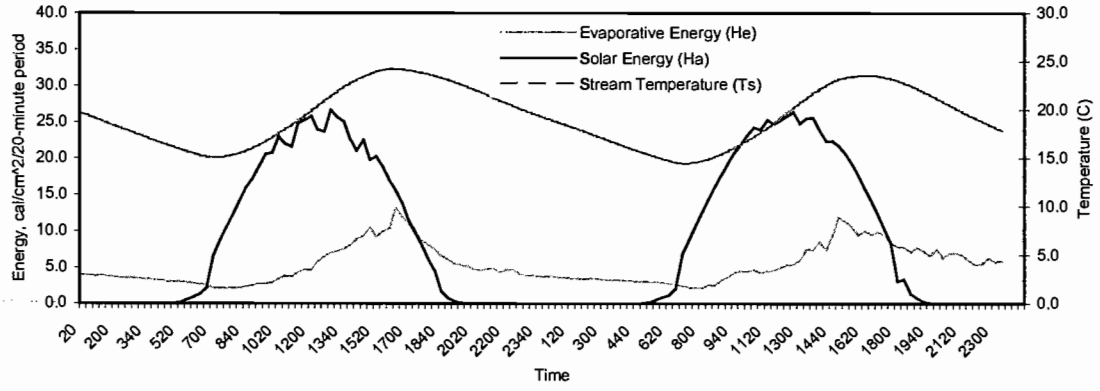

Figure 6.10. Plot of available solar energy (H_a) and evaporative energy (H_e) lost from the stream every 20-minutes, in addition to stream temperature, at Pan 3 (Site D) from August 14, 1998 to August 15, 1998.

From visual comparison of Figures 6.9 and 6.10, it can be seen that evaporative energy losses are dampened at Pan 3 (incised) relative to Pan 4 (floodplain). At Pan 3 on August 14, 1998, 365 cal/cm^2/d of energy was lost by evaporation as compared to 536

cal/cm^2/d for Pan 4. Similarly, on August 15, 1998, 387 cal/cm^2/d of energy was lost by evaporation as compared to 597 cal/cm^2/d for Pan 4. Differences in daily evaporation between pans can be attributed to lesser wind (see wind run, Table 6.1) reaching the stream surface at Pan 3 relative to Pan 4 (at Site D). These results indicate that channel incision on the MFJD River can reduce the capability of a stream reach to cool by evaporation, which, in turn, may adversely influence peak water temperatures.

6.2 Study #2

The intent of this study was to fulfill objective 3, which focused on determining the influence of water velocity/turbulence on rates of evaporation. Because all evaporation rates in Study #1 were recorded for stagnant water inside evaporation pans, it was desired to derive a correction that adjusted stagnant water evaporation rates for varying levels of water movement. The results of this study are divided into three parts that represent performed experimental tests. A detailed description of the equipment and procedures used in this study can be found in the study design and methods and data analysis sections of this paper.

6.2.1 Test #1

This experimental test was performed under the following laboratory conditions: vapor pressure deficit $\approx$ 1 kPa, windspeed = 0 m/s. Three different sub-tests were performed under the above conditions. The water velocity of the treatment evaporation pan was the only variable between sub-tests. Figure 6.11 graphically demonstrates the

results of Test #1 (Appendix D). Figure 6.11 indicates a strong relationship between water movement and percent increase in evaporation from a moving water body relative to a non-moving water body. According to this relationship, there is a significant difference between evaporation rates measured in moving water and those measured in stagnant water. This difference increases at a decreasing rate with increasing water movement (velocity). For example, a 49% average increase in evaporation was recorded in water moving between 0.03-0.06 m/s, where as, a 127% average increase in evaporation was recorded in water moving between 0.27-0.30 m/s.

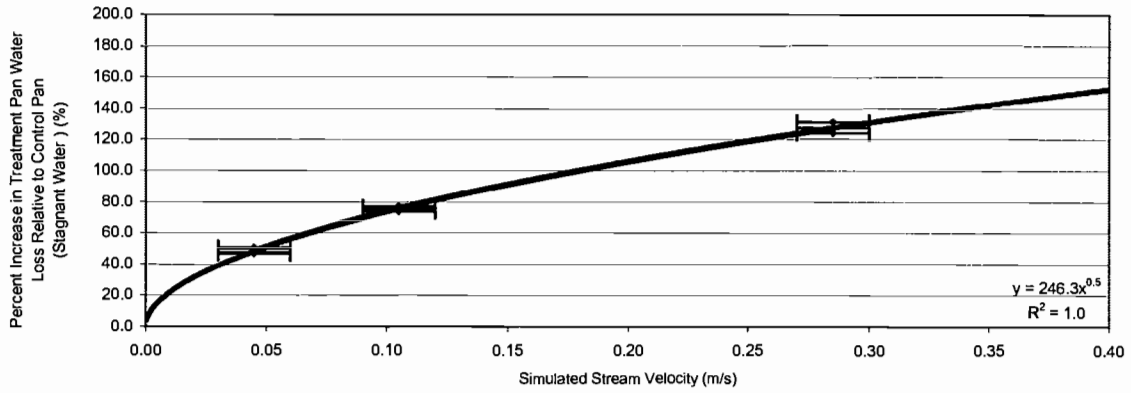

Figure 6.11. Percentage increase in water loss from a moving body of water as compared to that from a stagnant body of water, shown as function of the velocity of the moving water body (experimental conditions: e_s-$e_a \approx 1$ kPa, V = 0 m/s).

6.2.2 Test #2

The intent of Test #2 was to certify if the relationship discovered in Test #1 was identical at the following laboratory conditions: vapor pressure deficit ≈ 2 kPa,

windspeed = 0 m/s. This experimental test was conducted at only one simulated stream velocity, 0.12-0.18 m/s.

Results from this test were quite different from those seen in Test #1. From figure 6.11, an evaporation pan with a simulated velocity of between 0.12-0.18 m/s would be expected to produce 90% more water loss than a pan with non-moving water under constant meteorological conditions (e_s-$e_a \approx 1$ kPa, V = 0 m/s). However, the same simulated stream velocity produced only 9% more water loss than did a stagnant pan under the meteorological conditions of Test #2 (e_s-$e_a \approx 2$ kPa, V = 0 m/s). It should be emphasized that the only difference between the above examples was the vapor pressure deficit. Test #1 had a vapor pressure deficit of approximately 1 kPa, where as, Test #2 had a vapor pressure deficit of approximately 2 kPa. Results from this test indicate that increasing vapor pressure deficits reduce differences in evaporation rates recorded between moving and stagnant water.

6.2.3 Test #3

The intent of Test #3 was to determine the impact of a slight wind blowing over the surface of both the treatment and control evaporation pans. Test #3 exactly copied the experimental design and conditions of Test #1, but added a slight wind of approximately 0.3 m/s over the surfaces of both pans (e_s-$e_a \approx 1$ kPa, V $\approx$ 0.3 m/s). The simulated water velocity in this test was 0.12-0.18 m/s. Results from this study were again quite different from those recorded in Test #1. At a simulated stream velocity of 0.12-0.18 m/s, Test #1 indicted a water loss increase of 90% in the treatment pan (moving water) relative to the control pan (stagnant water). By adding a slight wind over the surfaces of both pans in

Test #3, only a 19% increase in water loss was recorded in the treatment pan compared to the control pan. Results from this experimental test indicate that the presence of wind vastly reduces differences in evaporation rates recorded between moving water and non-moving water.

The combined results from Study #2 suggest that differences in evaporation rates associated with moving water (relative to stagnant water) are significant for conditions of low vapor pressure deficit and no wind movement. However, as vapor pressure deficits increase and/or wind movement occurs near the water surface, differences in evaporation between moving and stagnant water become much less prominent. These results make the establishment of an evaporation rate correction factor for moving water very difficult. It would be essential that a correction factor be based not only upon the velocity of the water body, but also upon the average vapor pressure deficit and wind velocity recorded during any particular period of evaporation rate measurement. Because Study #2 did not involve the testing of numerous vapor pressure deficits and wind velocities, a correction factor for evaporation rates recorded in Study #1 could not be accurately derived. For appropriate evaporation rate corrections to be made, a more detailed examination similar to Study #2 would be essential. Also, it may be important to not only look at the velocity of the water at a stream section, but also at the direction of stream flow in relation to the direction of wind movement. For example, in the event that a stream was moving exactly opposite to wind movement, evaporation rates may be influenced more than if the two were moving in similar directions. This is the case in much of the west, daytime up valley winds.

Much of the meteorological data used in the production of Equation 6-2 was recorded during periods in which conditions equaled or exceeded those in Test #3 (e_s-$e_a \approx 1$ kPa, V ≈ 0.3 m/s). Over 94% of all data used in Equation 6-1(6-2) contained windspeeds greater than 0.3 m/s, of these data points 79% contained vapor pressure deficits of more than 1 kPa. Overall, most of the data used in Study #1 had windspeeds and vapor pressure deficits that were similar to tests #2 and #3 of Study #2. During these tests only small increases in treatment pan evaporation were recorded in comparison to control pan evaporation. However, because some data used in Study #1 contained meteorological information similar to that in Test #1, it can only be safely assumed that the evaporation rates predicted by Equation 6-2 are underestimates of the evaporation that would have occurred in an actual stream with moving water. However, it is expected that Equation 6-2 only slightly under estimates evaporation from the MFJD River, especially during periods of moderate to intense wind and vapor pressure deficits.

The following hypothesis is proposed in explanation of the differences noted between tests in Study #2:

> At the low vapor pressure deficit seen in Test #1, evaporated water vapor tended to accumulate above the surface of the control pan (stagnant water). This excess water vapor tended to reduce the vapor pressure deficit above the water surface and ultimately restrict rates of evaporation. However, water movement in the treatment pan (moving water) created enough micro-movement between the water surface and air to efficiently disperse lingering water vapor. In this case, the difference noted in evaporation rates between the treatment and control pans was very prominent. In Test #2, a steep vapor pressure deficit allowed less water vapor to accumulate over the control pan. The steeper vapor pressure deficit created increased motivation for water vapor molecules to not linger above the water surface. The slight wind introduced in Test #3 also prohibited the ponding of water vapor over the control pan. In these cases, differences noted in evaporation rates between treatment and control pans were minor.

7 - CONCLUSIONS

In northeastern Oregon, high stream temperatures are common during the summer months of the year (Boyd 1996, Hopson 1997, Torgersen 1997). Even so, evaporation is an important mechanism enabling a water body to dissipate energy. The research described in this study provides new information concerning the magnitude of evaporation and factors affecting evaporation from river and stream environments. This is the first known study to date that has used a mass-transfer approach for determining evaporation from a stream. By measuring evaporation loss along with each variable contributing to the evaporation process, a Dalton-type equation (Equation 3-1) was produced that can be used to predict evaporation from streams.

The evaporation relationship developed in this study (Equation 6-2) was statistically significant ($r^2 = 0.88$, $F_{2, 360} = 5572$, $p > F = 0.01$, $n = 363$). Using equation 6-2, evaporation can be easily estimated at a stream location by measuring windspeed, air temperature, relative humidity, and stream temperature. Inexpensive measurement equipment is available that records all of the above meteorological variables. For example, TRI-SENSE© makes a single instrument that accurately measures temperatures, relative humidity, and air velocity. The establishment of this equation also provides stream temperature models with a critical component that was otherwise lacking.

Additional research has focused on studying the influence of water movement on evaporation rates. Studies have shown that evaporation rates are notably accelerated in

moving water relative to non-moving water (i.e., 90% increase @ 0.12-0.18 m/s water movement) during periods of low vapor pressure deficit (≈ 1 kPa) and no wind movement. However, a study conducted at a high vapor pressure deficit (≈ 2 kPa) with no wind and a study performed under light wind movement (≈ 0.3 m/s) with a low vapor pressure deficit have shown less significant differences between evaporation from moving water and non-moving water (i.e., 9% and 19 % increases respectively @ 0.12-0.18 m/s water movement). Because water loss measurements in this study were recorded from stagnant water evaporation pans, it can only be safely concluded that Equation 6-2 underestimates rates of evaporation from a moving stream. However, many of the data points used in the development of Equation 6-2 were recorded during periods of atmospheric conditions similar to laboratory conditions where differences in evaporation from moving water relative to non-moving water were minimal, suggesting that underestimations are minor in most cases.

Comparison of Equation 6-2 to a relationship derived on the San Diego Aqueduct in California indicates that evaporative mechanisms are consistent for aridland environments. Other examples provided in this study suggest that Equation 6-2 may also be applicable to more moderate environments (i.e., western Oregon) during summertime conditions. However, it is suggested that caution be exercised when attempting to apply Equation 6-2 to more moderate climates until validated by further research.

Regression coefficients (α and β) that compose the wind function of the evaporation relationship provided were found to vary largely as a result of unstable atmospheric conditions (overcast periods and/or variable wind direction), and differing measurement

heights of meteorological variables. However, under stable conditions provided by clear-sky summer days and generally uniform wind direction, these coefficients (α and β) do not seem to vary to any large degree.

Because peak evaporation rates generally coincide with peak stream water temperatures, the evaporative process can be a useful mechanism for influencing daily maximum stream water temperatures. The cooling provided by evaporation is particularly important on smaller streams with shallow depths and relatively small volumes of stream water. While it takes more energy to heat larger bodies of water, more energy must also be lost to cool the larger volume of water. Smaller streams are critical from a temperature perspective based on their ability to both heat and cool quickly. Furthermore, the combined temperatures of several smaller tributary streams generally have a profound impact on the temperature of larger main-stem rivers. Therefore, stream temperatures are especially critical in the smaller tributary streams that are particularly susceptible to temperature loading. The subjects of this study, the MFJD River and its tributary Squaw Creek, were both lower order streams whose daily summertime temperatures often fluctuated by 10°C or more.

Previous research along the MFJD River demonstrated the presence of a certain degree of thermal "patchiness" that was not sufficiently explained by hyporeic or other sub-surface flow phenomenon. Results discovered in this study indicate that evaporation is a significant component of the energy balance of stream during summertime periods. The ability of a stream to loose heat by evaporation is influenced by a number of channel characteristics, including: the alignment of the stream channel with respect to wind

direction, the degree of incision of the stream channel, and the gradient of stream bank side slopes in the direction of wind. Each of these characteristics can influence the cooling of streams by affecting the amount of wind that occurs above the water surface. Possibly the most influential combination of the above characteristics would involve a severely incised stream section (low WEI) with steep stream bank side slopes and channel aligned perpendicular to wind direction. Figures 6.9 and 6.10 demonstrate the limited cooling potential for a stream section that is slightly incised. The effect seen in this example is likely magnified at higher levels of channel incision. While it is impossible to conclude that evaporative differences among reaches are the cause of the thermal "patchiness" seen on the MFJD River, the variable capacity of each reach to loose heat by evaporation may be an important contributing factor. However, it is more likely that multiple factors (i.e., variable shading, evaporative potential, groundwater inflows, etc.) have contributed to the thermal "patchiness" recorded along the MFJD River. Nonetheless, this study has shown that stream heat losses by evaporation are significant and must be considered when analyzing summertime stream temperature phenomenon.

Several suggestions for future research are:

1) Additional measurements of micrometeorological conditions and evaporation rates, especially in environments other than aridlands.
2) Additional research focused on studying the influence of water movement on evaporation rates over a range of vapor pressure deficits and rates of wind movement, and relating these influences to situations where wind is moving with or against the direction of water movement.

LITERATURE CITED

Baltz, D.M., P.B. Moyle, and N.J. Knight. 1982. Competitive interactions between benthic stream fishes, riffle sculpin, Cottus gulosus, and speckled dace Rhinichthys osculus. Canadian Journal of Fisheries and Aquatic Science 39:1502-1511.

Beschta, R.L. 1997. Riparian shade and stream temperature: an alternative perspective. Rangelands 19 (2): 25-28.

Beschta, R.L, R.E. Bilby, G.W. Brown, L.B. Hotlby, and T.D. Hofstra. 1987. Stream temperature and aquatic habitat: fisheries and forest interactions. *In*: Streamside Management: Forestry and Fisheries Interactions. E.O. Salo and T.W. Cundy (Editors). Contribution No. 57, University of Washington, Institute of Forest Resources, 471 pp.

Bowen, I.S. 1926. The ratio of heat losses by conduction and evaporation from any water surface. Physical Review 27: 779 – 787.

Bowie, G.L., W.B. Mills, D.B. Porcella, C.L. Campbell, J.R. Pagenkopf, , G.L. Rupp, K.M. Johnson, P.W. Chan, and S.A. Gherini. 1985. Rates, constants and kinetics formulation in surface water quality modeling, Second edition, EPA/600/3-85/040, U.S. Environmental Protection Agency, Athens, GA. 89 pp.

Boyd, M. 1996. HEAT Source: reach analysis of stream and river temperature dynamics. Masters Thesis, Oregon State University. 134 pp.

Brown, G.W. 1969. Predicting temperatures of small Streams. Water Resource Research 5(1): 68-75.

Brown, G.W. 1989. Forestry and water quality. Oregon State University Bookstore, Inc., Corvallis. 142 pp.

Camuffo, D., and A. Bernardi. 1982. An observational study of heat fluxes and their relationships with net radiation. Boundary Layer Meteorology 23: 359-368.

Constantz, J. 1998. Interaction between stream temperature, streamflow, and groundwater exchanges in alpine streams. Water Resources research 34(7): 1609-1615.

Delay, W.H., J. Senders, and R.T. Evans. 1964. Water temperature prediction and control study: Umpqua River Basin. Oregon State Water Resource Board, Salem, Oregon February 1964. 6 pp.

Dingman, S.L. 1994. Physical Hydrology. Prentice Hall, Inc., New Jersey. 575 pp.

Duncan, A. (ed.). 1998. A snapshot of salmon in Oregon. Oregon State University Extension Service. 24 pp.

Edinger, J.E., D.W. Duttweiler, and J.C. Geyer. 1968. The response of water temperatures to meteorological conditions. Water Resources Research 4(5): 1137-1143.

Feller, M.C. 1981. Effects of clearcutting and slashburning on stream temperature in southwestern British Columbia. Water Resources Bulletin 17(5): 863-867.

Heisel, J.E., R.E. Hoggatt, and C.H. Tate. 1972. Evaporation from Morse Reservoir, Indiana. U.S. Department of the Interior. Geological Survey Open-file report, Water Resources Division, Indianapolis, Indiana. 33 pp.

Heming, T.A., J.E. McInerney, and D.F. Alderdice. 1982. Effect of temperature on initial feeding in alevins of chinook salmon (Oncorhynchus tshawytscha). Canadian Journal of Fisheries and Aquatic Science 39: 1554-1562.

Hewlett, J.D., and J.C. Fortson. 1982. Stream temperature under an inadequate buffer strip in the southeast piedmont. Water Resource Bulletin 18(6): 983-988.

Hopson, R.G. 1997. Shallow aquifer characteristics adjacent to the upper Middle Fork John Day River. Masters Thesis, Oregon State University. 191 pp.

Hostetler, S.W. 1991. Analysis and modeling of long-term stream temperatures on the Steamboat Creek Basin, Oregon: implications for landuse and fish habitat. Water Resources Bulletin 27(4): 637-647.

Jackman, A.P. and N. Yotsukura. 1977. Thermal loading of natural streams. U.S. Geological Survey Professional Paper 991. 39 pp.

Jacobs, A.F.G., B.G. Hensinkveld, and D.C. Lucassen. 1998. Temperature variation in a class A evaporation pan. Journal of Hydrology 206: 75-83.

Janvario dos Reis, R., N. Luis Dias. 1998. Multi-season lake evaporation: energy-budget estimates and CRLE model assessment with limited meteorological observations. Journal of Hydrology 208: 135-147.

Jobson, H.E. 1980. Thermal modeling of flow in the San Diego Aqueduct, California, and its relation to evaporation. U.S. Geological Survey Professional Paper 1122. 24 pp.

Jobson, H.E. and T.N. Keefer. 1979. Modeling highly transient flow, mass, and heat transport in the Chattahoochee River near Atlanta, Georgia. U.S. Geological Survey Professional Paper 1136. 41 pp.

Jobson, H.E., and A.M. Sturrock. 1979. Comprehensive monitoring of meteorology, hydraulics and thermal regime of the San Diego Aqueduct, California. U.S. Geological Survey Professional Paper 1137. 29 pp.

Jones, H.G. 1992. Plants and microclimate: a quantitative approach to environmental plant physiology. Cambridge University Press, New York. 428 pp.

Kevern, N.R., and R.C. Ball. 1965. Primary productivity and energy relationships in artificial streams. Limnology and Oceanography 10: 74-87.

Krajewski, W.F., A.J. Kraszewski, and W.J. Grenney. 1982. A graphical technique for river water temperature predictions. Ecological Modeling 17: 209-224.

Lakshmi, V., and E.F. Wood. 1998. Diurnal cycles of evaporation using a two-layer hydrological model. Journal of Hydrology 204: 37-51.

Larson, L.L., and S.L. Larson. 1996. Riparian shade and stream temperature: a perspective. Rangelands 18(4): 149-152.

LeBlanc, R.T., R.D. Brown, and J.E. Fitzgibbon. 1997. Modeling the effects of land use change on the water temperature in unregulated urban streams. Journal of Environmental Management 49: 445–469.

Lindsey S.D. and R.K. Farnsworth. 1997. Sources of solar radiation estimates and their effect on daily potential evaporation for use in streamflow modeling. Journal of Hydrology 201 (1-4) 348-366.

Maidment, D.R. 1993. The handbook of hydrology. McGraw-Hill, New York.

McGurk, B.L. 1989. Predicting stream temperature after riparian vegetation removal. *In:* D.L. Abell (ed). Proceedings of the California Riparian Systems Conference, Berkley, California September 22-24, 1988. USDA Forest Service General Technical Report PSW-110. Pacific Southwest Forestry and Range Experimental Station. 541 pp.

Messinger, H. 1963. Dissipation of heat from a thermally loaded stream. U.S. Geological Survey professional Paper 475-C. 3 pp.

Minshall, G.W. 1968. Community dynamics of the benthic fauna in a woodland springbrook. Hydrobiologia 32: 305-337.

Mohseni, O., and H.G. Stephan. 1999. Stream temperature /air temperature relationships: a physical interpretation. Journal of Hydrology 218: 128 – 141.

Oregonian. 1999. Oregon, feds tussle to set thermostat for state's fish. *The Oregonian*. Friday August 6th, 1999. E4.

Oroud, I.M. 1998. The influence of heat conduction on evaporation from sunken pans in a hot, dry environment. Journal of Hydrology 210: 1-10.

Parker, F.L. and P.A. Krenkel. 1970. Physical and engineering aspects of thermal pollution. CRC Press, Ohio. 90 pp.

Priestly, C.H.B., and R.J. Taylor. 1972. On the assessment of surface heat flux and evaporation using large-scale parameters. Monthly Weather Review 100: 81-92.

Reeves, G.H. 1985. Interaction and behavior of the redside shiner (Richardsonins balteatus) and the steelhead trout (Salmo gairdneri) in Western Oregon: the influence of water temperature. Ph.D. Thesis, Oregon State University, Corvallis. 101p.

Ross, J.L., and A.J.H. Pieterse. 1994. Light, temperature and flow regimes of the Vaal River at Balkfontein, South Africa. Hydrobiologia 277: 1-15.

Satterlund, D.R., and P.W. Adams. 1992. Wildland watershed management. John Wiley & Sons, Inc., New York. 436 pp.

Shade, W.R., and A.F. Smith III. 1968. Engineering aspects of thermal pollution. *In:* F.L Parker and P.A. Krenkel (ed). Proceedings of National Symposium on Thermal Pollution, Nashville, Tennessee Aug 14-16, 1968. 308 pp.

Sinokrot, B.A., and H.G. Stefan. 1993. Stream temperature dynamics: measuring and modeling. Water Resource Research 29: 2299-2312.

Smith, K., and M.E. Lavis. 1975. Environmental influences on the temperature of a small upland stream. OIKOS 26: 228-236.

Steele, T.D. 1982. A characterization of stream temperatures in Pakistan using harmonic analysis. Hydrological Sciences 27: 451-467.

Torgersen, C.E. 1997. Multiscale assessment of thermal patterns and the distribution of chinook salmon in the John Day River Basin, Oregon. Masters Thesis, Oregon State University. 99 pp.

Unland, H.E., A.M. Arain, C. Harlow, P.R. Houser, J. Garatuza-Payan, P. Scott, O.L. Sen, and W.J. Shuttleworth. 1998. Evaporation from a riparian system in a semi-arid environment. Hydrological Processes 12: 527-542.

Vorosmarty, C.J., C.A. Federer, and A.L. Schloss. 1998. Potential evaporation functions compared on U.S. watersheds: possible implications for global-scale water balance and terrestrial ecosystem modeling. Journal of Hydrology 207: 147-169.

World Meteorological Organization, 1994. Guide to Hydrologic Practices. Fifth Edition. WMO-No. 168, Geneva, Switzerland.

Yelagina, L.G., V.I. Gorshkov, and E.T. Mironenko. 1970. Measurement of the turbulent vapor flux by infrared hygrometer. Atmospheric and Oceanic Physics 6(1): 49-51.

Yoshino, M.M. 1975. Climate in a small area. University of Tokyo Press. 549 pp.

Yuskavitch, J. 1998. Salmon recovery. Trout: the journal of coldwater fisheries conservation. Summer 1998: 14–20.

Zison, S.W., W.B. Mills, D. Diemer, and C.W. Chen. 1978. Rates, constants, and kinetic formulations in surface water quality modeling. Environmental Protection Agency. EPA-600/3-78-105, U.S. Environmental Protection Agency, Athens, GA. 318 pp.

APPENDICES

APPENDIX A: Calculated evaporative heat loss for the upper Middle Fork of the John Day River, August 9, 1996

Appendix A-1. Measured and calculated hourly data for the Middle Fork of the John Day River, August 9, 1996.

Measured Variables					Calculated Variables				
Time (hr)	Relative Humidity (%)	Wind Speed V (m/s)	Water Temperature Ts (C)	Air Temperature Ta (C)	Vapor Pressure of Evaporating Surface (water) Es (Kpa)	Vapor Pressure of Air Ea (Kpa)	Evaporation Rate (mm/d)	Latent Heat of Vaporization LHV (cal/g)	Heat Energy Lost By Evaporation Qe (cal/cm2/d)
1	0.25	0.0	18.0	20.0	2.1	0.6	4.5	587	262
2	0.25	0.0	18.0	19.0	2.1	0.6	4.6	587	268
3	0.26	0.0	17.0	18.0	1.9	0.5	4.2	588	248
4	0.28	0.5	16.0	18.0	1.8	0.5	4.7	588	276
5	0.29	0.0	16.0	15.0	1.8	0.5	4.0	588	235
6	0.27	0.5	15.0	14.0	1.7	0.4	4.6	589	269
7	0.25	0.5	15.0	13.0	1.7	0.4	4.8	589	281
8	0.24	1.0	14.0	12.0	1.6	0.3	5.2	589	309
9	0.23	2.0	15.0	13.0	1.7	0.3	7.2	589	423
10	0.21	3.0	16.0	15.0	1.6	0.4	9.4	588	551
11	0.19	4.0	18.0	18.0	2.1	0.4	12.6	587	741
12	0.15	3.0	20.0	21.0	2.3	0.4	12.6	588	739
13	0.13	4.0	21.0	23.0	2.5	0.4	16.0	585	938
14	0.11	4.0	22.0	26.0	2.7	0.4	17.2	585	1004
15	0.14	4.0	23.0	28.0	2.8	0.5	17.2	584	1006
16	0.16	2.5	24.0	30.0	3.0	0.7	13.5	584	787
17	0.15	3.0	24.0	30.0	3.0	0.6	15.1	584	880
18	0.17	1.0	23.0	29.0	2.8	0.7	8.6	584	516
19	0.20	1.0	23.0	28.0	2.8	0.8	8.5	584	498
20	0.22	0.0	22.0	26.0	2.7	0.7	5.7	585	336
21	0.23	0.0	21.0	25.0	2.5	0.7	5.3	585	311
22	0.23	0.0	21.0	23.0	2.5	0.6	5.6	585	325
23	0.23	0.5	20.0	22.0	2.3	0.6	6.2	586	363
24	0.23	0.0	19.0	21.0	2.2	0.6	4.9	587	288
AVERAGES =		1.4	19.2	21.0	2.3	0.5	8.4	586	494

Equations used for calculated values:

1. Vapor pressure of evaporating surface (e_s) = $0.1[6.11\exp((17.3T_s)/(T_s + 237.3))]$ (5-2)

Where: e_s = saturation vapor pressure of the air evaluated at a temperature equal to that of the water surface, kPa

T_s = temperature of the water surface, °C

2. Vapor pressure of the air (e_a) = $0.1[R_h\{6.11\exp((17.3T_a)/(T_a + 237.3))\}]$ (5-1)

Where: e_a = vapor pressure of the air, kPa

R_h = relative humidity expressed as a fraction

T_a = temperature of the air, °C

3. Evaporation rate (E) = $[3.01 + 1.13(V)](e_s - e_a)$ (Jobson's open channel evaporation equation, 3-3)

Where: E = evaporation, mm/d

V = windspeed, m/s

e_s and e_a = vapor pressures (defined above), kPa

4. Latent heat of vaporization, $LHV = 597.3 - 0.564\ (T_s)$ (5-3)

Where: LHV = latent heat of vaporization, cal/g
T_s = temperature of the water surface, °C

5. Heat energy lost by means of evaporating water $(H_e) = 0.10\ [(LHV)E]$ (5-4)

Where: H_e = evaporative heat energy, $cal/cm^2/d$
LHV = latent heat of vaporization, cal/g
E = evaporation, mm/d
ρ = density of water, g/cm^3

Calculated evaporative heat loss for the upper Middle Fork of the John Day River August 9, 1996

494 $cal/cm^2/d$

Appendix A-2. Stream surface heat energy flux calculations for MFJD River, August 9, 1996.

Equation to be used:

$$S = H_s - H_{sr} + H_a - H_{ar} - H_{br} - H_e \pm H_c \pm H_p \quad (1\text{-}1)$$

Where:

S = *net surface heat energy flux*
H_s = *shortwave solar radiation incident to water surface*
H_{sr} = *reflected solar shortwave radiation*
H_a = *incoming longwave radiation from atmosphere*
H_{ar} = *reflected longwave radiation*
H_{br} = *longwave back radiation emitted by body of water*
H_e = *energy utilized by evaporation*
H_c = *energy convected to or from water surface*
H_p = *advective heat flux due to precipitation*

H_s: From Figure 3-6 (Dingman 1994), under clear-sky conditions at approximately 44.5° N latitude for mid-August:

$$H_s \text{ (clear sky)} = 850 \text{ cal/cm}^2\text{/d}$$

H_{sr}: Reflected shortwave radiation

$H_{sn} = H_s - H_{sr}$
$H_{sn} = (1\text{-}R) * H_s$

Where:

H_{sn} = net shortwave radiation
R = reflectivity of water surface

Using substitution:
$H_s - H_{sr} = (1\text{-}R) * H_s$
$H_{sr} = H_s (R)$

From previous calculations:
$H_s = 850$ cal/cm^2/d
R = 0.06 (Mohseni and Stephan 1999)

$$\therefore H_{sr} = H_s (0.06)$$
$$H_{sr} = (850 \text{ cal/cm}^2\text{/d}) * 0.06$$
$$\mathbf{H_{sr} = 51 \text{ cal/ cm}^2\text{/d}}$$

H_a & H_{ar}:

$$H_{an} = H_a - H_{ar} = 0.2712 \left[1.16 \times 10^{-13} (1 + 0.17C^2) (1.8T_a + 492)^6\right] \quad (1\text{-}3)$$

Where:

$H_{an} = H_a - H_{ar}$ = net longwave atmospheric radiation, cal/cm^2/day
C = cloud cover, fraction (assume 0.05)
T_a = air temperature, °C

Average air temperature for MFJD River on august 9, 1996 (Appendix A-1)

$$T_s = 21°C$$

$$H_{an} = 0.2712*[1.16 \times 10^{-13} (1 + 0.17(0.05)^2)((1.8*21)+ 492)^6]$$

$$H_{an} = 696 \text{ cal/cm}^2\text{/d}$$

Assume $H_{ar} = H_a * R = H_a (0.06)$

$$H_{an} = H_a - H_{ar}$$

$$H_{an} = H_a - H_a (0.06)$$

$$H_{an} = 0.94 (H_a)$$

$$H_a = (696 \text{ cal/cm}^2\text{/d})/ 0.94$$

$$\mathbf{H_a = 740 \text{ cal/cm}^2\text{/d}}$$

$$H_{ar} = H_a - H_{an}$$

$$H_{ar} = (740 - 696) \text{ cal/ cm}^2\text{/d}$$

$$\mathbf{H_{ar} = 44 \text{ cal/cm}^2\text{/d}}$$

H_{br}:

$$H_{br} = 0.97\sigma T_s^4 \qquad (1\text{-}4)$$

Where H_{br} = longwave back radiation, cal/cm^2/d
T_s = surface water temperature, °K
σ = Stephan-Boltzman constant = 1.19×10^{-7}, cal/cm^2/d/°K

Average surface temperature for MFJD River on august 9, 1996 (Appendix A-1)

$$T_s = 19.2 \text{ °C} = 292.4 \text{ °K}$$

$$H_{br} = 0.97 (1.19 \times 10^{-7})(292.4^4)$$

$$\mathbf{H_{br} = 843 \text{ cal/cm}^2\text{/d}}$$

H_e: From previous calculations Appendix A-1:

$$\mathbf{H_e = 494 \text{ cal/cm}^2\text{/d}}$$

H_c:

$$R = H_c/H_e = (6.1 \times 10^{-4}) P [(T_s - T_a)/(e_s - e_a)] \qquad (1\text{-}5)$$

Where R = bowen ratio
P = atmospheric pressure, mb
T_a = air temperature, ° C
T_s = surface water temperature, ° C
e_s = saturation vapor pressure at the surface water temperature, mb
e_a = vapor pressure of the air, mb

From Appendix A-1, average values for the MFJD River are:

$$T_s = 19.2\ °C$$
$$T_a = 21\ °C$$
$$e_s - e_a = 2.3\text{kPa} - 0.5\ \text{kPa} = 1.8\ \text{kPa} = 18.0\ \text{mb}$$

Atmospheric pressure (Equation taken from Boyd 1996):

$$P_r = [(288 - 0.0065\ (Z))/288]^{5.256} \qquad \text{and } P_r = P_s/P_o$$

Where P_r = ratio of atmospheric pressure at stream surface to that at sea level
Z = elevation of stream surface, m
P_s = atmospheric pressure at elevation of stream surface
P_o = atmospheric pressure at sea level

Assume elevation is 1250 meters (4100 feet) and P_o = 1000 mb

$$P_r = [(288 - 0.0065\ (1250))/288]^{5.256}$$
$$P_r = 0.86$$
$$P_r = P_s/P_o$$
$$P_s = 0.86 * 1000$$
$$P_s = 860\ \text{mb}$$

$$R = (6.1 \times 10^{-4})\ 860\ |\ [(19.2 - 21)/(18.0)]\ | = 0.052$$
$$H_c/H_e = 0.052$$
$$H_c = H_e\ (0.052)$$
$$H_c = 494\ \text{cal/cm}^2\text{/d}\ (0.052)$$
$$\mathbf{H_c = 26\ cal/cm^2/d}$$

Because $T_a > T_s$: Assume that Hc is positive and the stream is gaining heat energy from the atmosphere

H_p: Advective heat flux

No precipitation fell on August 9, 1996. Therefore, the advective heat flux can be assumed to be zero.

TOTAL HEAT FLUX:

$S = H_s - H_{sr} + H_a - H_{ar} - H_{br} - H_e \pm H_c \pm H_p$

$S = 850 - 51 + 740 - 44 - 843 - 494 + 26$

$S = +184$ cal/cm^2/d

TOTAL IMPOSED HEAT LOSSES:

$H_{br} = 843$ cal/cm^2/d

$H_e = 494$ cal/cm^2/d

Total = 1337 cal/cm^2/d

PERCENT IMPOSED HEAT LOST BY EVAPORATION

$\%\ LOSS = 100\ (H_e/H_{TOTAL})$

$\%\ LOSS = 100\ (494/1337)$

$\%\ LOSS = 0.37(100)$

% LOSS = 37%

"Imposed heat loss" refers to physical heat loss from the water body and not to losses that would have been "imposed" heat if they were not reflected, etc. This means that reflected short and long wave radiation was not counted as an actual heat loss because this energy was never converted to actual stream heating. Essentially, heat losses in this case refer to those that contributed to the cooling of a heated body of water.

APPENDIX B: Characteristics of pan locations, channels, and windspeeds for field sites, upper Middle Fork of John Day River

SITE A: MIDDLEFORK CAMPGROUND

Plan View:

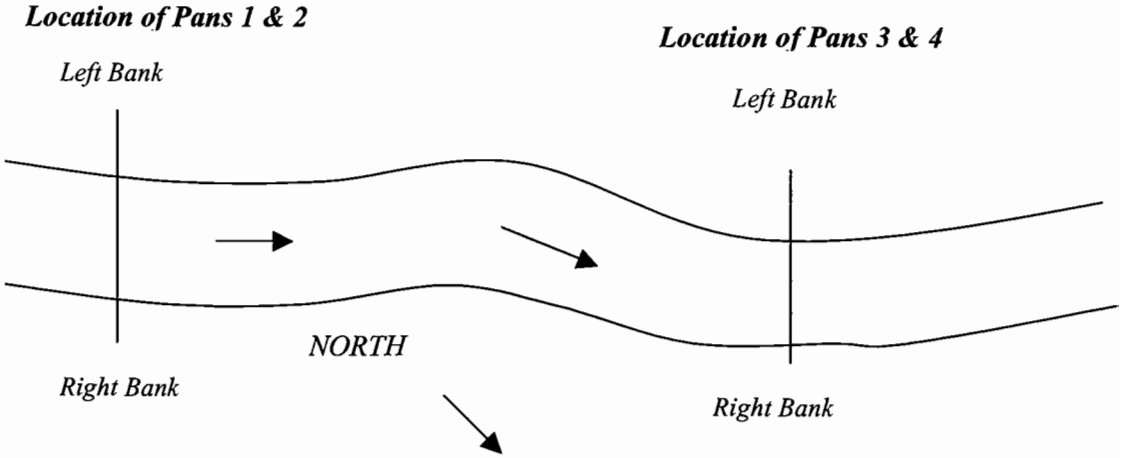

Cross-Sectional View:

Pans 1 & 2

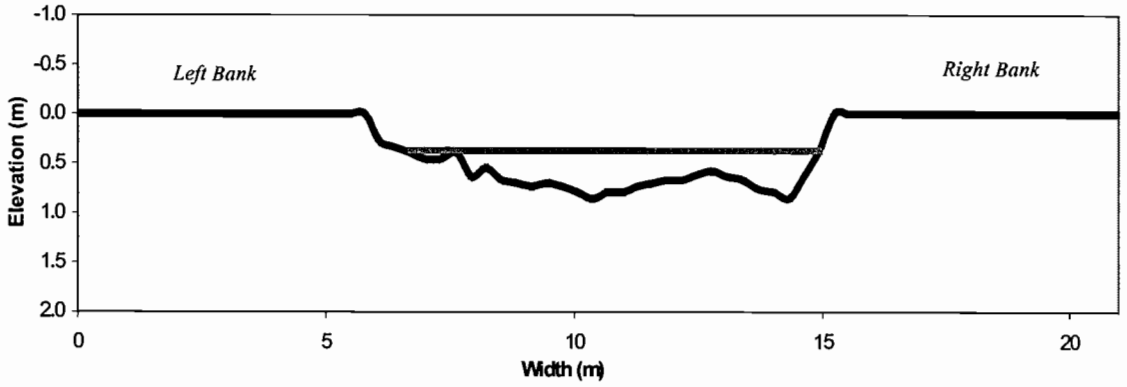

Depth (Floodplain Surface to Water Surface)	0.37 m
Average Water Depth	0.30 m
Average Channel Depth	0.63 m
Wetted Perimeter	8.76 m
Flow Area	2.47 m^2
Wetted Width	8.38 m
Channel Area	5.78 m^2
Channel Width	9.45 m
Channel Perimeter	10.12 m
Site Elevation	1220 m
Surface Velocity at Evaporation Pan	0.30 m/s
Exposure Index	*12.1*

Note: Channel information for Pans 3 & 4 was not collected.

Wind Direction Information (valley aligned northwest - southeast):
Dates of Analysis: 8-19-98 through 8-21-98

Pans 1 & 2:

Channel orientation: NW ↔ SE
Direction of flow: NW

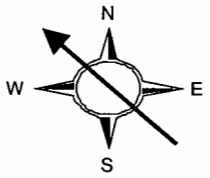

Pans 3 & 4:

Channel orientation: NW ↔ SE
Direction of flow: NW

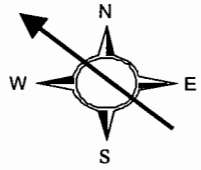

8-19-98: Daytime winds out of the south

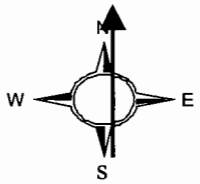

8-20-98: Daytime winds out of the northwest

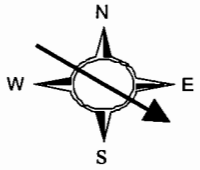

8-21-98: Daytime winds out of the northwest

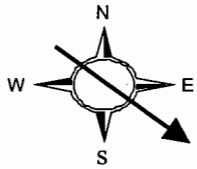

Average Daytime Windspeed Information

Date	Pan #1 In-stream windspeed (m/s)	Pan #2 Out-of-stream windspeed (m/s)	Ratio of: Pan #1 to Pan #2	Pan #3 In-stream windspeed (m/s)	Pan #4 Out-of-stream windspeed (m/s)	Ratio of: Pan #3 to Pan #4
8-19-98	0.28	0.23	1.26	0.23	0.22	1.06
8-20-98	0.63	0.27	2.32	0.43	0.38	1.15
8-21-98	0.72	0.29	2.47	0.63	0.62	1.01

SITE B: DEERHORN CAMPGROUND

Plan View:

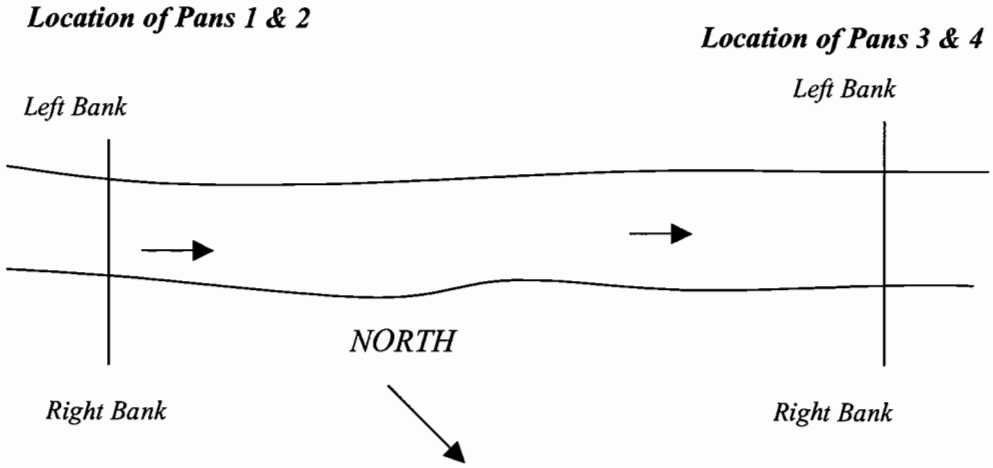

Cross-Sectional View:

Pans 1 & 2

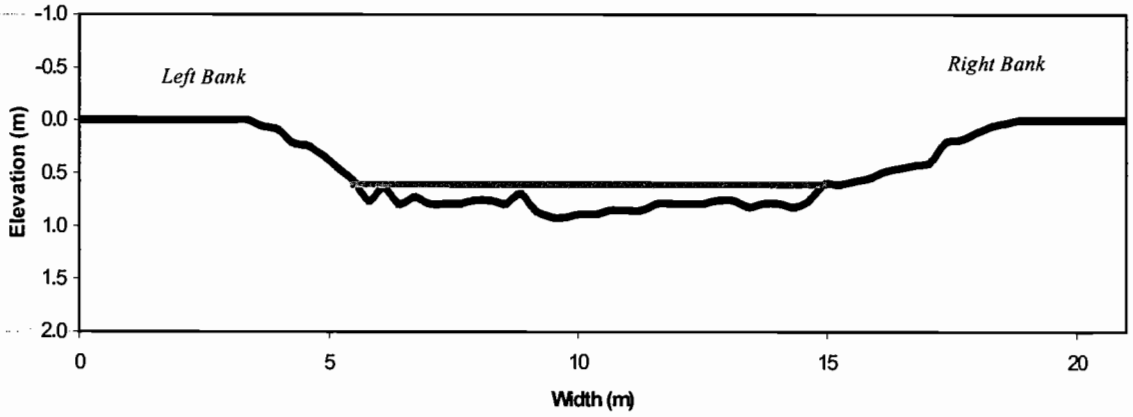

Depth (Floodplain Surface to Water Surface)	0.61 m
Average Water Depth	0.19 m
Average Channel Depth	0.61 m
Wetted Perimeter	9.63 m
Flow Area	1.74 m^2
Wetted Width	9.40 m
Channel Area	9.37 m^2
Channel Width	15.55 m
Channel Perimeter	15.97 m
Site Elevation	1220 m
Surface Velocity at Evaporation Pan	0.10 m/s
Exposure Index	*15.9*

Pans 3 & 4

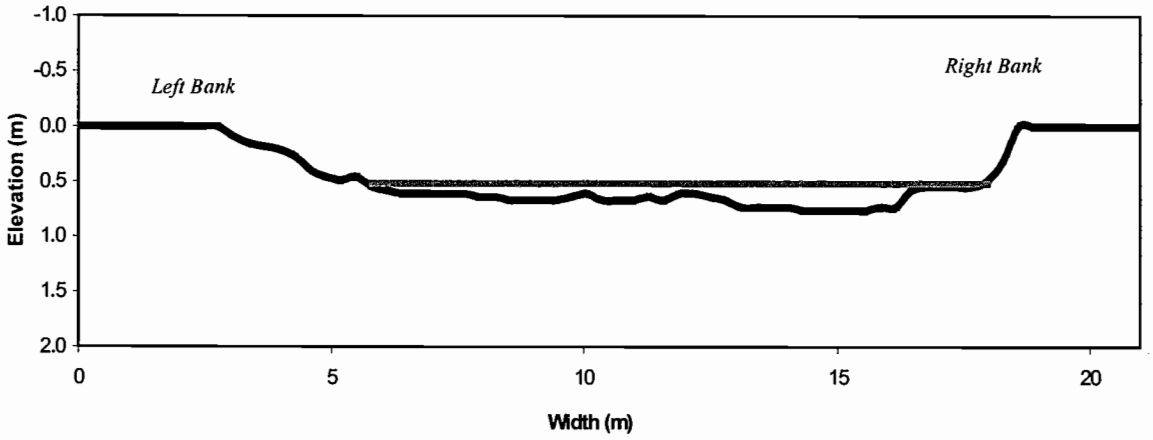

Depth (Floodplain Surface to Water Surface)	0.52 m
Average Water Depth	0.15 m
Average Channel Depth	0.59 m
Wetted Perimeter	12.23 m
Flow Area	1.67 m^2
Wetted Width	12.14 m
Channel Area	9.05 m^2
Channel Width	15.85 m
Channel Perimeter	16.19 m
Site Elevation	*1220 m*
Surface Velocity at Evaporation Pan	0.25 m/s
Exposure Index	*17.3*

Wind Direction Information (valley aligned northwest-southeast):
Dates of Analysis: 8-6-98, 8-11-98, 8-12-98

Pans 1 & 2:

Channel orientation: NW ↔ SE
Direction of flow: NW

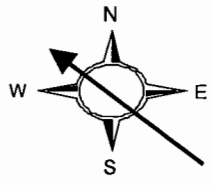

Pans 3 & 4:

Channel orientation: NW ↔ SE
Direction of flow: NW

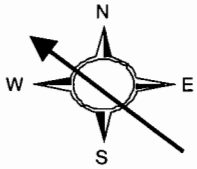

8-6-98: Daytime winds out of the northwest

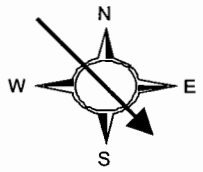

8-11-98: Daytime winds out of the northwest

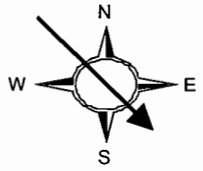

8-12-98: Daytime winds out of the northwest

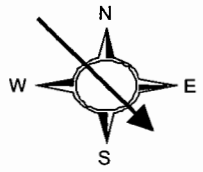

Average Daytime Windspeed Information

Date	Pan #1 In-stream windspeed (m/s)	Pan #2 Out-of-stream windspeed (m/s)	Ratio of: Pan #1 to Pan #2	Pan #3 In-stream windspeed (m/s)	Pan #4 Out-of-stream windspeed (m/s)	Ratio of: Pan #3 to Pan #4
8-6-98	1.39	0.88	1.57	0.99	1.08	0.91
8-11-98	0.77	0.81	0.94	0.77	1.07	0.71
8-12-98	0.75	0.75	1.00	0.64	0.90	0.71

SITE C: LOWER 580 POOL

Plan View:

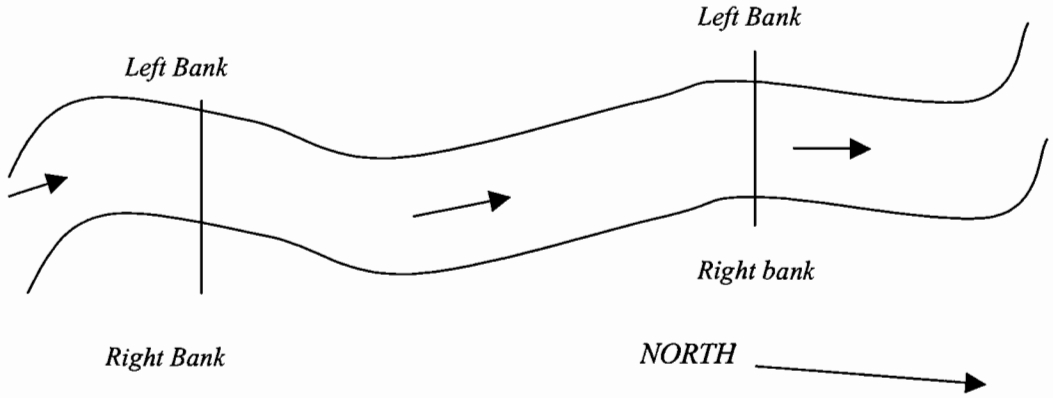

Cross-Sectional View:

Pans 1 & 2

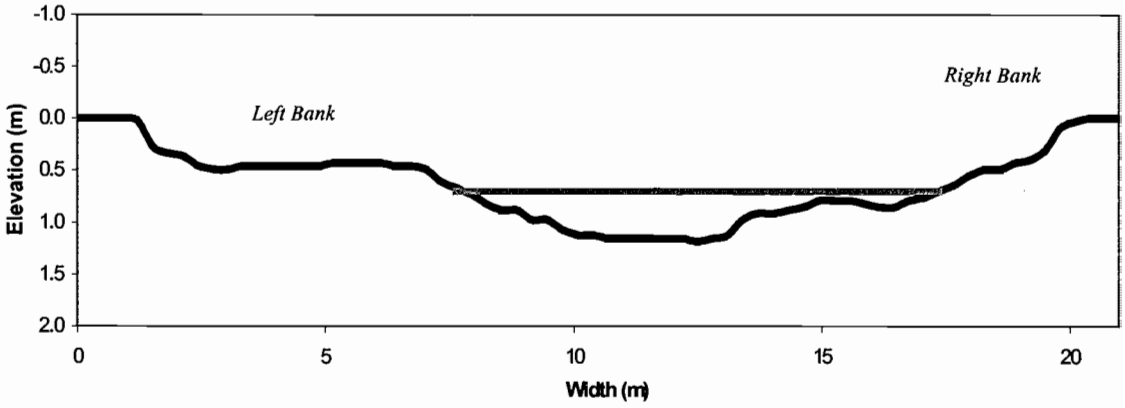

Depth (Floodplain Surface to Water Surface)	0.70 m
Average Water Depth	0.32 m
Average Channel Depth	0.69 m
Wetted Perimeter	9.73 m
Flow Area	2.53 m^2
Wetted Width	9.60 m
Channel Area	13.33 m^2
Channel Width	19.51 m
Channel Perimeter	19.91 m
Site Elevation	1220 m
Surface Velocity at Evaporation pan	0.22 m/s
Exposure Index	*18.7*

Pans 3 & 4

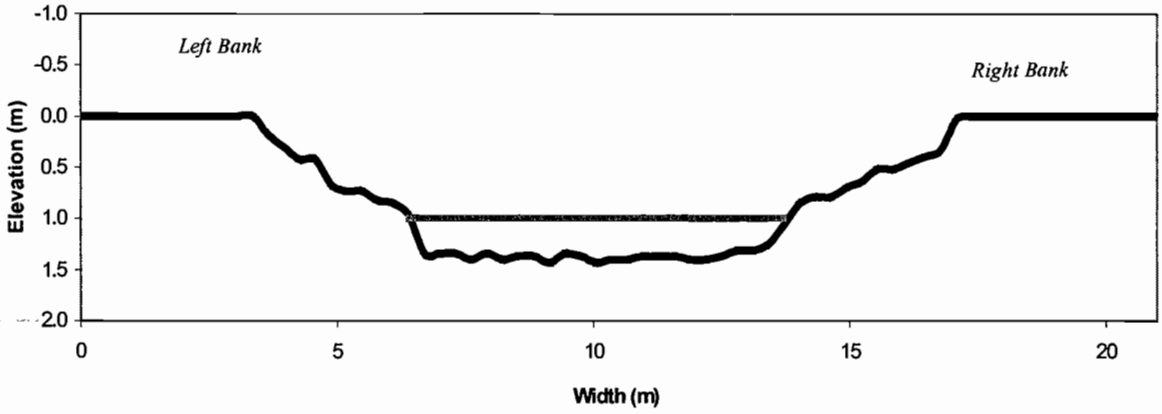

Depth (Floodplain Surface to Water Surface)	1.01 m
Average Water Depth	0.35 m
Average Channel Depth	0.99 m
Wetted Perimeter	7.67 m
Flow Area	2.54 m^2
Wetted Width	7.38 m
Channel Area	13.59 m^2
Channel Width	14.02 m
Channel Perimeter	14.81 m
Site Elevation	1220 m
Surface Velocity at Evaporation pan	0.05 m/s
Exposure Index	*9.1*

Wind Direction Information (valley aligned northwest-southeast):
Dates of Analysis: 8-16-98 through 8-18-98

Pans 1 & 2:

Channel orientation: N ↔ S
Direction of flow: N

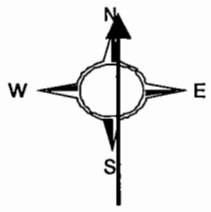

Pans 3 & 4:

Channel orientation: N ↔ S
Direction of flow: N

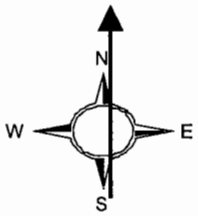

8-16-98: Daytime winds out of the northwest

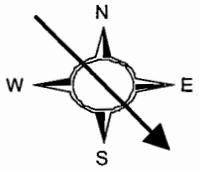

8-17-98: Daytime winds out of the northwest

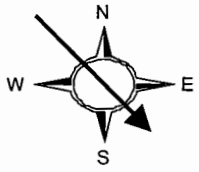

8-18-98: Daytime winds out of the northwest

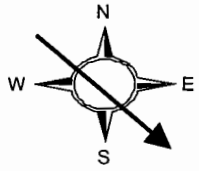

Average Daytime Windspeed Information

Date	Pan #1 In-stream windspeed (m/s)	Pan #2 Out-of-stream windspeed (m/s)	Ratio of: Pan #1 to Pan #2	Pan #3 In-stream windspeed (m/s)	Pan #4 Out-of-stream windspeed (m/s)	Ratio of: Pan #3 to Pan #4
8-16-98	2.47	3.30	0.75	1.91	3.32	0.58
8-17-98	2.96	4.04	0.73	2.40	4.07	0.59
8-18-98	1.95	2.60	0.75	1.39	2.59	0.54

SITE D: 580 POOL

Plan View:

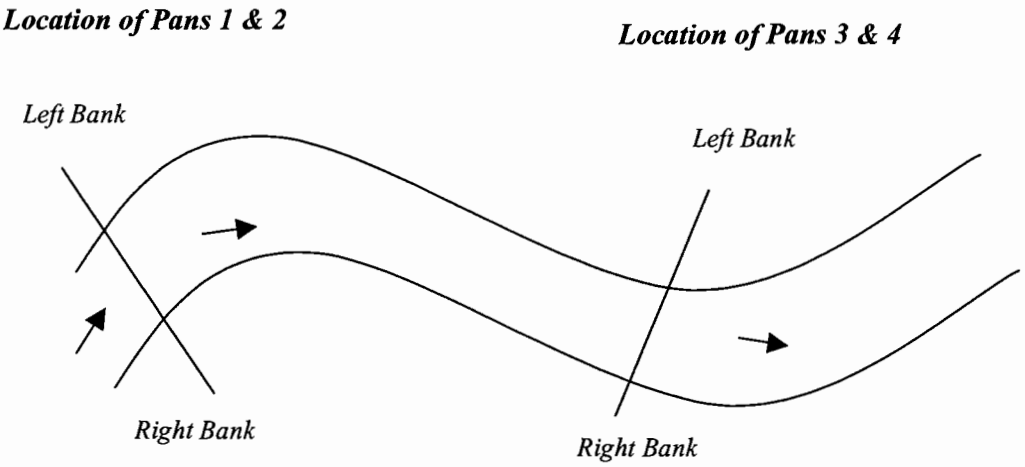

Cross-Sectional View:

Pans 1 & 2

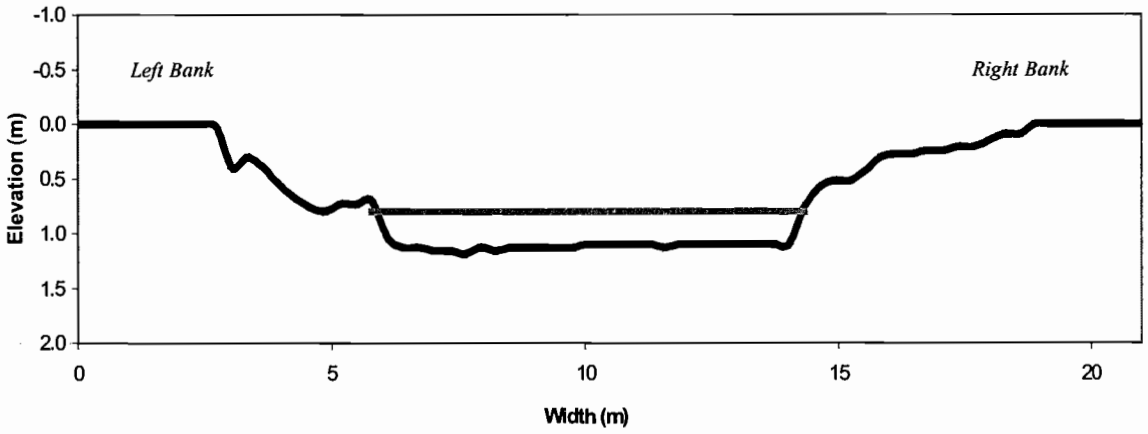

Depth (Floodplain Surface to Water Surface)	0.79 m
Average Water Depth	0.31 m
Average Channel Depth	0.78 m
Wetted Perimeter	8.47 m
Flow Area	2.57 m^2
Wetted Width	8.16 m
Channel Area	12.44 m^2
Channel Width	16.46 m
Channel Perimeter	17.23 m
Site Elevation	1220 m
Surface Velocity at Evaporation pan	0.08 m/s
Exposure Index	*13.9*

Pans 3 & 4

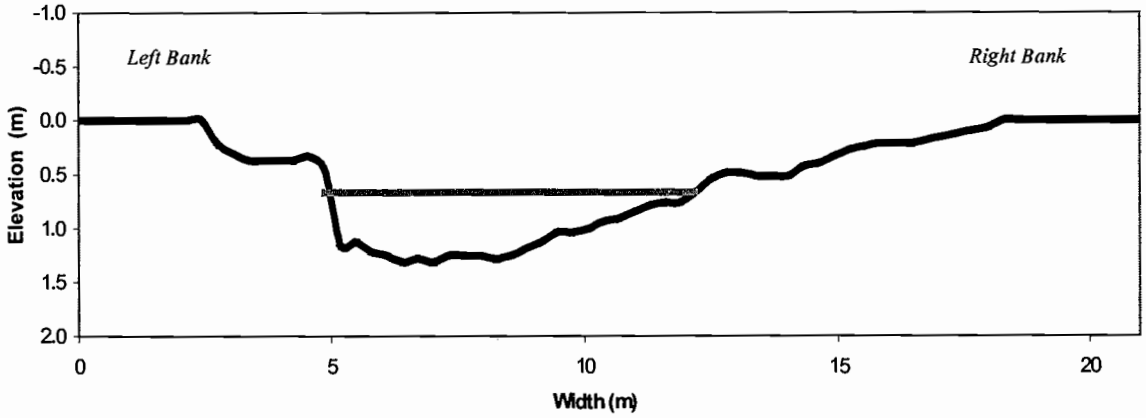

Depth (Floodplain Surface to Water Surface)	0.67 m
Average Water Depth	0.16 m
Average Channel Depth	0.55 m
Wetted Perimeter	7.64 m
Flow Area	3.01 m^2
Wetted Width	7.23 m
Channel Area	10.61 m^2
Channel Width	15.85 m
Channel Perimeter	16.60 m
Site Elevation	*1220* m
Surface Velocity at Evaporation pan	0.20 m/s
Exposure Index	*16.2*

Wind Direction Information (valley aligned northwest-southeast):
Dates of Analysis: 8-13-98 through 8-15-98

Pans 1 & 2:
Channel orientation: NW ↔ SE
Direction of flow: NW

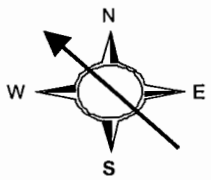

Pans 3 & 4:
Channel orientation: NE ↔ SW
Direction of flow: NE

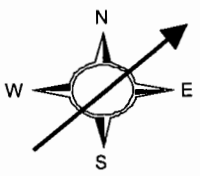

8-13-98: Daytime winds out of the northwest

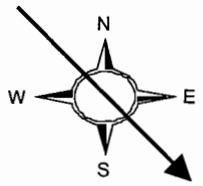

8-14-98: Daytime winds out of the northwest

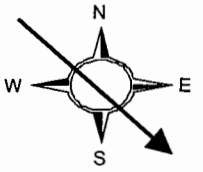

8-15-98: Daytime winds out of the northwest

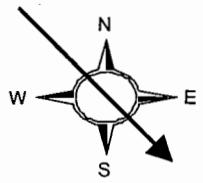

Average Daytime Windspeed Information

Date	Pan #1 In-stream windspeed (m/s)	Pan #2 Out-of-stream windspeed (m/s)	Ratio of: Pan #1 to Pan #2	Pan #3 In-stream windspeed (m/s)	Pan #4 Out-of-stream windspeed (m/s)	Ratio of: Pan #3 to Pan #4
8-13-98	1.66	1.87	0.89	0.80	1.85	0.43
8-14-98	2.50	2.86	0.87	1.19	2.94	0.41
8-15-98	2.56	2.76	0.94	1.16	2.80	0.41

SITE E: LOWER PHIPPS MEADOW

Plan View:

Location of Pans 1 & 2

Location of Pans 3 & 4

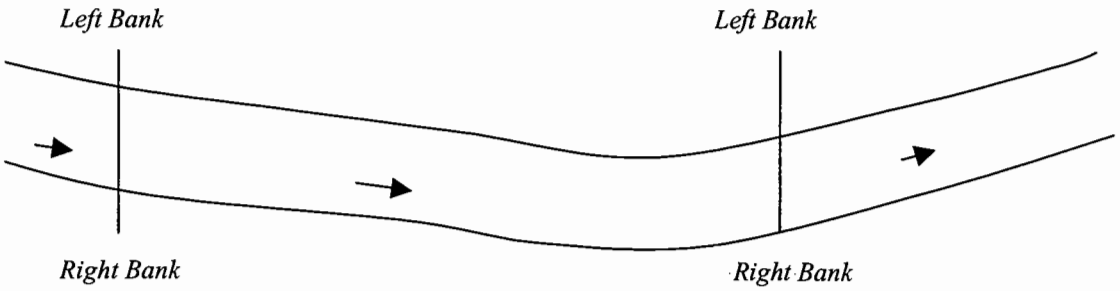

NORTH ⟶

Cross-Sectional View:

Pans 1 & 2

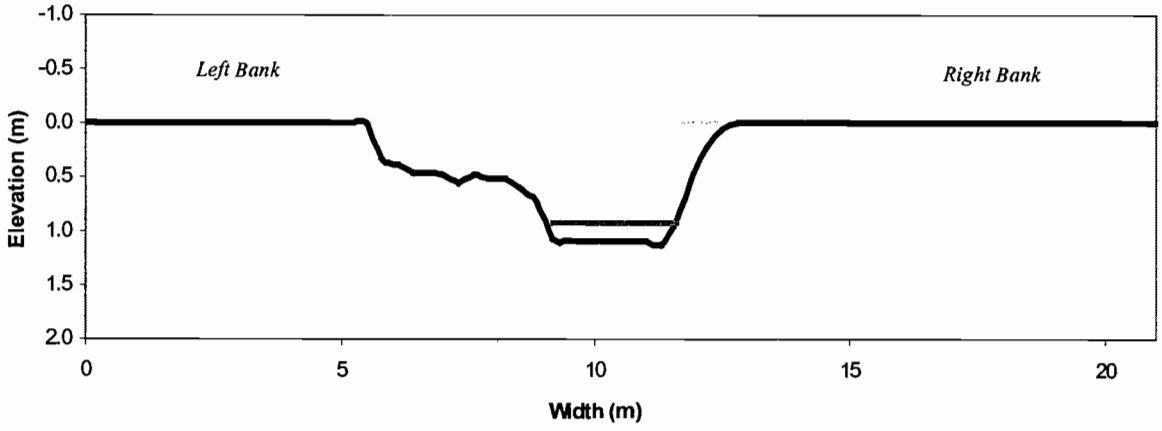

Depth (Floodplain Surface to Water Surface)	0.91 m
Average Water Depth	0.19 m
Average Channel Depth	0.69 m
Wetted Perimeter	2.69 m
Flow Area	0.43 m^2
Wetted Width	2.54 m
Channel Area	4.87 m^2
Channel Width	7.32 m
Channel Perimeter	8.11 m
Site Elevation	1300 m
Surface Velocity at Evaporation pan	0.07 m/s
Exposure Index	*6.0*

Pans 3 & 4

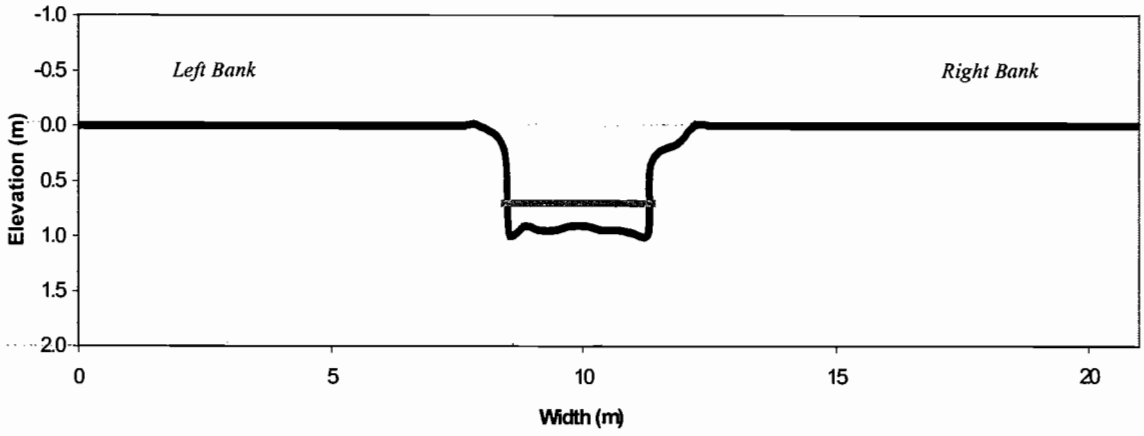

Depth (Floodplain Surface to Water Surface)	0.70 m
Average Water Depth	0.24 m
Average Channel Depth	0.78 m
Wetted Perimeter	3.36 m
Flow Area	0.69 m^2
Wetted Width	2.98 m
Channel Area	3.10 m^2
Channel Width	4.27 m
Channel Perimeter	5.35 m
Site Elevation	1300 m
Surface Velocity at Evaporation pan	0.02 m/s
Exposure Index	*3.6*

Wind Direction Information (valley aligned east-west)
Dates of Analysis: 7-21-98 through 7-24-98

Pans 1 & 2:
Channel orientation: N ↔ S
Direction of flow: N

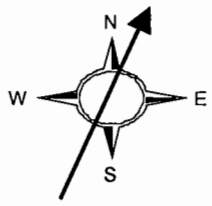

Pans 3 & 4:
Channel orientation: N ↔ S
Direction of flow: N

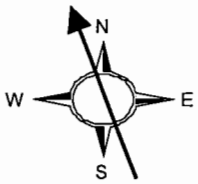

7-21-98: Daytime winds out of the northwest

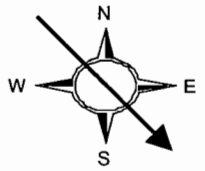

7-22-98: Daytime winds out of the northwest

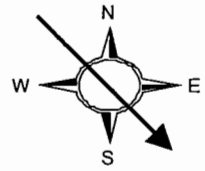

7-23-98: Daytime winds out of the northwest

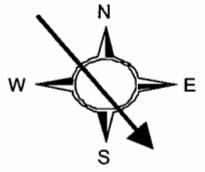

7-24-98: Daytime winds out of the northwest
(switch to northeast at end of day)

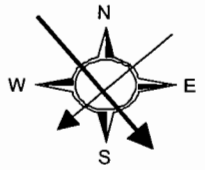

Average Daytime Windspeed Information

Date	Pan #1 In-stream windspeed (m/s)	Pan #2 Out-of-stream windspeed (m/s)	Ratio of: Pan #1 to Pan #2	Pan #3 In-stream windspeed (m/s)	Pan #4 Out-of-stream windspeed (m/s)	Ratio of: Pan #3 to Pan #4
7-21-98	0.77	1.75	0.44	1.06	1.76	0.60
7-22-98	0.63	1.38	0.46	0.80	1.34	0.60
7-23-98	0.39	0.74	0.53	0.35	0.71	0.50
7-24-98	0.77	1.50	0.52	0.84	1.52	0.56
7-24-98	1.07	1.30	0.82	0.59	1.19	0.49

SITE F: MID-PHIPPS MEADOW

Plan View:

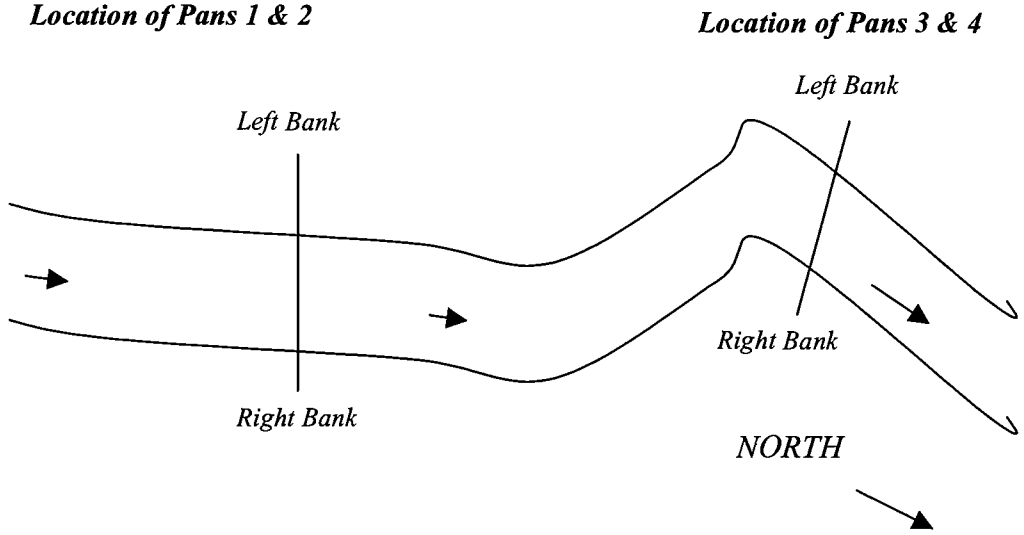

Cross-Sectional View:

Pans 1 & 2

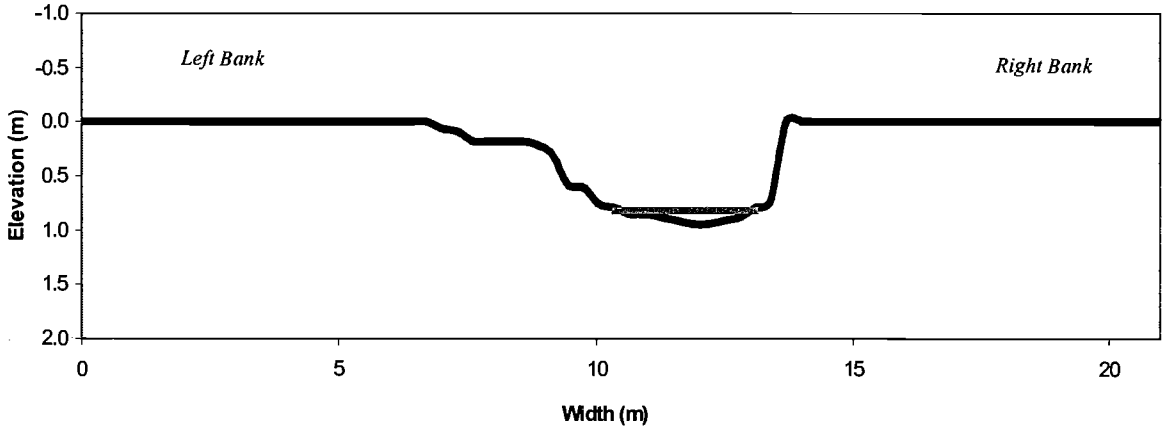

Depth (Floodplain Surface to Water Surface)	0.82 m
Average Water Depth	0.08 m
Average Channel Depth	0.58 m
Wetted Perimeter	2.51 m
Flow Area	0.18 m^2
Wetted Width	2.49 m
Channel Area	3.92 m^2
Channel Width	7.01 m
Channel Perimeter	7.71 m
Site Elevation	1300 m
Surface Velocity at Evaporation Pan	0.12 m/s
Exposure Index	*6.3*

Pans 3 & 4

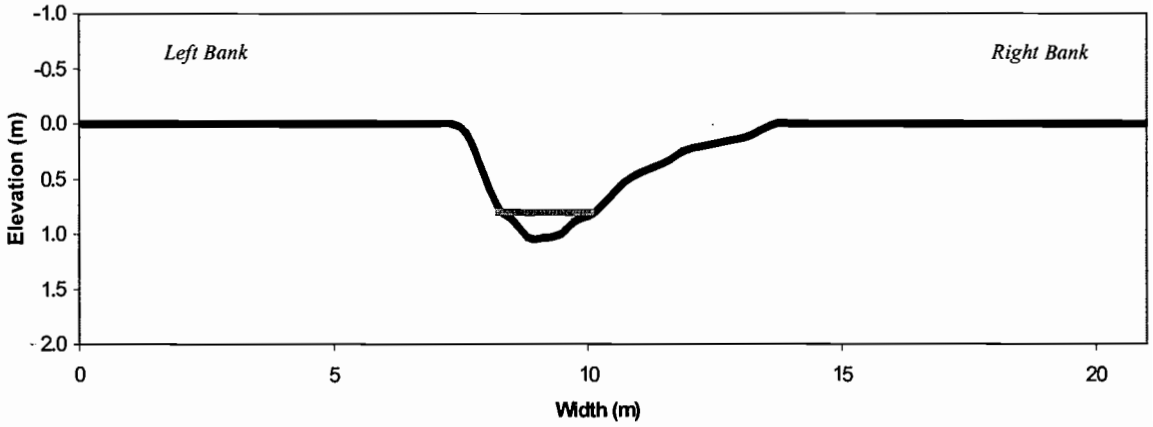

Depth (Floodplain Surface to Water Surface)	0.79 m
Average Water Depth	0.15 m
Average Channel Depth	0.52 m
Wetted Perimeter	1.92 m
Flow Area	0.27 m^2
Wetted Width	1.83 m
Channel Area	3.16 m^2
Channel Width	6.40 m
Channel Perimeter	6.92 m
Site Elevation	1300 m
Surface Velocity at Evaporation Pan	0.03 m/s
Exposure Index	*6.3*

Wind Direction Information (valley aligned east-west)
Dates of Analysis: 7-25-98 through 7-28-98

Pans 1 & 2:

Channel orientation: NW ↔ SE
Direction of flow: NW

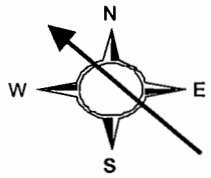

Pans 3 & 4:

Channel orientation: N ↔ S
Direction of flow: N

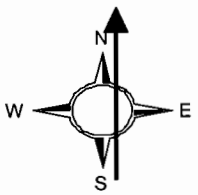

7-25-98: Daytime winds out of the west

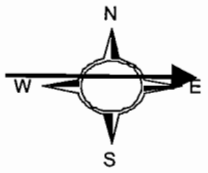

7-26-98: Daytime winds out of the west

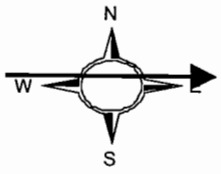

7-27-98: Daytime winds out of the west

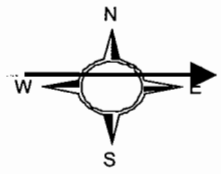

7-28-98: Daytime winds out of the west

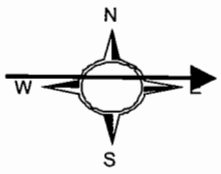

Average Daytime Windspeed Information

Date	Pan #1 In-stream windspeed (m/s)	Pan #2 Out-of-stream windspeed (m/s)	Ratio of: Pan #1 to Pan #2	Pan #3 In-stream windspeed (m/s)	Pan #4 Out-of-stream windspeed (m/s)	Ratio of: Pan #3 to Pan #4
7-25-98	1.38	1.76	0.79	0.40	1.69	0.24
7-26-98	0.94	1.18	0.80	0.36	1.12	0.32
7-27-98	0.94	1.30	0.73	0.41	1.18	0.35
7-28-98	1.27	1.75	0.73	0.47	1.69	0.28

SITE G: UPPER PHIPPS MEADOW

Plan View:

Location of Pans 1 & 2 ***Location of Pans 3 & 4***

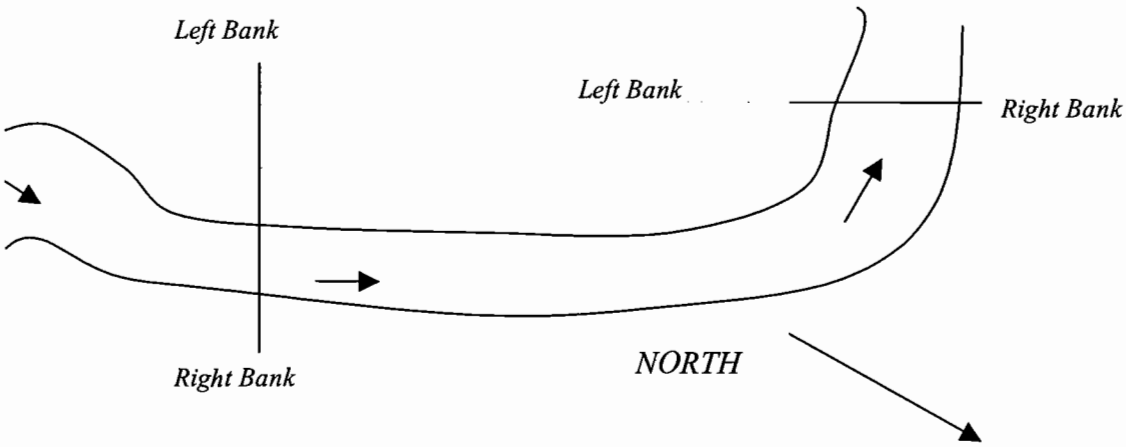

Cross-Sectional View:

Pans 1 & 2

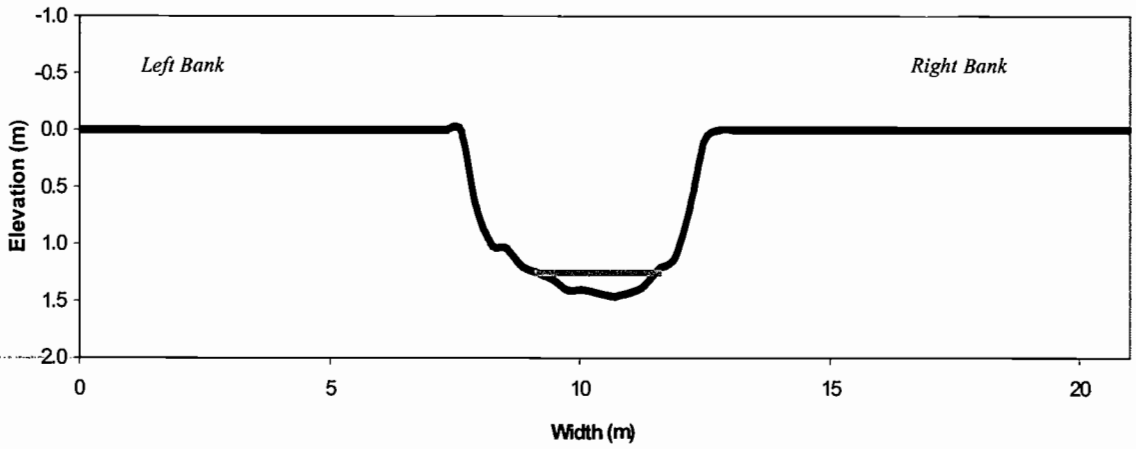

Depth (Floodplain Surface to Water Surface)	1.25 m
Average Water Depth	0.15 m
Average Channel Depth	1.13 m
Wetted Perimeter	2.44 m
Flow Area	0.32 m^2
Wetted Width	2.38 m
Channel Area	5.52 m^2
Channel Width	5.18 m
Channel Perimeter	6.49 m
Site Elevation	1300 m
Surface Velocity at Evaporation Pan	0.05 m/s
Exposure Index	*2.8*

Pans 3 & 4

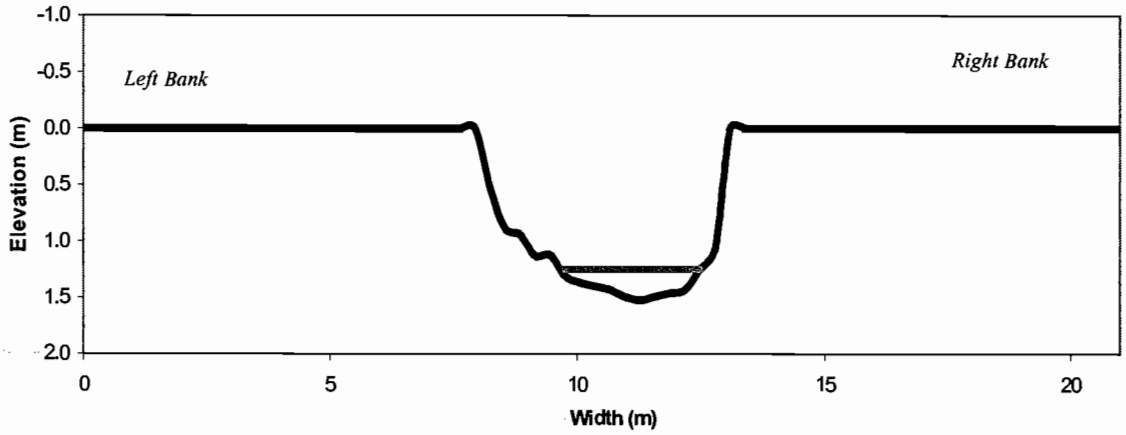

Depth (Floodplain Surface to Water Surface)	1.25 m
Average Water Depth	0.19 m
Average Channel Depth	1.24 m
Wetted Perimeter	2.93 m
Flow Area	0.50 m^2
Wetted Width	2.84 m
Channel Area	6.05 m^2
Channel Width	5.18 m
Channel Perimeter	6.69 m
Site Elevation	1300 m
Surface Velocity at Evaporation pan	0.03 m/s
Exposure Index	*2.7*

Wind Direction Information (valley aligned east-west)
Dates of Analysis: 8-2-98 through 8-5-98

Pans 1 & 2:

Channel orientation: NW ↔ SE
Direction of flow: NW

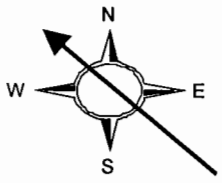

Pans 3 & 4:

Channel orientation: NE ↔ SW
Direction of flow: SW

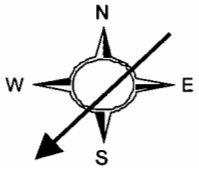

8-2-98: Daytime winds out of the west

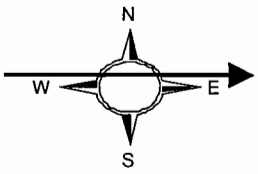

8-3-98: Daytime winds out of the southeast

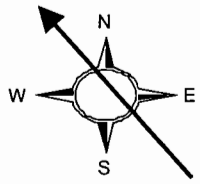

8-4-98: Daytime winds out of the east

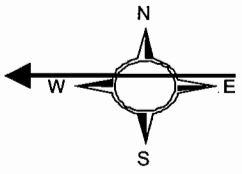

8-5-98: Daytime winds out of the east
(switch to northwest at end of day)

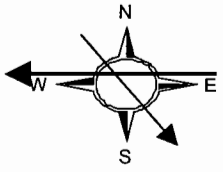

Average Daytime Windspeed Information

Date	Pan #1 In-stream windspeed (m/s)	Pan #2 Out-of-stream windspeed (m/s)	Ratio of: Pan #1 to Pan #2	Pan #3 In-stream windspeed (m/s)	Pan #4 Out-of-stream windspeed (m/s)	Ratio of: Pan #3 to Pan #4
8-2-98	0.57	0.99	0.58	0.41	0.76	0.54
8-3-98	0.55	1.13	0.48	0.43	0.92	0.46
8-4-98	0.79	2.24	0.35	0.93	2.08	0.45
8-5-98	0.91	2.19	0.42	1.06	2.09	0.51
8-5-98	0.69	1.32	0.52	0.40	1.10	0.36

SITE H: LOWER SQUAW CREEK

Plan View:

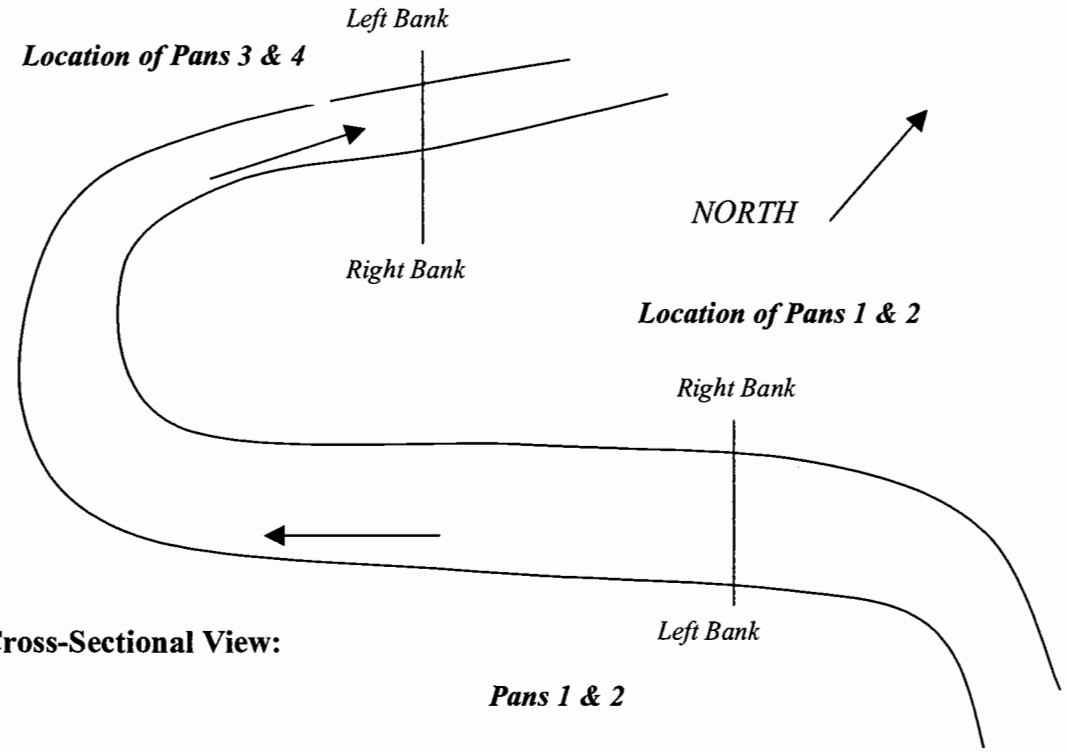

Cross-Sectional View:

Pans 1 & 2

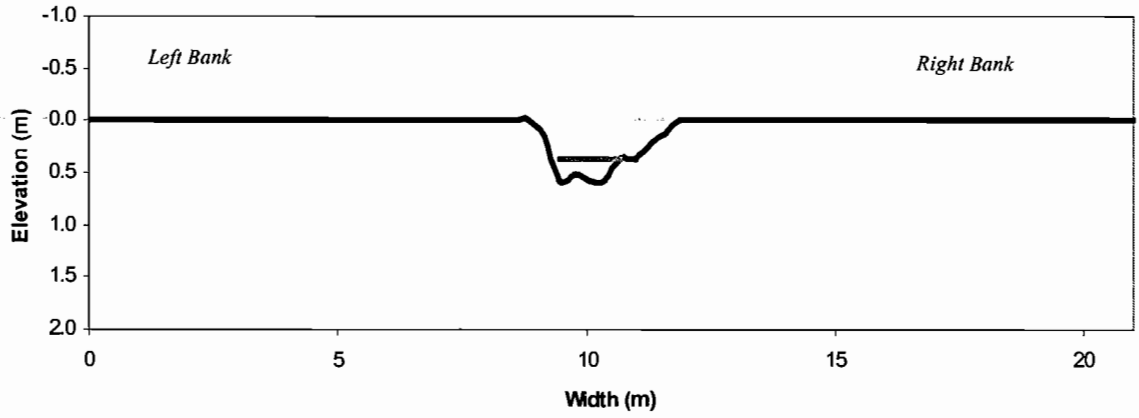

Depth (Floodplain Surface to Water Surface)	0.37 m
Average Water Depth	0.20 m
Average Channel Depth	0.39 m
Wetted Perimeter	1.56 m
Flow Area	0.22 m^2
Wetted Width	1.37 m
Channel Area	1.06 m^2
Channel Width	3.05 m
Channel Perimeter	3.46 m
Site Elevation	1460 m
Surface Velocity at Evaporation Pan	0.06 m/s
Exposure Index	*5.7*

Pans 3 & 4

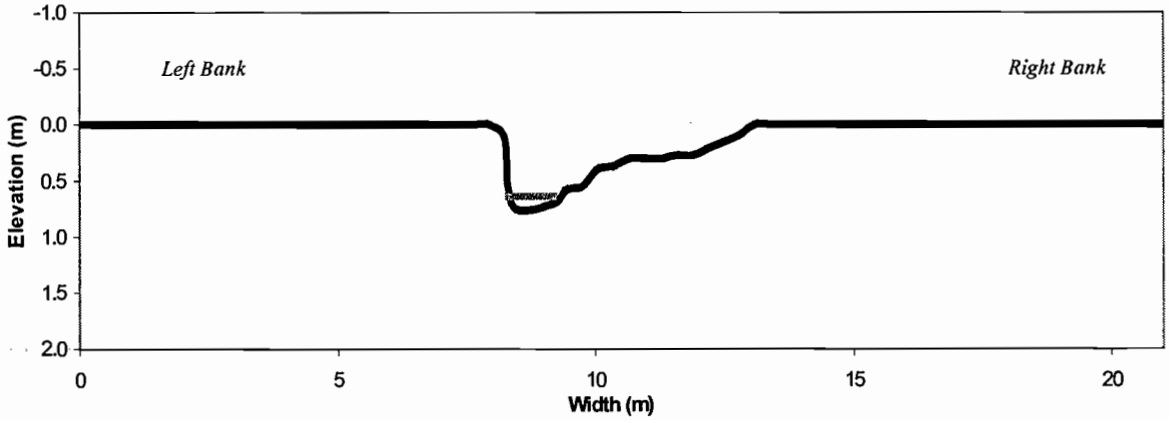

Depth (Floodplain Surface to Water Surface)	0.64 m
Average Water Depth	0.09 m
Average Channel Depth	0.37 m
Wetted Perimeter	0.69 m
Flow Area	0.04 m^2
Wetted Width	0.63 m
Channel Area	1.82 m^2
Channel Width	5.18 m
Channel Perimeter	5.60 m
Site Elevation	1460 m
Surface Velocity at Evaporation Pan	0.12 m/s
Exposure Index	*7.2*

Wind Direction Information (valley aligned northwest-southeast)
Dates of Analysis: 9-6-98 through 9-8-98

Pansl & 2:

Channel orientation: NE ↔ SW
Direction of flow: NE

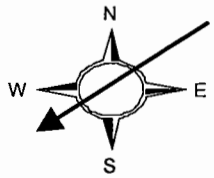

Pans 3 & 4:

Channel orientation: SW ↔ NE
Direction of flow: SW

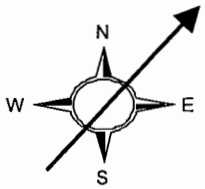

9-6-98: Daytime winds out of the south

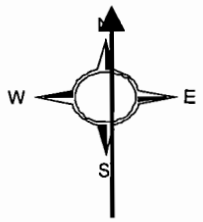

9-7-98: Daytime winds out of the northeast

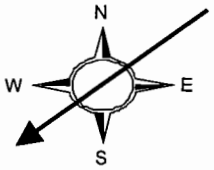

9-8-98: Daytime winds out of the north
(switch to south near end of day)

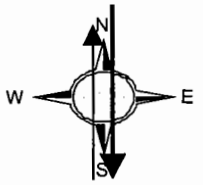

Average Daytime Windspeed Information

Date	Pan #1 In-stream windspeed (m/s)	Pan #2 Out-of-stream windspeed (m/s)	Ratio of: Pan #1 to Pan #2	Pan #3 In-stream windspeed (m/s)	Pan #4 Out-of-stream windspeed (m/s)	Ratio of: Pan #3 to Pan #4
9-6-98	0.76	1.20	0.63	0.38	1.51	0.25
9-7-98	0.55	1.10	0.50	0.40	1.07	0.37
9-8-98	0.47	1.27	0.36	0.57	1.27	0.45
9-8-98	0.75	1.19	0.63	0.34	1.22	0.28

SITE I: UPPER SQUAW CREEK

Plan View:

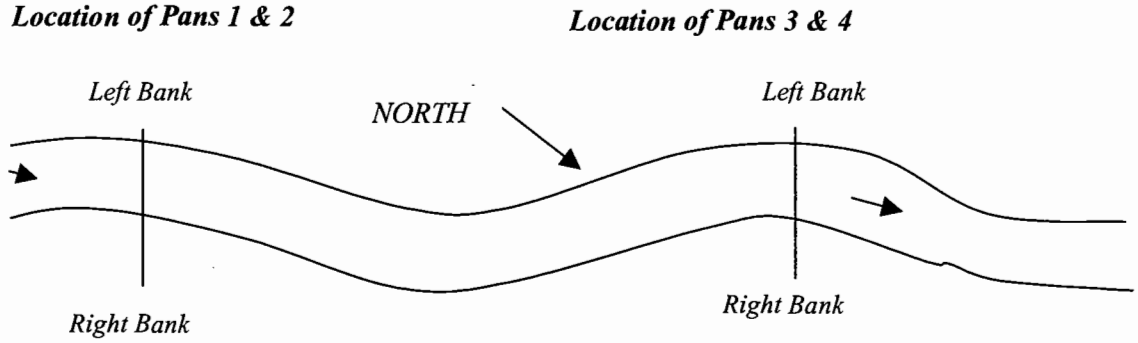

Cross-Sectional View:

Pans 1 & 2

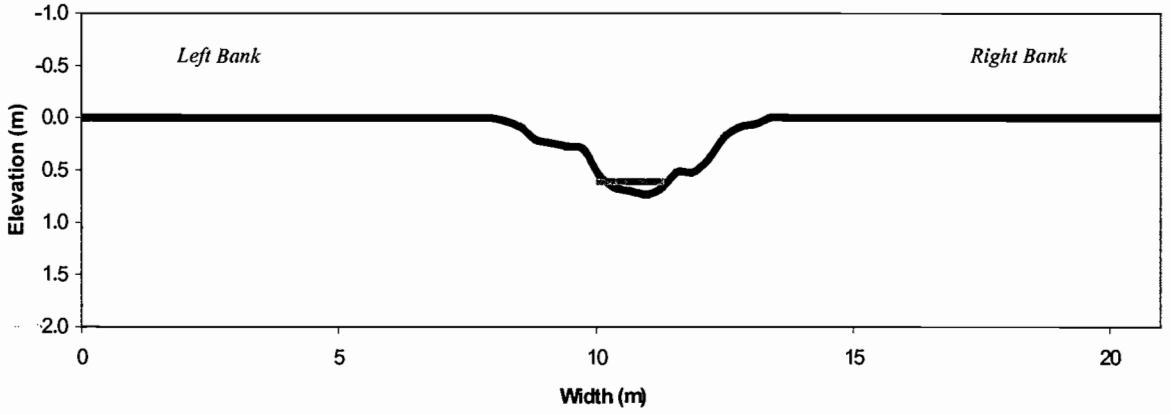

Depth (Floodplain Surface to Water Surface)	0.61 m
Average Water Depth	0.08 m
Average Channel Depth	0.37 m
Wetted Perimeter	1.23 m
Flow Area	0.09 m^2
Wetted Width	1.19 m
Channel Area	1.91 m^2
Channel Width	5.49 m
Channel Perimeter	5.79 m
Site Elevation	1460 m
Surface Velocity at Evaporation Pan	0.15 m/s
Exposure Index	*7.4*

Pans 3 & 4

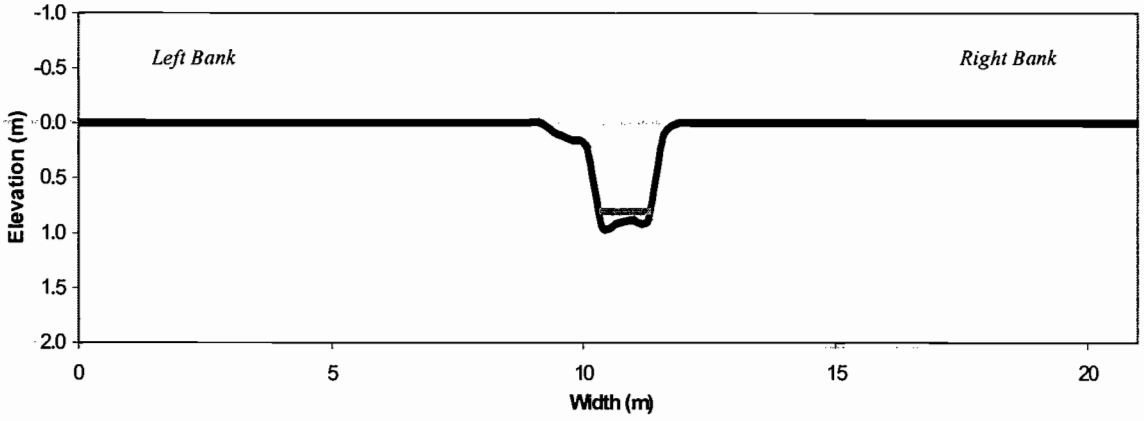

Depth (Floodplain Surface to Water Surface)	0.79 m
Average Water Depth	0.11 m
Average Channel Depth	0.53 m
Wetted Perimeter	1.18 m
Flow Area	0.11 m^2
Wetted Width	1.02 m
Channel Area	1.28 m^2
Channel Width	2.74 m
Channel Perimeter	3.80 m
Site Elevation	1460 m
Surface Velocity at Evaporation Pan	0.10 m/s
Exposure Index	2.5

Wind Direction Information (valley aligned northwest-southeast)
Dates of Analysis: 9-2-98 through 9-5-98

Pans 1 & 2:

Channel orientation: NW ↔ SE
Direction of flow: NW

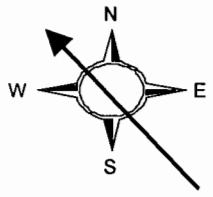

Pans 3 & 4:

Channel orientation: NW ↔ SE
Direction of flow: NW

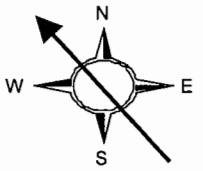

9-2-98: Daytime winds out of the northwest

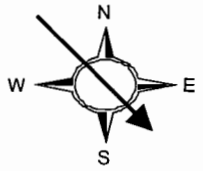

9-3-98: Daytime winds out of the southeast

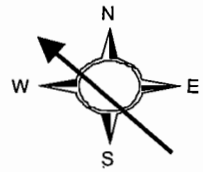

9-4-98: Daytime winds out of the northwest

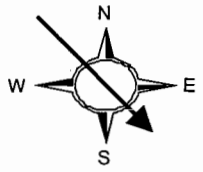

9-5-98: Daytime winds out of the northwest

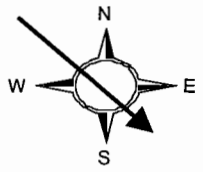

Average Daytime Windspeed Information

Date	Pan #1 In-stream windspeed (m/s)	Pan #2 Out-of-stream windspeed (m/s)	Ratio of: Pan #1 to Pan #2	Pan #3 In-stream windspeed (m/s)	Pan #4 Out-of-stream windspeed (m/s)	Ratio of: Pan #3 to Pan #4
9-2-98	0.99	1.31	0.76	0.35	1.13	0.31
9-3-98	0.95	1.05	0.91	0.27	1.09	0.25
9-4-98	0.69	0.96	0.72	0.26	0.75	0.33
9-5-98	0.76	1.09	0.70	0.31	0.78	0.40

APPENDIX C: Summary of data obtained at field sites and regression analysis, upper Middle Fork of John Day River

Appendix C-1. Data sets for field Sites A through I along the upper Middle Fork of the John Day River in northeastern Oregon. Data sets include: dates of measurement, evaporation rates, meteorological variables averaged over period that evaporation was measured, and calculated vapor pressures. Data used in statistical analysis are bolded.

Site A: Middle Fork Campground Data Set

19- August 1998 Partly cloudy
20 August 1998 Partly cloudy, nightime rain
21 August 1998 Morning sunshine, afternoon thunderstorms

Date	Time	Evaporation rate (mm/hr)	Windspeed V (m/s)	Air temp. Ta (C)	Relative humidity Rh (%)	Photosynth. active radiation (*m*mol/m^2/s)	Water temp. Ts (C)	Vap. pres. of water surface Es (Kpa)	Vap. pres. of air Ea (Kpa)	Vap. pres. deficit Es-Ea (Kpa)	Windspeed x Vap. pres. deficit V*(Es-Ea) [(m/s)* Kpa]
Pan #1											
19-Aug	**1150**	**0.047**	**0.33**	**22.9**	**39.9**	**415**	**17.8**	**2.04**	**1.12**	**0.92**	**0.30**
19-Aug	1550	0.013	0.25	21.9	47.4	108	19.2	2.23	1.25	0.98	0.25
19-Aug	1905	0.114	0.20	13.3	72.1	87	16.4	1.87	1.10	0.76	0.15
20-Aug	**945**	**0.184**	**0.71**	**22.5**	**41.2**	**851**	**16.7**	**1.90**	**1.13**	**0.78**	**0.55**
20-Aug	1315										
20-Aug	**1635**	**0.189**	**0.31**	**19.1**	**62.2**	**96**	**18.3**	**2.11**	**1.38**	**0.74**	**0.23**
20-Aug	1940	0.070	0.20	10.2	81.3	88	14.7	1.67	1.01	0.66	0.13
21-Aug	**938**	**0.205**	**0.76**	**21.2**	**44.4**	**692**	**15.9**	**1.81**	**1.12**	**0.69**	**0.53**
21-Aug	1445										
Pan #2											
19-Aug	1152	0.042	0.22	23.2	34.3	122	15.5	1.76	0.98	0.78	0.17
19-Aug	1552	0.029	0.22	21.9	41.5	56	16.1	1.83	1.10	0.74	0.16
19-Aug	1907	0.073	0.20	12.9	72.3	105	14.5	1.66	1.08	0.57	0.12
20-Aug	**947**	**0.092**	**0.27**	**22.5**	**41.4**	**347**	**15.1**	**1.72**	**1.13**	**0.59**	**0.16**
20-Aug	**1317**	**0.056**	**0.30**	**20.1**	**56.3**	**96**	**16.3**	**1.85**	**1.33**	**0.52**	**0.15**
20-Aug	1637	0.107	0.22	18.7	61.7	58	16.8	1.91	1.33	0.58	0.13
20-Aug	1942	0.063	0.22	9.8	82.8	104	13.7	1.57	1.00	0.56	0.12
21-Aug	**940**	**0.091**	**0.30**	**21.2**	**44.7**	**328**	**14.1**	**1.61**	**1.13**	**0.48**	**0.14**
21-Aug	1447										
Pan #3											
19-Aug	1220	0.090	0.25	23.6	39.8	469	18.2	2.10	1.16	0.94	0.24
19-Aug	1554	0.042	0.21	23.0	47.2	212	19.3	2.24	1.33	0.91	0.19
19-Aug	1909	0.075	0.22	13.5	71.5	65	16.4	1.87	1.11	0.76	0.17
20-Aug	**956**	**0.108**	**0.49**	**23.3**	**35.7**	**847**	**17.0**	**1.94**	**1.03**	**0.92**	**0.44**
20-Aug	**1319**	**0.079**	**0.45**	**20.9**	**53.0**	**100**	**18.8**	**2.17**	**1.31**	**0.86**	**0.39**
20-Aug	1639	0.038	0.24	19.4	61.9	73	18.3	2.11	1.40	0.71	0.17
20-Aug	1944	0.083	0.28	10.3	80.3	56	14.8	1.69	1.01	0.68	0.19
21-Aug	**942**	**0.132**	**0.66**	**22.2**	**38.5**	**877**	**16.6**	**1.89**	**1.04**	**0.86**	**0.57**
21-Aug	1449										
Pan #4											
19-Aug	1222	0.133	0.22	24.8	34.6	554	19.7	2.30	1.09	1.21	0.27
19-Aug	1556	0.052	0.21	24.1	40.9	264	21.9	2.63	1.23	1.40	0.29
19-Aug	1911	0.128	0.21	12.8	73.0	9	17.5	2.01	1.08	0.93	0.20
20-Aug	**958**	**0.113**	**0.44**	**23.1**	**38.6**	**202**	**15.6**	**1.77**	**1.09**	**0.68**	**0.30**
20-Aug	**1321**	**0.142**	**0.37**	**20.7**	**53.4**	**83**	**18.3**	**2.10**	**1.30**	**0.80**	**0.30**
20-Aug	1641	0.096	0.22	19.2	61.1	52	18.5	2.14	1.36	0.78	0.17
20-Aug	1946	0.072	0.24	9.5	82.3	8	14.5	1.65	0.98	0.67	0.16
21-Aug	**944**	**0.152**	**0.65**	**22.5**	**40.0**	**516**	**14.5**	**1.66**	**1.10**	**0.56**	**0.36**
21-Aug	1451										

Site B: Deerhorn Campground Data

6 August 1998 Clear skies
11 August 1998 Clear skies
12 August 1998 Clear Skies

Date	Time	Evaporation rate (mm/hr)	Windspeed V (m/s)	Air temp. Ta (C)	Relative humidity Rh (%)	Photosynth. active radiation (mmol/m^2/s)	Water temp. Ts (C)	Vap. pres. of water surface Es (Kpa)	Vap. pres. of air Ea (Kpa)	Vap. pres. deficit Es-Ea (Kpa)	Wind x Vap. pres. deficit V*(Es-Ea) [(m/s)* Kpa]
Pan #1											
6-Aug	1102	0.504	1.47	26.2	29.3	1610	20.5	2.42	1.00	1.42	2.09
6-Aug	1302	0.457	1.45	29.4	28.0	1497	22.8	2.78	1.15	1.63	2.37
6-Aug	1502	0.415	1.22	29.2	27.9	207	23.6	2.92	1.13	1.79	2.19
6-Aug	1702										
11-Aug	1002	0.394	0.38	25.2	31.4	1496	18.1	2.09	1.01	1.08	0.40
11-Aug	1225	0.476	1.51	28.4	27.3	1501	21.1	2.51	1.06	1.45	2.18
11-Aug	1448	0.363	1.06	28.4	26.1	174	22.1	2.68	1.01	1.66	1.77
11-Aug	1705	0.193	0.31	24.4	40.2	55	21.8	2.63	1.23	1.40	0.43
11-Aug	1956	0.119	0.20	11.9	73.9	54	17.6	2.02	1.03	0.99	0.20
12-Aug	930	0.352	0.24	24.6	35.0	1452	17.2	1.97	1.08	0.88	0.21
12-Aug	1200	0.500	1.40	29.5	21.6	1689	20.7	2.45	0.90	1.56	2.18
12-Aug	1415	0.333	0.79	29.7	24.4	483	22.4	2.72	1.02	1.70	1.34
12-Aug	1640	0.190	0.26	24.6	44.7	52	22.7	2.76	1.38	1.38	0.36
12-Aug	1955										
Pan #2											
6-Aug	1104	0.237	0.80	28.5	29.8	1589	20.5	2.41	1.16	1.25	0.99
6-Aug	1304	0.288	0.99	31.2	27.8	1326	25.1	3.19	1.27	1.92	1.90
6-Aug	1504	0.169	0.86	29.6	27.9	371	27.2	3.62	1.16	2.46	2.12
6-Aug	1704										
11-Aug	1004	0.131	1.04	27.0	31.2	1352	16.0	1.82	1.11	0.71	0.74
11-Aug	1227	0.334	1.17	30.5	26.5	1342	21.4	2.56	1.16	1.40	1.63
11-Aug	1450	0.315	0.86	28.8	25.9	272	24.3	3.04	1.03	2.01	1.73
11-Aug	1707	0.190	0.29	23.9	39.9	66	23.5	2.91	1.19	1.72	0.51
11-Aug	1958	0.107	0.26	11.0	76.4	57	17.1	1.95	1.01	0.95	0.24
12-Aug	932	0.179	0.79	26.1	34.9	1097	14.9	1.69	1.18	0.51	0.40
12-Aug	1202	0.342	0.89	32.6	21.3	1552	20.9	2.48	1.05	1.43	1.28
12-Aug	1442	0.284	0.69	30.0	24.9	274	24.8	3.14	1.06	2.08	1.44
12-Aug	1642	0.198	0.25	24.5	40.1	75	24.4	3.07	1.24	1.83	0.46
12-Aug	1957										
Pan #3											
6-Aug	1106	0.423	1.02	26.4	27.1	1267	20.6	2.43	0.94	1.49	1.52
6-Aug	1306	0.436	1.02	29.7	25.5	1082	22.8	2.78	1.06	1.72	1.75
6-Aug	1506	0.360	0.92	29.5	24.3	224	23.5	2.90	1.01	1.89	1.73
6-Aug	1706										
11-Aug	1006	0.323	1.04	25.4	28.9	1288	18.1	2.08	0.94	1.14	1.18
11-Aug	1229	0.352	1.06	28.6	24.8	1101	21.0	2.49	0.97	1.52	1.60
11-Aug	1452	0.337	0.71	28.8	22.7	144	22.0	2.65	0.90	1.74	1.23
11-Aug	1709	0.146	0.25	24.8	37.5	39	21.8	2.62	1.17	1.45	0.36
11-Aug	2000	0.128	0.21	12.0	72.6	23	17.6	2.02	1.02	1.01	0.21
12-Aug	934	0.271	0.71	24.6	32.8	1251	17.2	1.97	1.01	0.95	0.68
12-Aug	1204	0.466	0.80	29.9	19.8	1226	20.8	2.47	0.84	1.63	1.30
12-Aug	1444	0.246	0.47	29.8	22.3	142	22.3	2.71	0.94	1.77	0.83
12-Aug	1644	0.175	0.23	25.3	38.3	46	22.6	2.75	1.24	1.51	0.35
12-Aug	1959										
Pan #4											
6-Aug	1108	0.660	1.10	27.9	25.1	1652	21.6	2.59	0.95	1.64	1.80
6-Aug	1308	0.605	1.15	31.3	23.3	1602	26.3	3.43	1.07	2.37	2.72
6-Aug	1508	0.516	1.00	30.5	22.7	530	28.2	3.83	1.00	2.83	2.83
6-Aug	1708										
11-Aug	1006	0.316	1.46	26.4	27.3	1367	15.6	1.78	0.94	0.84	1.22
11-Aug	1231	0.444	1.48	30.1	22.6	1517	22.1	2.66	0.97	1.69	2.51
11-Aug	1454	0.671	1.02	29.7	21.0	327	25.4	3.25	0.88	2.37	2.43
11-Aug	1711	0.193	0.29	24.9	34.2	44	23.6	2.92	1.08	1.84	0.54
11-Aug	2002	0.107	0.22	11.0	75.1	35	16.7	1.90	0.99	0.92	0.20
12-Aug	936										
12-Aug	940	0.272	1.15	25.9	30.1	1148	14.5	1.65	1.01	0.65	0.74
12-Aug	1206	0.419	1.02	32.1	17.1	1652	21.3	2.55	0.82	1.72	1.76
12-Aug	1446	0.610	0.65	31.3	19.5	406	26.1	3.39	0.90	2.49	1.61
12-Aug	1646	0.263	0.27	25.4	34.5	42	24.6	3.09	1.13	1.97	0.54
12-Aug	2001										

Site C: Lower 580 Pool Data Set

16 August 1998 *Clear, cool, windy*
17 August 1998 *Clear, cool, windy*
18 August 1998 *Clear, cool, windy*

Date	Time	Evaporation rate (mm/hr)	Windspeed V (m/s)	Air temp. Ta (C)	Relative humidity Rh (%)	Photosynth. active radiation (mmol/m^2/s)	Water temp. Ts (C)	Vap. pres. of water surface Es (Kpa)	Vap. pres. of air Ea (Kpa)	Vap. pres. deficit Es-Ea (Kpa)	Wind x Vap. pres. deficit V*(Es-Ea) [(m/s)* Kpa]
Pan #1											
18-Aug	1146	0.404	2.38	19.1	46.7	1722	18.1	2.09	1.03	1.06	2.51
18-Aug	1414	0.481	2.56	21.5	39.4	1406	20.7	2.46	1.01	1.44	3.69
18-Aug	1622	0.621	2.49	20.6	34.2	628	21.1	2.51	0.83	1.68	4.18
18-Aug	1900	0.167	0.88	8.2	71.7	171	15.1	1.72	0.78	0.94	0.83
17-Aug	955	0.454	3.37	17.7	40.8	1642	15.2	1.73	0.83	0.90	3.03
17-Aug	1330	0.637	3.13	21.0	30.3	1521	18.8	2.18	0.76	1.42	4.45
17-Aug	1600	0.679	2.60	21.4	23.9	864	19.8	2.32	0.61	1.71	4.44
17-Aug	1805	0.470	1.23	17.4	32.5	145	19.0	2.20	0.65	1.55	1.91
17-Aug	2005	0.120	0.23	4.3	74.3	146	13.4	1.54	0.62	0.93	0.21
18-Aug	930										
18-Aug	938	0.326	1.22	18.0	38.3	1544	13.1	1.51	0.79	0.71	0.87
18-Aug	1220	0.332	1.87	21.9	30.6	1668	17.0	1.94	0.80	1.14	2.14
18-Aug	1445	0.470	1.85	23.4	28.1	1262	19.8	2.32	0.81	1.51	2.79
18-Aug	1645	0.488	1.52	20.9	28.9	405	20.2	2.37	0.72	1.65	2.51
18-Aug	1945										
Pan #2											
18-Aug	1148	0.579	3.11	19.6	44.6	1693	19.1	2.22	1.02	1.20	3.74
18-Aug	1416	0.819	3.50	21.6	37.9	1374	22.2	2.68	0.98	1.70	5.96
18-Aug	1624	0.866	3.28	20.5	34.0	600	21.7	2.60	0.82	1.78	5.84
18-Aug	1902	0.175	1.26	7.8	72.5	176	12.1	1.42	0.77	0.65	0.81
17-Aug	957										
17-Aug	959	0.553	4.56	18.0	38.9	1626	15.1	1.72	0.81	0.92	4.19
17-Aug	1332	0.928	4.29	21.1	29.3	1492	20.2	2.38	0.73	1.64	7.04
17-Aug	1602	0.854	3.50	21.1	23.6	838	20.8	2.47	0.59	1.88	6.57
17-Aug	1807	0.665	1.65	16.9	32.6	127	19.2	2.23	0.63	1.60	2.64
17-Aug	2007	0.117	0.64	3.7	75.0	152	9.9	1.22	0.60	0.62	0.40
18-Aug	932										
18-Aug	940	0.379	2.81	18.8	35.8	1533	11.3	1.35	0.78	0.57	1.59
18-Aug	1222	0.577	2.39	22.9	28.5	1643	18.8	2.17	0.80	1.37	3.28
18-Aug	1447	0.618	2.56	23.7	27.1	1229	22.4	2.72	0.80	1.92	4.91
18-Aug	1647	0.756	2.03	20.6	28.3	382	21.8	2.62	0.69	1.93	3.92
18-Aug	1947										
Pan #3											
18-Aug	1154	0.247	1.79	19.3	43.2	1512	18.1	2.08	0.97	1.11	1.99
18-Aug	1418	0.441	1.94	21.6	36.3	1251	20.7	2.45	0.94	1.51	2.91
18-Aug	1626	0.670	1.96	21.0	31.8	586	21.1	2.51	0.79	1.72	3.37
18-Aug	1904	0.138	0.64	8.4	69.8	147	15.2	1.73	0.77	0.96	0.61
17-Aug	1001	0.463	2.89	18.0	37.3	1431	15.1	1.72	0.77	0.95	2.74
17-Aug	1334	0.488	2.54	21.2	27.6	1349	18.7	2.17	0.70	1.47	3.73
17-Aug	1604	0.528	2.00	21.4	21.8	785	19.8	2.32	0.56	1.76	3.51
17-Aug	1809	0.377	0.74	17.6	31.9	148	19.0	2.20	0.64	1.56	1.15
17-Aug	2009	0.131	0.23	4.3	73.0	122	13.4	1.54	0.61	0.94	0.22
18-Aug	934										
18-Aug	942	0.282	1.58	18.2	35.4	1338	12.9	1.49	0.74	0.74	1.18
18-Aug	1224	0.304	1.32	21.9	28.2	1474	16.9	1.92	0.75	1.18	1.55
18-Aug	1449	0.203	1.31	23.4	26.0	1127	19.7	2.31	0.75	1.56	2.04
18-Aug	1649	0.485	1.02	21.2	26.7	381	20.1	2.36	0.67	1.68	1.72
18-Aug	1949										
Pan #4											
18-Aug	1156	0.459	3.06	19.6	42.3	1764	19.2	2.23	0.97	1.27	3.87
18-Aug	1420	0.751	3.46	21.7	35.8	1439	22.3	2.71	0.93	1.78	6.15
18-Aug	1628	0.808	3.36	20.7	31.9	645	21.9	2.64	0.78	1.86	6.24
18-Aug	1906	0.177	1.15	7.7	71.7	180	11.8	1.39	0.76	0.63	0.73
17-Aug	1003										
17-Aug	1005	0.594	4.58	16.1	36.4	1687	15.0	1.71	0.76	0.95	4.34
17-Aug	1336	0.772	4.42	21.2	27.0	1561	20.2	2.37	0.68	1.69	7.48
17-Aug	1606	0.898	3.59	21.3	21.5	885	20.9	2.48	0.54	1.94	6.96
17-Aug	1811	0.555	1.56	17.1	31.6	149	19.3	2.25	0.62	1.63	2.55
17-Aug	2011	0.130	0.49	3.6	74.7	152	9.4	1.18	0.59	0.59	0.29
18-Aug	936										
18-Aug	944	0.339	2.69	18.8	34.1	1581	11.3	1.34	0.74	0.60	1.61
18-Aug	1226	0.490	2.34	22.6	27.5	1716	18.6	2.15	0.76	1.39	3.24
18-Aug	1451	0.571	2.47	23.6	25.5	1293	22.3	2.70	0.75	1.95	4.83
18-Aug	1651	0.759	2.15	20.9	26.1	411	21.8	2.62	0.65	1.97	4.23
18-Aug	1951										

Site D: 580 Pool Data Set

13 August 1998 Clear sky
14 August 1998 Mostly sunny, windy
15 August 1998 Clear sky, windy

Date	Time	Evaporation rate (mm/hr)	Windspeed V (m/s)	Air temp. Ta (C)	Relative humidity Rh (%)	Photosynth. active radiation (mmol/m^2/s)	Water temp. Ts (C)	Vap. pres. of water surface Es (Kpa)	Vap. pres. of air Ea (Kpa)	Vap. pres. deficit Es-Ea (Kpa)	Wind x Vap. pres. deficit V*(Es-Ea) ((m/s)* Kpa)
Pan #1											
13-Aug	1055	0.294	1.50	31.5	24.2	1689	19.9	2.33	1.12	1.21	1.82
13-Aug	1355	0.456	1.67	33.5	21.1	1481	23.8	2.95	1.09	1.86	3.11
13-Aug	1612	0.575	1.78	32.2	23.1	651	24.9	3.16	1.12	2.04	3.63
13-Aug	1908	0.148	0.21	13.1	73.5	146	18.7	2.16	1.11	1.05	0.22
14-Aug	932	0.248	0.72	28.5	30.3	1448	17.9	2.06	1.18	0.87	0.63
14-Aug	1218	0.326	2.54	31.6	25.8	1656	21.4	2.56	1.21	1.35	3.44
14-Aug	1418	0.622	3.08	32.0	24.1	1384	23.7	2.94	1.15	1.78	5.51
14-Aug	1618	0.787	2.95	31.2	22.3	726	24.0	2.99	1.01	1.98	5.83
14-Aug	1852	0.171	0.28	13.0	70.1	125	18.2	2.09	1.05	1.04	0.29
15-Aug	907										
15-Aug	920	0.331	2.23	24.0	35.1	1511	17.5	2.00	1.05	0.95	2.12
15-Aug	1250	0.244	2.14	28.6	26.9	1609	21.9	2.63	1.06	1.57	3.37
15-Aug	1524	0.739	3.36	28.7	25.6	1088	23.5	2.91	1.01	1.90	6.38
15-Aug	1804	0.612	2.85	24.6	35.0	210	22.5	2.74	1.08	1.65	4.70
15-Aug	1950	0.281	2.87	13.2	64.8	181	16.1	1.83	0.98	0.85	2.44
16-Aug	1022										
Pan #2											
13-Aug	1057	0.373	1.69	33.6	20.9	1649	21.6	2.59	1.09	1.49	2.51
13-Aug	1357	0.760	1.91	35.1	18.5	1410	27.3	3.64	1.05	2.59	4.95
13-Aug	1614	0.847	1.92	32.5	21.5	605	28.1	3.81	1.06	2.75	5.30
13-Aug	1910	0.205	0.49	12.6	73.2	148	18.2	2.09	1.07	1.02	0.50
14-Aug	934	0.287	1.55	30.7	27.9	1464	18.1	2.08	1.24	0.84	1.31
14-Aug	1220	0.690	2.73	33.3	23.2	1607	24.6	3.10	1.19	1.91	5.21
14-Aug	1420	0.978	3.32	33.2	21.8	1296	27.3	3.64	1.11	2.52	8.37
14-Aug	1620	1.054	3.12	31.5	20.6	635	26.7	3.52	0.95	2.56	8.00
14-Aug	1854	0.193	0.59	12.7	69.6	118	17.3	1.98	1.02	0.96	0.56
15-Aug	909										
15-Aug	922	0.389	2.35	25.5	31.9	1541	18.1	2.08	1.04	1.03	2.44
15-Aug	1252	0.675	2.41	30.2	24.1	1583	25.0	3.17	1.04	2.14	5.15
15-Aug	1526	0.977	3.55	29.2	24.1	936	26.0	3.38	0.98	2.40	8.55
15-Aug	1806	0.851	3.03	24.2	34.2	116	23.8	2.95	1.04	1.91	5.79
15-Aug	1952	0.280	3.06	13.0	64.2	225	13.9	1.59	0.97	0.62	1.91
16-Aug	1024										
Pan #3											
13-Aug	1120	0.272	0.80	31.6	22.3	1468	20.0	2.35	1.04	1.31	1.04
13-Aug	1359	0.397	0.87	33.4	19.3	1299	23.6	2.92	1.00	1.92	1.68
13-Aug	1616	0.436	0.70	32.1	21.4	594	24.8	3.15	1.03	2.12	1.47
13-Aug	1912	0.143	0.20	13.6	67.9	117	18.8	2.18	1.06	1.12	0.22
14-Aug	936	0.226	0.61	28.5	28.9	1258	17.8	2.04	1.13	0.91	0.55
14-Aug	1222	0.313	1.16	31.7	24.8	1432	21.2	2.52	1.17	1.36	1.58
14-Aug	1422	0.428	1.42	32.0	23.0	1186	23.5	2.91	1.10	1.81	2.57
14-Aug	1622	0.659	1.29	30.9	20.8	619	24.0	2.99	0.93	2.06	2.65
14-Aug	1856	0.144	0.22	13.7	64.7	93	18.3	2.10	1.01	1.09	0.24
15-Aug	911										
15-Aug	924	0.269	1.02	24.0	34.1	1311	17.3	1.98	1.02	0.96	0.99
15-Aug	1254	0.527	1.17	28.6	25.5	1380	21.7	2.61	1.00	1.61	1.87
15-Aug	1538	0.491	1.40	28.4	24.5	878	23.4	2.89	0.95	1.94	2.71
15-Aug	1808	0.512	0.97	24.4	33.4	146	22.6	2.75	1.02	1.73	1.67
15-Aug	1954	0.223	1.23	13.2	62.8	179	16.1	1.84	0.96	0.88	1.08
16-Aug	1026										
Pan #4											
13-Aug	1122	0.482	1.66	32.8	20.2	1720	21.9	2.64	1.01	1.63	2.71
13-Aug	1401	0.953	1.88	34.5	17.7	1479	27.3	3.64	0.97	2.67	5.02
13-Aug	1618	0.980	1.88	32.2	20.3	651	28.1	3.82	0.98	2.84	5.33
13-Aug	1914	0.219	0.48	13.2	68.3	147	18.2	2.09	1.04	1.05	0.51
14-Aug	938										
14-Aug	940	0.323	1.57	30.2	26.4	1486	18.6	2.15	1.14	1.02	1.60
14-Aug	1224	0.864	2.82	32.2	23.4	1663	25.0	3.18	1.13	2.05	5.78
14-Aug	1424	1.215	3.36	32.3	21.8	1370	27.3	3.63	1.06	2.57	8.66
14-Aug	1624	1.321	3.23	30.9	20.1	688	26.7	3.51	0.90	2.60	8.40
14-Aug	1858	0.209	0.50	13.3	65.0	117	17.5	2.00	0.99	1.01	0.50
15-Aug	913										
15-Aug	926	0.426	2.38	24.5	32.4	1576	18.3	2.11	1.00	1.11	2.63
15-Aug	1256	0.896	2.47	29.3	23.9	1650	24.8	3.14	0.98	2.17	5.37
15-Aug	1530	1.132	3.61	28.4	24.0	994	25.8	3.34	0.93	2.41	8.68
15-Aug	1810	0.885	3.01	24.1	33.7	133	23.7	2.94	1.02	1.92	5.78
15-Aug	1956	0.305	3.08	12.9	63.8	223	14.0	1.60	0.95	0.65	2.00
16-Aug	1028										

Site E: Lower Phipps Meadow Data Set

21 July 1998 Clear skies
22 July 1998 Clear Skies
23 July 1998 Very overcast/ off and on drizzle most of day
24 July 1998 Clear skies most of day/some afternoon cloud cover

Date	Time	Evaporation rate (mm/hr)	Windspeed V (m/s)	Air temp. Ta (C)	Relative humidity Rh (%)	Photosynth. active radiation m mol/m^2/s	Water temp. Ts (C)	Vap. pres. of water surface Es (Kpa)	Vap. pres. of air Ea (Kpa)	Vap. pres. deficit Es-Ea (Kpa)	Wind x Vap. pres. deficit V*(Es-Ea) I(m/s)* Kpa
Pan #1											
21-Jul	**1220**	**0.412**	**0.97**	**30.7**	**20.1**	**1837**	**21.8**	**2.62**	**0.89**	**1.73**	**1.67**
21-Jul	**1430**	**0.416**	**0.88**	**31.9**	**20.2**	**1595**	**24.0**	**2.99**	**0.96**	**2.03**	**1.79**
21-Jul	**1610**	**0.485**	**0.62**	**31.5**	**20.9**	**1013**	**24.5**	**3.08**	**0.97**	**2.12**	**1.31**
21-Jul	1825	0.149	0.23	116	75.4	88	18.4	2.12	103	109	0.25
22-Jul	848										
22-Jul	**915**	**0.097**	**0.29**	**24.4**	**36.3**	**1457**	**16.7**	**1.91**	**1.11**	**0.79**	**0.23**
22-Jul	**1115**	**0.285**	**0.75**	**29.6**	**26.3**	**1809**	**20.2**	**2.38**	**1.09**	**1.28**	**0.96**
22-Jul	**1325**	**0.391**	**0.81**	**31.6**	**23.7**	**1751**	**23.4**	**2.88**	**1.11**	**1.78**	**1.44**
22-Jul	**1522**	**0.422**	**0.68**	**31.9**	**21.7**	**1129**	**24.8**	**3.15**	**1.03**	**2.12**	**1.45**
22-Jul	**1826**	**0.159**	**0.25**	**14.8**	**72.9**	**87**	**19.3**	**2.25**	**1.23**	**1.01**	**0.26**
23-Jul	900										
23-Jul	1400										
23-Jul	1828	0.042	0.21	114	88.6	100	15.8	180	1.19	0.60	0.12
24-Jul	**920**	**0.252**	**0.55**	**23.0**	**51.5**	**1461**	**16.0**	**1.82**	**1.45**	**0.37**	**0.20**
24-Jul	**1123**	**0.167**	**0.74**	**27.1**	**39.9**	**1816**	**19.5**	**2.27**	**1.44**	**0.83**	**0.62**
24-Jul	**1325**	**0.325**	**1.02**	**29.8**	**32.4**	**1762**	**23.1**	**2.83**	**1.36**	**1.47**	**1.50**
24-Jul	**1558**	**0.409**	**1.01**	**29.2**	**32.3**	**932**	**24.5**	**3.08**	**1.31**	**1.77**	**1.79**
24-Jul	1913										
Pan #2											
21-Jul	**1225**	**0.722**	**1.96**	**32.5**	**17.8**	**1797**	**23.0**	**2.82**	**0.87**	**1.94**	**3.81**
21-Jul	**1433**	**0.667**	**1.99**	**33.1**	**18.1**	**1535**	**26.6**	**3.49**	**0.92**	**2.57**	**5.12**
21-Jul	**1615**	**0.720**	**1.72**	**31.9**	**19.2**	**964**	**27.7**	**3.73**	**0.91**	**2.82**	**4.85**
21-Jul	1827	0.220	0.27	10.7	78.0	145	19.2	2.23	101	123	0.33
22-Jul	850										
22-Jul	**917**	**0.152**	**0.42**	**28.5**	**30.4**	**1465**	**16.9**	**1.93**	**1.19**	**0.73**	**0.31**
22-Jul	**1117**	**0.453**	**1.47**	**32.0**	**23.2**	**1782**	**22.1**	**2.67**	**1.10**	**1.56**	**2.30**
22-Jul	**1327**	**0.667**	**1.90**	**33.1**	**21.3**	**1699**	**27.1**	**3.61**	**1.08**	**2.53**	**4.82**
22-Jul	**1525**	**0.801**	**1.70**	**32.5**	**19.9**	**1079**	**29.1**	**4.04**	**0.98**	**3.06**	**5.20**
22-Jul	**1829**	**0.215**	**0.30**	**14.0**	**73.9**	**111**	**20.7**	**2.45**	**1.19**	**1.27**	**0.38**
23-Jul	902										
23-Jul	1402										
23-Jul	1830	0.070	0.22	10.6	93.7	126	15.8	180	120	0.61	0.13
24-Jul	922										
24-Jul	**925**	**0.174**	**1.20**	**25.2**	**46.3**	**1485**	**15.8**	**1.79**	**1.49**	**0.31**	**0.37**
24-Jul	**1125**	**0.293**	**1.58**	**29.3**	**35.6**	**1792**	**21.0**	**2.50**	**1.45**	**1.05**	**1.65**
24-Jul	**1328**	**0.511**	**1.79**	**31.3**	**29.8**	**1715**	**26.9**	**3.56**	**1.37**	**2.19**	**3.92**
24-Jul	**1602**	**0.825**	**1.47**	**29.6**	**30.1**	**890**	**29.2**	**4.07**	**1.26**	**2.81**	**4.14**
24-Jul	1916										
Pan #3											
21-Jul	**1235**	**0.398**	**1.26**	**30.4**	**19.1**	**1656**	**22.0**	**2.66**	**0.63**	**1.83**	**2.31**
21-Jul	**1435**	**0.489**	**1.25**	**31.2**	**19.6**	**1419**	**24.1**	**3.00**	**0.89**	**2.11**	**2.63**
21-Jul	**1620**	**0.457**	**0.93**	**31.0**	**20.1**	**868**	**24.4**	**3.07**	**0.91**	**2.17**	**2.02**
21-Jul	1830	0.166	0.22	11.8	73.4	108	18.3	2.11	102	109	0.24
22-Jul	855										
22-Jul	**907**	**0.134**	**0.28**	**24.8**	**33.0**	**1323**	**16.7**	**1.91**	**1.04**	**0.87**	**0.25**
22-Jul	**1120**	**0.277**	**0.89**	**29.5**	**24.7**	**1657**	**20.4**	**2.40**	**1.02**	**1.38**	**1.23**
22-Jul	**1330**	**0.525**	**1.28**	**31.0**	**22.6**	**1576**	**23.5**	**2.90**	**1.02**	**1.88**	**2.41**
22-Jul	**1528**	**0.434**	**0.84**	**31.4**	**21.1**	**986**	**24.8**	**3.14**	**0.98**	**2.16**	**1.82**
22-Jul	1833	0.149	0.23	14.9	71.8	83	19.2	2.23	122	102	0.23
23-Jul	905										
23-Jul	1404										
23-Jul	1832	0.056	0.22	11.6	85.3	113	15.8	179	1.16	0.63	0.14
24-Jul	926										
24-Jul	**928**	**0.098**	**0.77**	**23.1**	**48.7**	**1368**	**16.1**	**1.84**	**1.38**	**0.46**	**0.35**
24-Jul	**1127**	**0.225**	**0.85**	**26.9**	**38.3**	**1660**	**19.7**	**2.30**	**1.36**	**0.93**	**0.79**
24-Jul	**1331**	**0.362**	**0.89**	**29.3**	**31.9**	**1584**	**23.2**	**2.85**	**1.30**	**1.55**	**1.38**
24-Jul	**1604**	**0.458**	**0.77**	**29.4**	**30.4**	**809**	**24.4**	**3.07**	**1.25**	**1.82**	**1.40**
24-Jul	1918										
Pan #4											
21-Jul	**1240**	**0.419**	**2.03**	**31.5**	**17.5**	**1879**	**23.5**	**2.91**	**0.61**	**2.10**	**4.26**
21-Jul	**1440**	**0.563**	**1.96**	**32.0**	**18.2**	**1593**	**27.0**	**3.57**	**0.87**	**2.70**	**5.30**
21-Jul	**1622**	**0.857**	**1.67**	**31.2**	**18.9**	**980**	**28.1**	**3.82**	**0.86**	**2.96**	**4.94**
21-Jul	1833	0.218	0.25	10.8	76.3	154	18.9	2.19	0.99	120	0.30
22-Jul	858										
22-Jul	**910**	**0.050**	**0.38**	**27.6**	**28.5**	**1513**	**16.3**	**1.85**	**1.06**	**0.79**	**0.30**
22-Jul	**1122**	**0.297**	**1.44**	**31.0**	**22.6**	**1866**	**21.7**	**2.61**	**1.02**	**1.58**	**2.27**
22-Jul	**1332**	**0.758**	**2.01**	**31.9**	**21.1**	**1776**	**26.9**	**3.56**	**1.00**	**2.56**	**5.13**
22-Jul	**1530**	**0.514**	**1.59**	**31.8**	**19.7**	**1112**	**29.0**	**4.02**	**0.93**	**3.10**	**4.92**
22-Jul	**1835**	**0.247**	**0.28**	**14.0**	**72.9**	**114**	**20.5**	**2.41**	**1.17**	**1.25**	**0.35**
23-Jul	907										
23-Jul	1407										
23-Jul	1835										
23-Jul	1840	0.076	0.23	10.4	92.5	141	15.6	178	1.17	0.61	0.14
24-Jul	**930**	**0.076**	**1.24**	**24.3**	**46.1**	**1562**	**15.4**	**1.75**	**1.41**	**0.35**	**0.43**
24-Jul	**1130**	**0.270**	**1.62**	**28.0**	**35.8**	**1884**	**20.7**	**2.45**	**1.36**	**1.09**	**1.76**
24-Jul	**1334**	**0.618**	**1.78**	**30.2**	**29.9**	**1795**	**26.7**	**3.51**	**1.29**	**2.23**	**3.97**
24-Jul	**1607**	**0.663**	**1.42**	**29.3**	**29.2**	**912**	**29.0**	**4.02**	**1.20**	**2.83**	**4.01**
24-Jul	1921										

Site F: Mid-Phipps Meadow Data Set

25 July 1998 Clear skies
26 July 1998 Rain off and on
27 July 1998 Somewhat cloudy, windy at times
28 July 1998 Somewhat cloudy at times, extremely windy evening

Date	Time	Evaporation rate (mm/hr)	Windspeed V (m/s)	Air temp. Ta (C)	Relative humidity Rh (%)	Photosynth. active radiation (m mol/m^2/s)	Water temp. Ts (C)	Vap. pres. of water surface Es (Kpa)	Vap. pres. of air Ea (Kpa)	Vap. pres. deficit Es-Ea (Kpa)	Wind * Vap. pres. deficit V*(Es-Ea) [(m/s)* Kpa]
Pan #1											
25-Jul	1508	0.610	1.39	31.37	20.87	1338	25.54	3.28	0.96	2.32	3.22
25-Jul	1708	0.432	0.96	30.89	23.10	657	25.77	3.33	1.03	2.29	2.19
25-Jul	1908	0.130	0.21	14.31	75.10	173	19.75	2.31	1.23	1.08	0.22
26-Jul	930										
26-Jul	1255										
26-Jul	1835										
27-Jul	923	0.218	0.49	28.65	37.91	1581	18.01	2.07	1.49	0.58	0.28
27-Jul	1159										
27-Jul	1501	0.390	1.41	29.37	30.48	1114	22.94	2.81	1.25	1.56	2.19
27-Jul	1744	0.221	0.60	26.45	39.18	294	23.11	2.84	1.36	1.48	0.89
27-Jul	2009	0.120	0.20	12.25	79.80	172	17.81	2.04	1.14	0.90	0.18
28-Jul	930										
28-Jul	933	0.200	0.49	29.36	29.73	1631	18.45	2.13	1.22	0.91	0.44
28-Jul	1231	0.381	1.23	29.35	27.57	849	22.54	2.74	1.13	1.61	1.98
28-Jul	1631	0.462	1.73	28.54	29.02	594	23.03	2.82	1.14	1.69	2.92
28-Jul	1940										
Pan #2											
25-Jul	1247	0.568	2.17	32.08	19.51	1737	26.05	3.38	0.94	2.45	5.31
25-Jul	1510	0.948	1.77	32.34	19.19	1320	28.58	3.92	0.93	2.99	5.29
25-Jul	1710	0.733	1.27	30.95	21.07	652	28.54	3.91	0.95	2.97	3.78
25-Jul	1912	0.191	0.23	13.36	78.64	173	19.81	2.32	1.21	1.11	0.26
26-Jul	932										
26-Jul	941										
26-Jul	1257										
26-Jul	1837										
27-Jul	925	0.264	0.71	30.92	34.82	1538	18.65	2.16	1.56	0.59	0.42
27-Jul	1201										
27-Jul	1503	0.629	1.81	30.17	28.07	1082	26.40	3.45	1.21	2.25	4.06
27-Jul	1746	0.431	1.18	26.70	35.53	300	26.08	3.39	1.25	2.14	2.53
27-Jul	2011	0.141	0.22	11.39	85.15	177	18.04	2.07	1.15	0.92	0.20
28-Jul	936										
28-Jul	937	0.266	0.73	31.58	27.49	1591	19.23	2.23	1.28	0.95	0.70
28-Jul	1233	0.552	1.68	29.98	25.86	827	25.02	3.18	1.10	2.08	3.50
28-Jul	1633	0.702	2.35	28.83	27.94	584	25.67	3.31	1.11	2.19	5.16
28-Jul	1942										
Pan #3											
25-Jul	1250	0.354	0.54	31.28	21.83	1614	23.15	2.84	1.00	1.84	0.99
25-Jul	1512	0.567	0.38	31.36	21.92	1213	25.32	3.24	1.01	2.23	0.84
25-Jul	1712	0.400	0.23	29.88	26.49	573	25.54	3.28	1.12	2.16	0.50
25-Jul	1914	0.137	0.20	13.83	75.79	146	19.71	2.30	1.20	1.10	0.22
26-Jul	926										
26-Jul	943										
26-Jul	1300										
26-Jul	1839										
27-Jul	927	0.166	0.21	29.16	35.98	1436	18.02	2.07	1.46	0.61	0.13
27-Jul	1203										
27-Jul	1505	0.309	0.56	29.30	30.91	970	22.85	2.79	1.26	1.53	0.85
27-Jul	1748	0.345	0.52	25.76	40.05	244	22.95	2.81	1.33	1.48	0.77
27-Jul	2014	0.115	0.20	12.17	79.33	164	17.82	2.05	1.13	0.92	0.18
28-Jul	939	0.199	0.26	29.54	28.49	1496	18.29	2.11	1.18	0.93	0.24
28-Jul	1235	0.345	0.37	28.99	28.47	765	22.29	2.70	1.14	1.56	0.57
28-Jul	1635	0.430	0.71	27.95	30.11	501	22.96	2.81	1.14	1.67	1.19
28-Jul	1944										
Pan #4											
25-Jul	1257	0.593	2.09	32.15	18.89	1783	26.29	3.43	0.91	2.52	5.28
25-Jul	1515	0.745	1.70	32.23	18.16	1344	28.75	3.96	0.88	3.08	5.25
25-Jul	1715	0.722	1.12	30.81	20.13	651	28.80	3.97	0.90	3.07	3.44
25-Jul	1916	0.174	0.21	13.39	77.71	171	20.10	2.36	1.20	1.16	0.24
26-Jul	929										
26-Jul	945										
26-Jul	1302										
26-Jul	1841										
27-Jul	929	0.203	0.58	30.78	33.17	1606	19.54	2.28	1.48	0.80	0.47
27-Jul	1204										
27-Jul	1507	0.661	1.70	29.87	27.66	1094	26.86	3.55	1.17	2.38	4.05
27-Jul	1750	0.422	1.02	26.23	35.41	300	26.39	3.45	1.21	2.24	2.30
27-Jul	2018	0.154	0.20	11.52	83.73	191	18.06	2.08	1.14	0.94	0.19
28-Jul	941										
28-Jul	943	0.236	0.63	31.52	25.80	1675	20.22	2.38	1.20	1.18	0.74
28-Jul	1237	0.572	1.63	29.78	25.08	855	25.63	3.30	1.05	2.25	3.66
28-Jul	1637	0.653	2.37	28.51	27.10	589	25.96	3.36	1.06	2.31	5.46
28-Jul	1946										

Site G: Upper-Phipps Meadow Data Set

2 August 1998 Clear sky conditions all day
3 August 1998 Clear sky conditions
4 August 1998 Clear sky conditions, windy
5 August 1998 Clear sky conditions, windy

Date	Time	Evaporation rate (mm/hr)	Windspeed V(m/s)	Air temp. Ta(C)	Relative humidity Rh(%)	Photosynth. active radiation (mmol/m^2/s)	Water temp. Ts(C)	Vap. pres. of water surface Es(Kpa)	Vap. pres. of air Ea(Kpa)	Vap. pres. deficit Es-Ea(Kpa)	Wind x Vap. pres. deficit V*(Es-Ea) [(m/s)*Kpa]
Pan#1											
2-Aug	932	0.307	0.39	23.6	32.5	1529	18.6	1.90	0.96	0.94	0.36
2-Aug	1146	0.327	0.73	27.3	26.0	1603	20.3	2.39	0.95	1.45	1.06
2-Aug	1344	0.322	0.77	29.3	23.6	1646	23.6	2.92	0.97	1.95	1.49
2-Aug	1552	0.266	0.42	29.9	24.1	1116	25.2	3.22	1.02	2.20	0.92
2-Aug	1745	0.156	0.22	27.5	37.8	328	24.5	3.09	1.39	1.70	0.37
2-Aug	1928	0.124	0.20	11.0	83.8	139	17.8	2.02	1.10	0.92	0.19
3-Aug	939	0.172	0.50	26.0	35.2	1575	18.2	2.10	1.33	0.76	0.36
3-Aug	1227	0.437	0.82	31.0	26.2	1792	22.5	2.73	1.18	1.55	0.95
3-Aug	1414	0.373	0.83	32.3	24.4	1537	25.2	3.21	1.19	2.02	1.27
3-Aug	1618	0.294	0.35	31.0	29.9	660	25.8	3.34	1.35	1.99	0.69
3-Aug	1923	0.122	0.22	12.4	83.4	127	18.8	2.18	1.20	0.98	0.21
4-Aug	930	0.324	0.79	29.4	31.7	1602	19.6	2.29	1.31	0.98	0.76
4-Aug	1311	0.550	0.86	32.6	25.6	1711	24.4	3.06	1.27	1.79	1.56
4-Aug	1512	0.852	0.86	33.1	24.1	1306	26.1	3.36	1.23	2.16	1.89
4-Aug	1704	0.505	0.56	30.1	27.6	387	24.9	3.15	1.16	1.97	1.14
4-Aug	2004	0.141	0.25	12.8	80.5	125	18.7	2.18	1.19	0.97	0.24
5-Aug	939										
5-Aug	941	0.329	0.79	29.7	30.9	1551	19.4	2.26	1.29	0.97	0.76
5-Aug	1214	0.466	0.62	33.2	26.1	1504	23.3	2.67	1.33	1.54	0.96
5-Aug	1423	0.391	1.29	33.4	22.6	1130	24.9	3.15	1.17	1.98	2.58
5-Aug	1633	0.429	0.93	30.6	26.6	431	24.3	3.05	1.19	1.87	1.74
5-Aug	2007										
Pan#2											
2-Aug	935	0.126	0.75	26.4	27.5	1520	17.2	1.97	0.95	1.02	0.76
2-Aug	1146	0.543	1.24	29.1	22.6	1777	22.6	2.79	0.92	1.87	2.32
2-Aug	1345	0.571	1.13	30.7	21.1	1620	27.0	3.56	0.94	2.64	2.99
2-Aug	1554	0.726	0.90	31.1	20.9	1103	29.0	4.02	0.94	3.08	2.76
2-Aug	1747	0.402	0.34	30.1	25.6	485	26.9	4.01	1.10	2.91	0.99
2-Aug	1928	0.164	0.21	10.8	87.0	168	18.5	2.14	1.13	1.01	0.21
3-Aug	941	0.306	1.12	30.2	29.9	1565	20.0	2.35	1.29	1.06	1.19
3-Aug	1229	0.542	1.26	32.6	22.7	1764	26.4	3.46	1.13	2.33	2.93
3-Aug	1416	0.777	1.22	33.7	21.5	1515	29.7	4.16	1.13	3.05	3.73
3-Aug	1620	0.571	0.62	32.6	23.4	724	30.6	4.40	1.16	3.24	2.03
3-Aug	1925	0.200	0.29	12.2	87.5	158	19.8	2.31	1.24	1.07	0.31
4-Aug	932										
4-Aug	934	0.520	2.23	30.7	26.0	1595	22.2	2.66	1.24	1.44	3.21
4-Aug	1313	0.936	2.34	33.4	22.6	1666	26.2	3.63	1.17	2.66	6.22
4-Aug	1513	1.043	2.35	33.6	21.5	1293	29.7	4.20	1.12	3.07	7.22
4-Aug	1706	0.661	1.76	30.9	24.1	469	26.4	3.67	1.06	2.79	4.96
4-Aug	2006	0.169	0.48	12.4	82.4	146	17.8	2.05	1.19	0.86	0.41
5-Aug	943										
5-Aug	945	0.457	2.30	31.0	27.2	1552	20.4	2.40	1.23	1.17	2.71
5-Aug	1216	0.662	1.60	34.7	22.4	1462	26.6	3.49	1.24	2.25	3.59
5-Aug	1425	0.960	2.54	34.5	19.9	1137	26.5	3.91	1.09	2.81	7.14
5-Aug	1635	0.666	1.96	31.7	23.6	491	27.3	3.63	1.11	2.52	5.00
5-Aug	2009										
Pan#3											
2-Aug	939	0.213	0.35	24.4	29.1	1416	16.7	1.91	0.89	1.01	0.35
2-Aug	1150	0.374	0.54	27.6	23.9	1637	20.4	2.40	0.90	1.50	0.82
2-Aug	1346	0.335	0.39	29.4	22.7	1470	23.7	2.93	0.94	2.00	0.78
2-Aug	1557	0.331	0.36	30.0	22.1	979	25.3	3.23	0.94	2.28	0.87
2-Aug	1749	0.251	0.21	26.8	31.6	390	24.6	3.10	1.25	1.84	0.39
2-Aug	1932	0.140	0.20	11.4	80.7	149	17.5	2.01	1.09	0.92	0.18
3-Aug	942	0.255	0.42	26.5	31.6	1436	16.3	2.10	1.23	0.87	0.37
3-Aug	1231	0.399	0.50	31.1	24.5	1610	22.5	2.74	1.11	1.63	0.81
3-Aug	1416	0.411	0.46	32.3	22.7	1366	25.3	3.23	1.10	2.13	0.98
3-Aug	1623	0.375	0.26	31.4	27.4	624	25.9	3.36	1.27	2.10	0.55
3-Aug	1927	0.135	0.22	12.8	80.4	140	18.7	2.17	1.19	0.98	0.22
4-Aug	936										
4-Aug	936	0.345	0.97	29.6	29.0	1476	19.6	2.31	1.21	1.10	1.06
4-Aug	1316	0.741	1.14	32.3	23.7	1537	24.5	3.06	1.15	1.93	2.19
4-Aug	1516	0.635	0.97	32.7	22.6	1158	26.1	3.40	1.12	2.28	2.22
4-Aug	1706	0.466	0.62	30.0	26.1	401	25.1	3.21	1.12	2.09	1.29
4-Aug	2008	0.119	0.25	13.1	77.1	135	18.6	2.15	1.17	0.98	0.24
5-Aug	947	0.566	1.02	29.9	26.3	1427	19.5	2.27	1.20	1.07	1.09
5-Aug	1218	0.209	0.56	33.2	24.0	1340	23.4	2.89	1.22	1.67	0.93
5-Aug	1427	0.734	1.50	33.5	21.1	1022	24.9	3.16	1.10	2.06	3.10
5-Aug	1637	0.567	0.96	30.6	25.0	425	24.4	3.07	1.12	1.95	1.86
5-Aug	2011										
Pan#4											
2-Aug	942	0.231	0.60	26.6	26.1	1567	17.5	2.01	0.92	1.09	0.65
2-Aug	1152	0.435	1.03	29.4	21.0	1637	22.6	2.75	0.87	1.89	1.95
2-Aug	1350	0.504	0.82	30.7	19.6	1652	27.3	3.64	0.86	2.77	2.27
2-Aug	1559	0.540	0.87	31.2	19.2	1097	29.6	4.16	0.86	3.29	2.20
2-Aug	1752	0.453	0.25	30.0	23.6	435	29.6	4.16	1.00	3.16	0.80
2-Aug	1933	0.160	0.20	10.9	84.5	181	19.5	2.27	1.11	1.17	0.24
3-Aug	944	0.304	0.91	30.0	26.9	1636	19.4	2.26	1.23	1.03	0.94
3-Aug	1233	0.451	1.07	32.4	22.0	1620	25.9	3.35	1.06	2.27	2.43
3-Aug	1420	0.622	1.01	33.4	20.3	1537	29.9	4.23	1.05	3.16	3.21
3-Aug	1625	0.507	0.46	32.4	22.7	711	31.1	4.55	1.11	3.43	1.57
3-Aug	1929	0.193	0.29	12.3	84.9	175	20.8	2.46	1.22	1.24	0.37
4-Aug	940										
4-Aug	943	0.354	2.09	30.3	27.3	1676	21.6	2.59	1.18	1.41	2.95
4-Aug	1316	0.859	2.31	32.6	22.1	1730	26.1	3.62	1.10	2.71	6.27
4-Aug	1516	0.907	2.15	33.1	21.1	1303	29.7	4.19	1.07	3.12	6.71
4-Aug	1710	0.796	1.49	30.5	24.0	455	26.7	3.94	1.06	2.89	4.31
4-Aug	2010	0.153	0.42	12.4	80.1	163	18.8	2.18	1.16	1.02	0.43
5-Aug	949										
5-Aug	951	0.365	2.13	30.6	26.7	1627	19.6	2.31	1.18	1.13	2.42
5-Aug	1220	0.563	1.30	34.2	21.6	1509	25.6	3.34	1.18	2.16	2.80
5-Aug	1429	0.979	2.81	34.5	18.5	1173	26.2	3.64	1.02	2.62	7.37
5-Aug	1639	0.743	1.69	31.5	22.6	463	27.3	3.63	1.05	2.58	4.66
5-Aug	2012										

Site H: Lower Squaw Creek Data Set

6 September 1998 Hot, somewhat cloudy
7 September 1998 Clear, hot
8 September 1998 Some clouds, hot

Date	Time	Evaporation rate (mm/hr)	Windspeed V (m/s)	Air temp. Ta (C)	Relative humidity Rh (%)	Photosynth. active radiation (m mol/m^2/s)	Water temp. Ts (C)	Vap. Pres. of water surface Es (Kpa)	Vap. pres. of air Ea (Kpa)	Vap. pres. deficit Es-Ea (Kpa)	Wind x Vap. pres. deficit V*(Es-Ea) [(m/s)* Kpa]
Pan #1											
6-Sep	1100	0.188	0.90	28.7	33.6	1270	18.6	2.15	1.33	0.82	0.74
6-Sep	1420	0.301	0.99	29.1	34.2	997	21.3	2.55	1.38	1.17	1.15
6-Sep	1620	0.192	0.36	25.0	46.1	283	20.7	2.45	1.47	0.98	0.35
6-Sep	1920	0.009	0.20	13.2	89.0	40	15.0	1.71	1.35	0.36	0.07
7-Sep	940	0.087	0.69	25.5	51.6	1070	16.8	1.92	1.69	0.23	0.16
7-Sep	1240	0.186	0.54	25.7	46.6	800	20.5	2.42	1.55	0.87	0.47
7-Sep	1600	0.211	0.48	24.5	46.4	284	20.2	2.38	1.43	0.95	0.45
7-Sep	1820										
6-Sep	1000	0.083	0.63	22.5	64.9	998	17.5	2.01	1.77	0.23	0.15
8-Sep	1400	0.197	0.73	20.9	58.2	334	19.0	2.20	1.44	0.76	0.55
8-Sep	1640										
Pan #2											
6-Sep	1100										
6-Sep	1420	0.521	1.45	29.7	30.6	992	24.1	3.01	1.28	1.72	2.51
6-Sep	1620	0.412	0.59	26.0	38.0	284	25.2	3.22	1.28	1.94	1.14
6-Sep	1920	0.053	0.21	13.1	88.6	40	18.6	2.15	1.34	0.80	0.17
7-Sep	940	0.246	1.27	25.6	49.6	1056	18.0	2.07	1.63	0.44	0.56
7-Sep	1240	0.325	1.24	25.8	44.2	794	23.0	2.81	1.47	1.34	1.66
7-Sep	1600	0.385	0.79	24.9	42.7	284	24.0	2.99	1.35	1.64	1.30
7-Sep	1820										
8-Sep	1000	0.155	1.29	22.0	65.5	974	18.7	2.17	1.74	0.43	0.56
8-Sep	1400	0.381	1.22	21.1	55.9	331	22.0	2.64	1.40	1.24	1.52
8-Sep	1640										
Pan #3											
6-Sep	1100	0.308	0.45	29.0	30.8	1138	18.6	2.15	1.24	0.91	0.41
6-Sep	1420	0.250	0.35	29.4	31.6	893	21.4	2.55	1.30	1.25	0.43
6-Sep	1620	0.262	0.23	25.4	42.7	253	20.8	2.46	1.39	1.07	0.25
6-Sep	1920	0.017	0.20	13.2	86.7	36	15.0	1.71	1.32	0.39	0.08
7-Sep	940	0.102	0.42	25.6	48.0	965	16.8	1.91	1.58	0.34	0.14
7-Sep	1240	0.216	0.47	25.8	42.7	721	20.5	2.42	1.43	1.00	0.47
7-Sep	1600	0.214	0.30	24.9	42.3	257	20.3	2.38	1.33	1.05	0.31
7-Sep	1820										
8-Sep	1000	0.066	0.46	22.1	63.2	904	17.5	2.01	1.69	0.32	0.15
8-Sep	1400	0.212	0.34	21.1	55.0	302	19.1	2.21	1.38	0.83	0.28
8-Sep	1640										
Pan #4											
6-Sep	1100	0.287	1.52	29.0	29.6	1303	19.7	2.30	1.19	1.11	1.68
6-Sep	1420	0.495	1.73	29.1	30.5	1019	24.5	3.08	1.23	1.85	3.20
8-Sep	1620	0.392	0.66	25.9	37.0	290	25.3	3.24	1.24	2.00	1.32
6-Sep	1920	0.058	0.21	13.3	87.1	41	18.7	2.16	1.33	0.83	0.18
7-Sep	940	0.164	1.24	25.6	47.1	1103	18.5	2.13	1.56	0.58	0.72
7-Sep	1240	0.371	1.19	26.1	41.2	821	23.6	2.93	1.39	1.53	1.83
7-Sep	1600	0.345	0.79	25.1	40.7	291	24.5	3.09	1.30	1.79	1.42
7-Sep	1820										
8-Sep	1000	0.193	1.27	21.9	63.9	1016	19.4	2.26	1.69	0.57	0.73
8-Sep	1400	0.320	1.23	21.0	54.4	343	22.3	2.70	1.36	1.34	1.64
8-Sep	1640										

Site I: Upper Squaw Meadow Data Set

2 September 1998 Clear, hot
3 September 1998 Clear, hot
4 September 1998 Clear, hot
5 September 1998 Some clouds, hot

Date	Time	Evaporation rate (mm/hr)	Windspeed V (m/s)	Air temp. Ta (C)	Relative humidity Rh (%)	Photosynth. active radiation (mmol/m^2/s)	Water temp. Ts (C)	Vap. pres. of water surface Es (Kpa)	Vap. pres. of air Ea (Kpa)	Vap. pres. deficit Es-Ea (Kpa)	Wind x Vap. pres. deficit V*(Es-Ea) [(m/s)* Kpa]
Pan #1											
2-Sep	**1220**	**0.411**	**1.02**	**33.1**	**15.7**	**1434**	**21.0**	**2.49**	**0.80**	**1.69**	**1.73**
2-Sep	**1600**	**0.157**	**0.39**	**14.8**	**63.3**	**345**	**14.0**	**1.60**	**1.07**	**0.53**	**0.21**
3-Sep	**1240**	**0.407**	**1.02**	**33.0**	**17.7**	**1452**	**20.6**	**2.43**	**0.89**	**1.53**	**1.56**
3-Sep	1500	0.000									
3-Sep	**1500**	**0.489**	**0.92**	**31.3**	**18.0**	**666**	**21.1**	**2.51**	**0.83**	**1.68**	**1.54**
3-Sep	1900	0.094	0.20	9.7	83.9	101	13.3	1.53	1.01	0.52	0.10
4-Sep	**1000**	**0.223**	**0.69**	**30.4**	**24.2**	**1418**	**15.8**	**1.80**	**1.06**	**0.75**	**0.51**
4-Sep	**1300**	**0.411**	**0.72**	**34.1**	**17.8**	**1305**	**22.1**	**2.67**	**0.96**	**1.72**	**1.24**
4-Sep	**1640**	**0.292**	**0.35**	**28.9**	**31.7**	**368**	**21.3**	**2.54**	**1.27**	**1.27**	**0.45**
4-Sep	1920	0.095	0.20	9.5	84.3	103	13.2	1.52	1.00	0.52	0.10
5-Sep	**1000**	**0.099**	**0.49**	**29.8**	**29.5**	**1250**	**15.5**	**1.77**	**1.24**	**0.53**	**0.26**
5-Sep	**1300**	**0.361**	**0.96**	**30.2**	**28.2**	**936**	**20.8**	**2.46**	**1.21**	**1.25**	**1.19**
5-Sep	**1620**	**0.296**	**0.58**	**27.9**	**31.0**	**379**	**20.1**	**2.36**	**1.17**	**1.19**	**0.68**
5-Sep	1920	0.070	0.20	9.8	82.4	82	13.5	1.55	1.00	0.55	0.11
6-Sep	920										
Pan #2											
2-Sep	**1220**	**0.579**	**1.34**	**34.7**	**12.6**	**1434**	**23.0**	**2.82**	**0.70**	**2.12**	**2.83**
2-Sep	**1600**	**0.250**	**0.47**	**15.3**	**58.3**	**343**	**18.1**	**2.08**	**1.02**	**1.06**	**0.49**
3-Sep	**1240**	**0.531**	**1.15**	**35.1**	**14.0**	**1447**	**23.7**	**2.94**	**0.80**	**2.15**	**2.46**
3-Sep	**1500**	**0.643**	**0.93**	**32.8**	**14.9**	**675**	**27.4**	**3.66**	**0.74**	**2.92**	**2.70**
3-Sep	1900	0.171	0.22	10.3	69.3	126	17.1	1.95	0.87	1.08	0.24
4-Sep	1000										
4-Sep	**1000**	**0.325**	**0.88**	**32.0**	**20.3**	**1402**	**17.6**	**2.02**	**0.97**	**1.05**	**0.92**
4-Sep	**1300**	**0.586**	**1.05**	**35.8**	**14.0**	**1307**	**25.9**	**3.36**	**0.83**	**2.53**	**2.67**
4-Sep	**1640**	**0.460**	**0.49**	**30.1**	**22.8**	**375**	**28.3**	**3.86**	**0.98**	**2.88**	**1.40**
4-Sep	1920										
5-Sep	**1000**	**0.200**	**0.89**	**30.9**	**26.0**	**1233**	**17.3**	**1.97**	**1.17**	**0.81**	**0.72**
5-Sep	**1300**	**0.442**	**1.27**	**31.4**	**24.6**	**926**	**24.1**	**3.01**	**1.14**	**1.87**	**2.39**
5-Sep	**1620**	**0.437**	**0.80**	**29.0**	**25.7**	**378**	**25.6**	**3.30**	**1.03**	**2.27**	**1.81**
5-Sep	1920	0.154	0.22	9.9	77.3	81	17.5	2.01	0.95	1.06	0.23
6-Sep	920										
Pan #3											
2-Sep	**1220**	**0.284**	**0.40**	**32.8**	**16.8**	**1252**	**21.0**	**2.50**	**0.84**	**1.66**	**0.66**
2-Sep	1500	0.113	0.22	14.4	62.0	291	13.9	1.59	1.02	0.57	0.12
3-Sep	**1240**	**0.258**	**0.28**	**32.9**	**17.7**	**1261**	**20.5**	**2.42**	**0.89**	**1.53**	**0.43**
3-Sep	**1500**	**0.366**	**0.27**	**30.6**	**19.0**	**535**	**21.0**	**2.49**	**0.84**	**1.65**	**0.44**
3-Sep	1900	0.090	0.20	9.9	73.9	109	12.6	1.46	0.90	0.56	0.11
4-Sep	**1000**	**0.093**	**0.28**	**29.3**	**25.0**	**1236**	**15.6**	**1.77**	**1.02**	**0.75**	**0.21**
4-Sep	**1300**	**0.309**	**0.25**	**33.9**	**18.4**	**1127**	**22.1**	**2.66**	**0.98**	**1.68**	**0.41**
4-Sep	1640	0.187	0.21	26.5	39.4	262	21.3	2.54	1.37	1.16	0.24
4-Sep	1920	0.088	0.20	9.6	80.9	87	13.2	1.52	0.97	0.55	0.11
5-Sep	1000										
5-Sep	**1000**	**0.082**	**0.26**	**28.6**	**30.6**	**1067**	**15.4**	**1.75**	**1.21**	**0.54**	**0.14**
5-Sep	**1300**	**0.140**	**0.39**	**29.6**	**29.1**	**782**	**20.6**	**2.44**	**1.21**	**1.23**	**0.48**
5-Sep	1620	0.257	0.23	26.3	36.1	273	20.0	2.35	1.24	1.11	0.26
5-Sep	1920	0.074	0.20	9.9	79.0	69	13.5	1.55	0.97	0.58	0.12
6-Sep	920										
Pan #4											
2-Sep	**1220**	**0.600**	**1.17**	**34.2**	**12.9**	**1486**	**22.7**	**2.77**	**0.69**	**2.08**	**2.43**
2-Sep	**1600**	**0.231**	**0.42**	**15.2**	**57.2**	**354**	**18.0**	**2.07**	**0.99**	**1.08**	**0.46**
3-Sep	**1240**	**0.563**	**1.22**	**34.5**	**13.8**	**1499**	**23.1**	**2.84**	**0.76**	**2.08**	**2.54**
3-Sep	1500										
3-Sep	**1500**	**0.656**	**1.06**	**32.6**	**13.9**	**700**	**26.9**	**3.56**	**0.69**	**2.87**	**3.06**
3-Sep	1900	0.169	0.22	10.2	68.6	127	16.9	1.93	0.85	1.08	0.24
4-Sep	1000										
4-Sep	**1000**	**0.262**	**0.65**	**31.8**	**19.9**	**1445**	**17.1**	**1.95**	**0.94**	**1.01**	**0.66**
4-Sep	**1300**	**0.540**	**0.94**	**35.3**	**14.2**	**1355**	**25.6**	**3.28**	**0.82**	**2.47**	**2.32**
4-Sep	**1640**	**0.415**	**0.39**	**29.7**	**23.5**	**388**	**28.4**	**3.88**	**0.98**	**2.90**	**1.12**
4-Sep	1920	0.165	0.20	9.4	79.0	103	17.8	2.05	0.93	1.11	0.22
5-Sep	1000										
5-Sep	**1000**	**0.130**	**0.81**	**30.8**	**25.6**	**1269**	**16.8**	**1.92**	**1.14**	**0.78**	**0.63**
5-Sep	**1300**	**0.348**	**0.76**	**31.4**	**24.3**	**951**	**23.5**	**2.91**	**1.12**	**1.78**	**1.35**
5-Sep	**1620**	**0.423**	**0.56**	**28.8**	**25.8**	**393**	**25.5**	**3.27**	**1.02**	**2.25**	**1.27**
5-Sep	1920	0.133	0.21	9.8	75.6	81	17.5	2.00	0.92	1.09	0.23
6-Sep	920										

Appendix C-2. Stepwise determination of evaporation model using SAS© statistical software. Determination made using data from all sites that could be used for regression analysis (wind > 0.20 m/s, etc.: 363 total data points).

Full Model:

$$E = \beta_o + \beta_1 (e_s-e_a) + \beta_2 (V) + \beta_3 (e_s-e_a)^2 + \beta_4 (V)^2 + \beta_5 [V*(e_s-e_a)] + \beta_6[V^2*(e_s-e_a)] + \beta_7[V*(e_s-e_a)^2] + \beta_8[(V)^2*(e_s-e_a)^2]$$

Coefficient	Estimate	Standard Error	Probability Equal to Zero
β_o	0.006	0.030	0.8392
β_1	0.176	0.036	0.0001
β_2	0.024	0.032	0.4477
β_3	-0.015	0.012	0.1975
β_4	0.006	0.011	0.6239
β_5	0.089	0.021	0.0001
β_6	-0.016	0.013	0.2097
β_7	-0.011	0.009	0.2594
β_8	0.007	0.005	0.1110

Reduced Model:

$$E = \beta_1 (e_s-e_a) + \beta_5 [V*(e_s-e_a)]$$

Coefficient	Estimate	Standard Error	Probability Equal to Zero
β_1	0.144	0.005	0.0001
β_5	0.085	0.003	0.0001

$r^2 = 0.88$

$F_{2,360} = 5572$

$p > F = 0.0001$

Note: Regression coefficients β_1 and β_3 will be referred to as α and β from this point forward in appendices and in thesis text in agreement with the theoretical equations presented in the literature review.

Appendix C-3. Regressions generated by SAS© statistical software and used to identify regression coefficients for in-stream and out-of-stream evaporation relationships for each site using the reduced form of the evaporation model established in Appendix C-2. Regression equations are presented with standard errors in parenthesis below each regression coefficient and with the square of the correlation coefficient. Also included is a summary of the statistical test used to determine if the data from each sub-site yielded significantly different regression constants than the coefficients produced using all data other than that of the sub-site.

		α	β	
Site A				
A $_{\text{In-stream}}$:	$E = 0.011\,(e_s-e_a) + 0.282\,[V^*(e_s-e_a)]$	(0.102)	(0.188)	$r^2 = 0.08$
A $_{\text{Out-of-stream}}$:	$E = 0.057\,(e_s-e_a) + 0.309\,[V^*(e_s-e_a)]$	(0.042)	(0.103)	$r^2 = 0.79$
Site B				
B $_{\text{In-stream}}$:	$E = 0.122\,(e_s-e_a) + 0.123\,[V^*(e_s-e_a)]$	(0.032)	(0.032)	$r^2 = 0.50$
B $_{\text{Out-of-stream}}$:	$E = 0.069\,(e_s-e_a) + 0.150\,[V^*(e_s-e_a)]$	(0.039)	(0.043)	$r^2 = 0.54$
Site C				
C $_{\text{In-stream}}$:	$E = 0.142\,(e_s-e_a) + 0.093\,[V^*(e_s-e_a)]$	(0.034)	(0.017)	$r^2 = 0.75$
C $_{\text{Out-of-stream}}$:	$E = 0.156\,(e_s-e_a) + 0.088\,[V^*(e_s-e_a)]$	(0.025)	(0.009)	$r^2 = 0.89$
Site D				
D $_{\text{In-stream}}$:	$E = 0.202\,(e_s-e_a) + 0.047\,[V^*(e_s-e_a)]$	(0.029)	(0.022)	$r^2 = 0.80$
D $_{\text{Out-of-stream}}$:	$E = 0.166\,(e_s-e_a) + 0.084\,[V^*(e_s-e_a)]$	(0.025)	(0.009)	$r^2 = 0.96$

Site E

$E_{\text{In-stream}}$: $E = 0.169\,(e_s-e_a) + 0.059\,[V^*(e_s-e_a)]$ $r^2 = 0.87$
(0.026) (0.028)

$E_{\text{Out-of-stream}}$: $E = 0.167\,(e_s-e_a) + 0.049\,[V^*(e_s-e_a)]$ $r^2 = 0.85$
(0.050) (0.029)

Site F

$F_{\text{In-stream}}$: $E = 0.202\,(e_s-e_a) + 0.026\,[V^*(e_s-e_a)]$ $r^2 = 0.77$
(0.017) (0.017)

$F_{\text{Out-of-stream}}$: $E = 0.190\,(e_s-e_a) + 0.040\,[V^*(e_s-e_a)]$ $r^2 = 0.87$
(0.031) (0.018)

Site G

$G_{\text{In-stream}}$: $E = 0.109\,(e_s-e_a) + 0.194\,[V^*(e_s-e_a)]$ $r^2 = 0.68$
(0.024) (0.033)

$G_{\text{Out-of-stream}}$: $E = 0.120\,(e_s-e_a) + 0.094\,[V^*(e_s-e_a)]$ $r^2 = 0.94$
(0.010) (0.006)

Site H

$H_{\text{In-stream}}$: $E = 0.204\,(e_s-e_a) + 0.057\,[V^*(e_s-e_a)]$ $r^2 = 0.82$
(0.027) (0.046)

$H_{\text{Out-of-stream}}$: $E = 0.157\,(e_s-e_a) + 0.081\,[V^*(e_s-e_a)]$ $r^2 = 0.88$
(0.029) (0.025)

Site I

$I_{\text{In-stream}}$: $E = 0.149\,(e_s-e_a) + 0.123\,[V^*(e_s-e_a)]$ $r^2 = 0.86$
(0.019) (0.029)

$I_{\text{Out-of-stream}}$: $E = 0.109\,(e_s-e_a) + 0.122\,[V^*(e_s-e_a)]$ $r^2 = 0.94$
(0.016) (0.017)

Question: Are the regression coefficients (α and β) produced by using only the data associated with a single sub-site significantly different from those coefficients that are obtained using all other data (entire useable data set minus sub-site data set)?

Two-sided Test at 5% Level of Significance

Null Hypothesis (H_o): $\mu_o = \mu_T$

Alternate Hypothesis (H_a): $\mu_o \neq \mu_T$

Where

μ_o = Mean regression coefficient estimate of data from sub-site

μ_T = Mean regression coefficient estimate using all data other than that from sub-site of comparison

Reject H_o if μ_T is located outside of 95% C.I. of μ_o

95 % Confidence Interval for μ_o

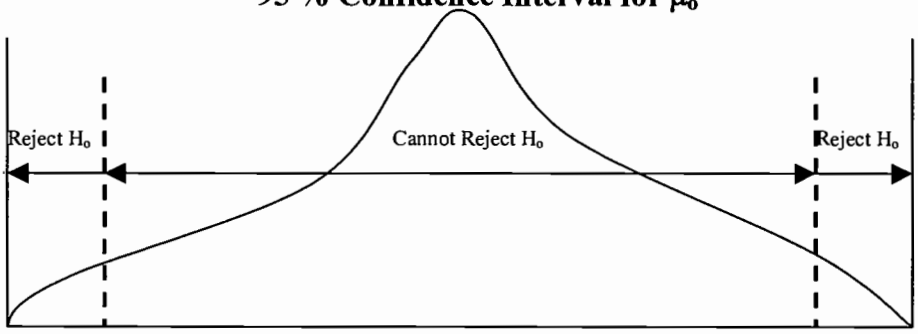

Sub-Site	95 % Confidence Interval for Alpha (α) Regression Coefficient for Sub-Site	Mean Alpha (α) Regression Coefficient Using all Data Other Than Sub-Site	Significantly Different? ($p > 0.05$)
A In-stream	-0.251, 0.272	0.144	No
A Out-of-stream	-0.060, 0.173	0.144	No
B In-stream	0.054, 0.190	0.143	No
B Out-of-stream	-0.012, 0.149	0.148	No
C In-stream	0.071, 0.212	0.144	No
C Out-of-stream	0.104, 0.208	0.147	No
D In-stream	0.140, 0.263	0.143	No
D Out-of-stream	0.114, 0.218	0.147	No
E In-stream	0.114, 0.224	0.144	No
E Out-of-stream	0.064, 0.270	0.145	No
F In-stream	0.166, 0.238	0.142	Yes
F Out-of-stream	0.124, 0.257	0.144	No
G In-stream	0.059, 0.159	0.137	No
G Out-of-stream	0.100, 0.140	0.148	Yes
H In-stream	0.146, 0.261	0.143	Yes
H Out-of-stream	0.094, 0.219	0.144	No
I In-stream	0.108, 0.190	0.142	No
I Out-of-stream	0.076, 0.143	0.145	Yes

Sub-Site	95 % Confidence Interval for Beta (β) Regression Coefficient for Sub-Site	Beta (β) Regression Coefficient Using all Data Other Than Sub-Site	Significantly Different? ($p > 0.05$)
$A_{In\text{-}stream}$	-0.202, 0.765	0.085	No
$A_{Out\text{-}of\text{-}stream}$	0.023, 0.595	0.085	No
$B_{In\text{-}stream}$	0.056, 0.190	0.085	No
$B_{Out\text{-}of\text{-}stream}$	0.060, 0.240	0.083	No
$C_{In\text{-}stream}$	0.058, 0.128	0.084	No
$C_{Out\text{-}of\text{-}stream}$	0.069, 0.106	0.082	No
$D_{In\text{-}stream}$	0.001, 0.093	0.085	No
$D_{Out\text{-}of\text{-}stream}$	0.064, 0.103	0.081	No
$E_{In\text{-}stream}$	-0.001, 0.118	0.085	No
$E_{Out\text{-}of\text{-}stream}$	-0.011, 0.110	0.087	No
$F_{In\text{-}stream}$	-0.010, 0.062	0.086	Yes
$F_{Out\text{-}of\text{-}stream}$	0.001, 0.079	0.087	Yes
$G_{In\text{-}stream}$	0.128, 0.261	0.088	Yes
$G_{Out\text{-}of\text{-}stream}$	0.081, 0.107	0.084	No
$H_{In\text{-}stream}$	-0.043, 0.157	0.086	No
$H_{Out\text{-}of\text{-}stream}$	0.026, 0.135	0.085	No
$I_{In\text{-}stream}$	0.061, 0.185	0.086	No
$I_{Out\text{-}of\text{-}stream}$	0.086, 0.158	0.084	Yes

Appendix C-4. Plots of evaporation rate versus the individual variables e_s-e_a and V* e_s-e_a (the main components of the reduced form of the multiple regression model). Plots shown use all 363 data points.

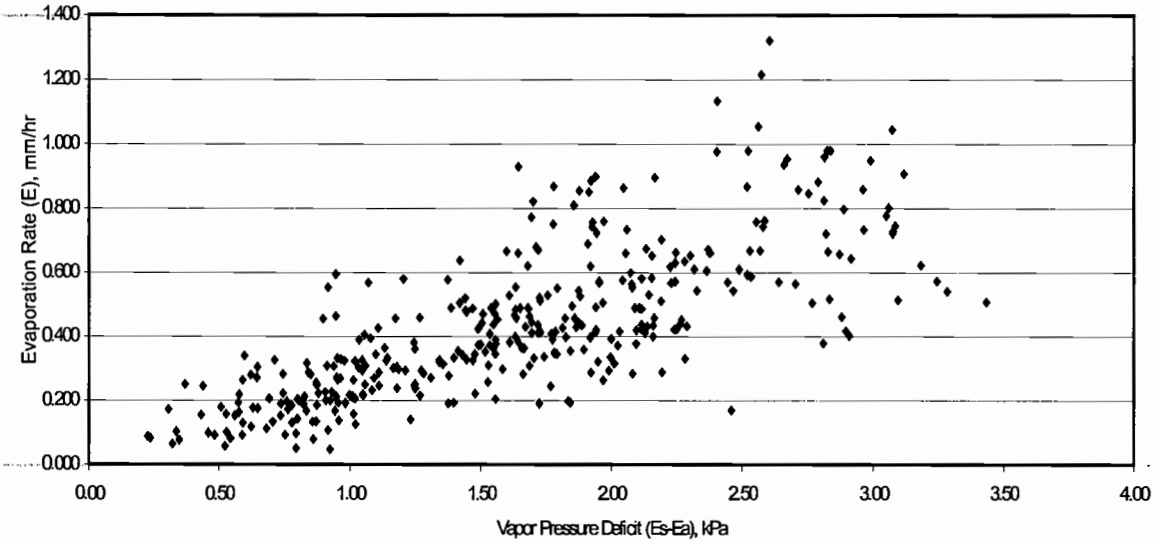

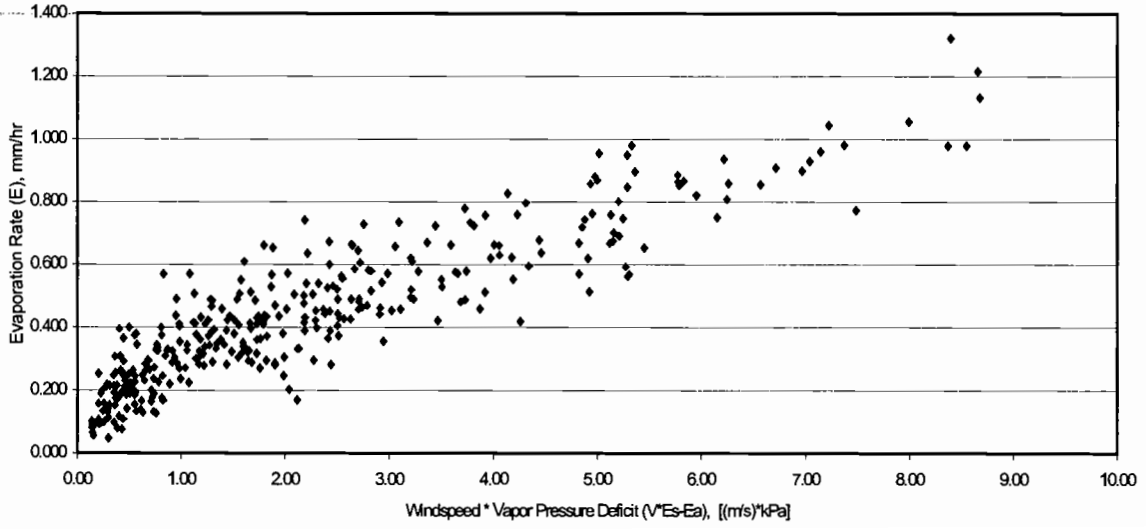

APPENDIX D: Results of water velocity and turbulence study conducted under laboratory conditions

Appendix D-1. Results of experiments testing the influence of water velocity and/or turbulence on the rate of evaporation.

TEST #1:

All tests conducted at the following conditions:

Vapor pressure deficit ≈ 1 kPa
Windspeed = 0 m/s

Treatment evaporation pan:

Water velocity = variable
Test 1a = 0.03-0.06 m/s (0.1-0.2 ft/s)
Test 1b = 0.09-0.12 m/s (0.3-0.4 ft/s)
Test 1c = 0.27-0.30 m/s (0.9-1.0 ft/s)

Control evaporation pan:

Water velocity = 0 m/s

Test 1a Results:

	Treatment Pan Evaporation (mm)	***Control Pan Evaporation (mm)***	***% Increase***
Run #1	2.39	1.63	47
Run #2	3.20	2.18	47
Run #3	1.70	1.12	52

Average % increase in evaporation with water moving at 0.03-0.06 m/s = ***49%***
(at low vapor pressure deficit and no air movement)

Test 1b Results:

	Treatment Pan Evaporation (mm)	***Control Pan Evaporation (mm)***	***% Increase***
Run #1	4.11	2.34	76
Run #2	2.69	1.55	74
Run #3	7.39	4.22	75

Average % increase in evaporation with water moving at 0.09-0.12 m/s = ***75%***
(at low vapor pressure deficit and no air movement)

Test 1c Results:

	Treatment Pan Evaporation (mm)	***Control Pan Evaporation (mm)***	***% Increase***
Run #1	4.04	1.75	131
Run #2	3.53	1.58	123
Run #3	2.82	1.25	126

Average % increase in evaporation with water moving at 0.27-0.30 m/s = ***127%***
(at low vapor pressure deficit and no air movement)

TEST #2:

All tests conducted at the following conditions:

Vapor pressure deficit ≈ 2 kPa
Windspeed = 0 m/s

Treatment evaporation pan:

Water velocity = 0.12-0.18 m/s (0.4-0.6 ft/s)

Control evaporation pan:

Water velocity = 0 m/s

Test 2a Results:

	Treatment Evaporation Pan Evaporation (mm)	***Control Pan Evaporation (mm)***	***% Increase***
Run #1	5.79	5.28	10
Run #2	1.83	1.52	20
Run #3	3.53	3.53	0
Run #4	2.11	2.01	5

Average % increase in evaporation with water moving at 0.12-0.18 m/s = ***9 %***
(at high vapor pressure deficit and no air movement)

TEST #3:

All tests conducted at the following conditions:

Vapor pressure deficit ≈ 1 kPa
Windspeed = 0.3 m/s

Treatment evaporation pan:

Water velocity = 0.12-0.18 m/s (0.4-0.6 ft/s)

Control evaporation pan:

Water velocity = 0 m/s

Test 3a Results:

	Treatment Evaporation Pan Evaporation (mm)	***Control Pan Evaporation (mm)***	***% Increase***
Run #1	5.05	4.34	16
Run #2	2.41	2.08	16
Run #3	3.68	2.98	25

Average % increase in evaporation with water moving at 0.12-0.18 m/s = ***19 %***
(at low vapor pressure deficit and low air movement)

APPENDIX E: Determination of wind exposure index

Appendix E-1. The Wind Exposure Index was determined based on a formula used to calculate "ventilation" in valleys established by Yoshino (1975). This formula was modified slightly to estimate the exposure of wind at the water surface of streams. Mathematical calculations using this formula are demonstrated below on hypothetical channel cross sections. Cross-sections and indices are compared for agreement.

Definition of Variables:

a = width of channel at beginning of floodplain surface (m)
b = depth from floodplain surface to water surface (m)
c = width of water surface (m)

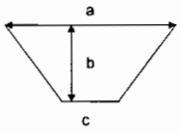

Wind Exposure Index (WEI) = [a/(a + c)] * (a/b)

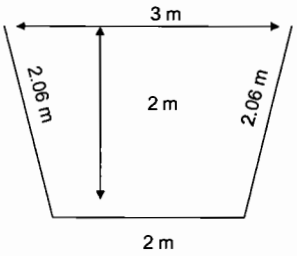

WEI = 0.9

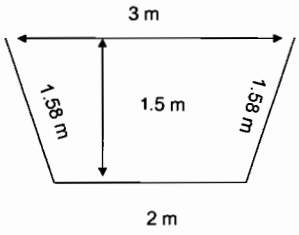

WEI = 1.2

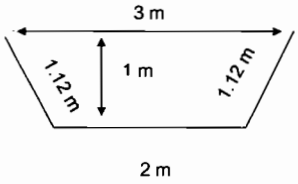

WEI = 1.8

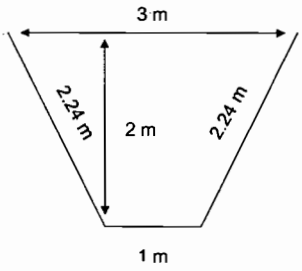

WEI = 1.1

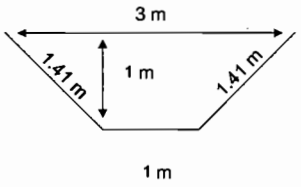

WEI = 2.3

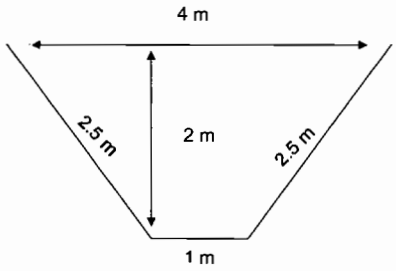

WEI = 1.6

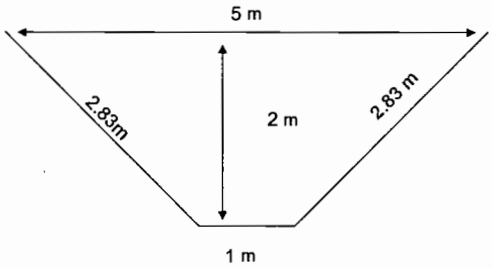

WEI = 2.1

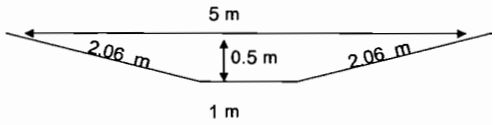

WEI = 8.3

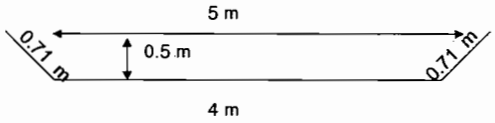

WEI = 5.6